

Khovanov homology for links in $\#^r(S^2 \times S^1)$

Michael Willis

Department of Mathematics, UCLA

msw188@ucla.edu

October 24, 2019

Abstract

We revisit Rozansky's construction of Khovanov homology for links in $S^2 \times S^1$, extending it to define Khovanov homology $Kh(L)$ for links L in $M^r = \#^r(S^2 \times S^1)$ for any r . The graded Euler characteristic of $Kh(L)$ can be used to recover WRT invariants at certain roots of unity, and also recovers the evaluation of L in the skein module $\mathcal{S}(M^r)$ of Hoste and Przytycki when L is null-homologous in M^r . The construction also allows for a clear path towards defining a Lee's homology $Kh'(L)$ and associated s -invariant for such L , which we will explore in an upcoming paper. We also give an equivalent construction for the Khovanov homology of the knotification of a link in S^3 and show directly that this is invariant under handle-slides, in the hope of lifting this version to give a stable homotopy type for such knotifications in a future paper.

1 Introduction

In [Kho00] Mikhail Khovanov introduced the Khovanov homology $Kh(L)$ of any link L in S^3 , which categorifies the Jones polynomial of L . This construction was generalized for tangles in the 3-ball in two different, but equivalent, ways. In [Kho02], Khovanov considered tangles with $2n$ 'incoming' and $2m$ 'outgoing' strands. In the spirit of topological quantum field theories (TQFTs), Khovanov defined corresponding 'arc algebras' H_n and H_m and assigned to any such tangle a complex of H_n, H_m -bimodules with proper gluing properties that could be used to recover $Kh(L)$. Meanwhile, in [BN05], Dror Bar-Natan constructed a universal categorification of the Temperley-Lieb algebra allowing him to assign to a tangle a formal complex of cobordisms between Temperley-Lieb diagrams in the 2-disk, again from which $Kh(L)$ could be recovered.

Later in [Roz], Lev Rozansky used Khovanov's framework to assign complexes of H_n, H_n -bimodules to tangles in $S^2 \times [0, 1]$ with $2n$ endpoints at both ends. From this Rozansky was able to define the Khovanov homology of the closure of such a tangle in $S^2 \times S^1$ by passing to the derived category of such complexes and taking the Hochschild homology, as expected under the axioms of a TQFT. He then showed that the projective resolution needed for this computation could be approximated by concatenating large numbers of full twists to the given tangle and computing the Khovanov homology of the usual closure in S^3 .

This work was funded in part by the NSF grant DMS-1563615

The main goal of this manuscript is to revisit the argument of Rozansky and extend it to define Khovanov homology invariants for links in $M^r := \#^r(S^2 \times S^1)$, the connect sum of r copies of $S^2 \times S^1$.

Theorem 1.1. *Let \mathcal{L} be a link in M^r having even geometric intersection numbers n_i with all of the belt spheres $S_i^2 \subset M^r$, represented by a diagram L . Then there exists a \mathbb{Z} -graded chain complex $KC^j(L)$ whose (graded) homology groups $H^{*,j}(\mathcal{L}) := H^*(KC^j(L))$ are invariants of the link \mathcal{L} up to overall grading shifts which vanish if \mathcal{L} is null-homologous in M^r . For links \mathcal{L} in $M^0 = S^3$, these homology groups are precisely the traditional Khovanov homology groups of \mathcal{L} .*

Theorem 1.1 provides link invariants that categorify both the skein module $\mathcal{S}(M^r)$ of Hoste and Przytycki [HP92] and the WRT invariants of links in M^r in the proper sense (see Section 5 for precise statements). To prove Theorem 1.1, we revise Rozansky's original construction and avoid the use of Khovanov's derived category and Hochschild homology, for which such an extension might be unclear. Instead, we choose to remain in Bar-Natan's setting throughout our construction and utilize Rozansky's arguments involving infinite full twists, only applying Khovanov's functor at the end to produce homology groups. We present a rough outline of this construction below.

Consider M^r as built by performing r S^0 -surgeries on S^3 . We draw M^r on the plane by specifying the projections of the surgery spheres $S^0 \times S^2$ for the 0-surgeries, using dashed lines to match corresponding spheres. Then any link $\mathcal{L} \subset M^r$ can be projected onto this plane as a tangle diagram with n_i matching endpoints on the attaching spheres $(S^0 \times S^2)_i$ (see Figure 1 for an example; these notions will be made precise in Section 3).

To construct the link invariant, we imagine connecting the corresponding endpoints of the link using n_i parallel copies of the dashed lines, giving us a diagram for a link in S^3 . We further augment this diagram by inserting a large number of full right-handed twists $\mathcal{F}_{n_i}^{k_i}$ into each of these connections (see Figure 1). Rozansky's arguments in [Roz] give a prescription for defining a limiting chain complex (in Bar-Natan's universal Temperley-Lieb category) for this diagram as the quantities $k_i \rightarrow \infty$. If we apply Khovanov's functor to this limiting complex, we have an infinite complex of chain groups; the Khovanov homology groups $Kh(\mathcal{L})$ of $\mathcal{L} \subset M^r$ are then defined to be the (graded) homology groups of this complex.

In order to show that $Kh(\mathcal{L})$ is indeed a link invariant, one must show that this construction is invariant with respect to isotopies in M^r . In terms of our diagram $L(\vec{k})$, such isotopies incorporate the usual Reidemeister moves in the plane as well as movements of tangle endpoints on corresponding spheres, pushing strands 'through' the attaching spheres, and the ability to 'pull strands around' the spheres (and through the twists introduced into the diagram for L along these dashed lines). The usual Reidemeister moves are handled automatically from Khovanov's original construction. The movements of the tangle endpoints, as well as the ability to push a strand through a sphere, are handled via simple properties of the full twist. For pulling strands *through* the twisting strands, the basic idea is that, for even numbers of strands n_i , the limiting complexes for the torus braids $\mathcal{F}_{n_i}^{k_i}$ as $k_i \rightarrow \infty$ can be written entirely in terms of diagrams where no strands pass from 'top to bottom', and thus there are always gaps through which one can 'pull' other strands in a consistent manner.

Many of these considerations follow directly from Rozansky's work in $S^2 \times S^1$ [Roz], but we present the details here for completion. In addition, there are two somewhat more substantial modifications to the arguments regarding the simplifications of multicones (Section 8.1 in [Roz]; see Remark 2.15 here) and the use of 'quasi-triviality' of certain tangles (Section 7.3 in [Roz]; see Remark 3.13 here).

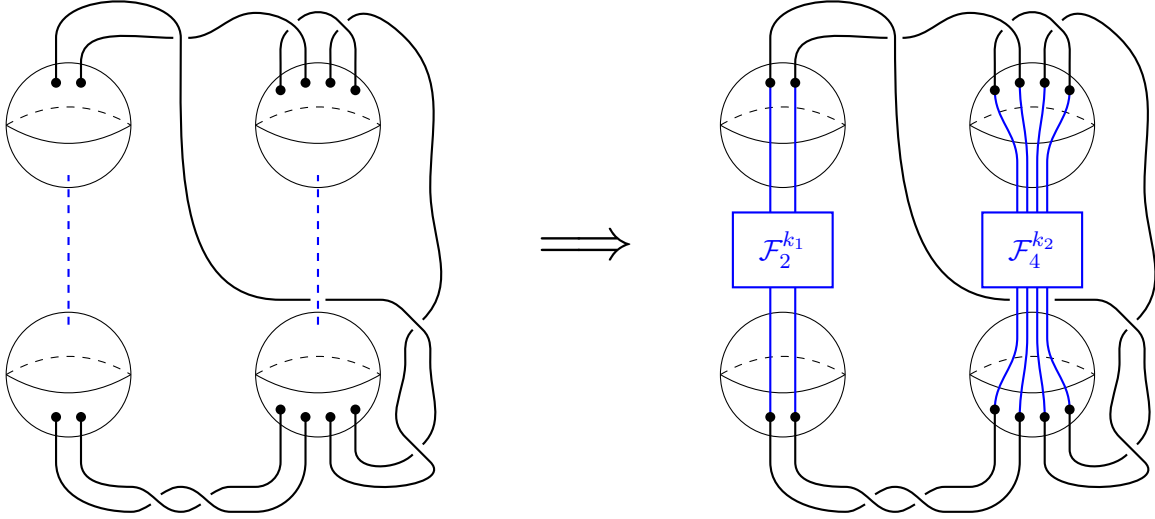


Figure 1: On the left is an example of a link diagram L for $\mathcal{L} \subset M^2$, with intersection numbers $n_1 = 2$ and $n_2 = 4$. The dashed lines in blue indicate corresponding surgery spheres. We then convert this into the diagram $L(\vec{k})$ on the right by changing the dashed lines into torus braids $\mathcal{F}_{n_i}^{k_i}$, also drawn in blue. The complex $KC(L)$ is defined by letting the various k_i go to infinity.

1.1 Future work

The construction above gives Khovanov homology groups for links up to isotopies within a fixed M^r , well-defined up to grading shifts. It is not hard to generalize all of this to Bar-Natan's deformed Temperley-Lieb category, allowing for a Lee's homology for such links and a definition of an s -invariant similar to that of Jacob Rasmussen in [Ras10]. We will explore this invariant and its associated bounds on the genus of cobordisms between links in a future paper with Ciprian Manolescu, Marco Marengon, and Sucharit Sarkar, to appear soon.

We will also show that, for knotifications $\mathcal{K}_{\mathcal{L}} \subset M^r$ of links $\mathcal{L} \subset S^3$ (used to define knot Floer homology for links [OS04]), handle slides of the underlying M^r do not affect the chain homotopy equivalence class of our complexes, and using this will allow us to construct the Khovanov homology for these knotifications directly from the link diagram for \mathcal{L} in S^3 . It is our hope that this alternative construction will be amenable to further study, including a lifting to the stable homotopy category following the work of [LS14, LLS] in a future paper.

1.2 Organization of the paper

This paper will be organized as follows. Section 2 will review the necessary homological algebra as it pertains to the Khovanov complexes in question before going on to produce a simplified Khovanov complex for the full twist on n strands which satisfies certain important properties. Much of this work is equivalent to similar work in [Roz], but is presented in a way that emphasizes the precise homological algebra being used. In Section 3 we explore diagrams for links in M^r before proving Theorem 1.1, making precise the ideas presented here in the introduction. We present example computations for some simple links in M^1 and M^2 in Section 4. Section 5 discusses the decategorification of the invariant, and its relationships with the skein module $\mathcal{S}(M^r)$ and WRT

invariants. Finally, in Section 6 we present an alternative construction geared towards defining Khovanov homology for knotifications of links in S^3 directly from the given link diagram.

Acknowledgements

The author would like to thank an anonymous referee for several very helpful suggestions that have improved the paper. He would also like to thank Slava Krushkal, Sucharit Sarkar, Ciprian Manolescu, Andy Manion, and especially Matt Hogancamp for many very enlightening discussions.

2 The Khovanov complex for the infinite full twist

2.1 Overview, conventions, and notation

Let R denote an arbitrary ground-ring. In this section we will construct a semi-infinite chain complex for the infinite right-handed twist on an even number of strands. This complex will be viewed as living in Bar-Natan's homotopy category of complexes of Temperley-Lieb diagrams and R -linear combinations of dotted cobordisms between them [BN05]. In order to state the desired theorem, we first introduce some notational conventions.

Definition 2.1. The following definitions and notations will be used throughout this paper.

- The variable n will generally be reserved for the number of strands in a braid; when n is even, it will be written as $n = 2p$.
- Tangles will generally be written as script capital letters. In particular, we will use the notation \mathcal{F}_n^k to indicate the torus braid of k right-handed full-twists on n strands, shown in Figure 2 below (\mathcal{F}_n without the superscript will denote a single full twist).
- The meaning of positive and negative crossings, as well as the meanings of 0-resolutions and 1-resolutions, is presented in Figure 3.
- The variable $n_{\mathcal{F}}^-$ represents the number of negative crossings present in a single copy of \mathcal{F}_n (this is non-zero when the strands of \mathcal{F}_n are not all oriented in the same direction). Similarly we define $N_{\mathcal{F}} := 2n_{\mathcal{F}}^- - n_{\mathcal{F}}^+$, where $n_{\mathcal{F}}^+$ is the number of positive crossings in \mathcal{F}_n . Later in Section 3, when there are several \mathcal{F}_{n_i} involved, we will use n_i^- and N_i (see Definition 3.4).
- If \mathcal{Z} is some oriented tangle, then the notation $KC^*(\mathcal{Z})$ will denote the Khovanov complex of \mathcal{Z} as described by Bar-Natan in [BN05]. We will be employing Bar-Natan's conventions for the homological grading of terms in the complex:

The homological degree of a diagram δ is computed as the number of 1-resolutions taken to arrive at δ , subtracted by the total number of negative crossings n^- of the original oriented tangle \mathcal{Z} .

The q -degree of a diagram δ is computed as the number of 1-resolutions taken to arrive at δ , subtracted by the normalization shift $N := 2n^- - n^+$ coming from the numbers of positive (n^+) and negative (n^-) crossings in \mathcal{Z} .

In this way, $KC^*(\mathcal{Z})$ is a genuine graded invariant of the oriented \mathcal{Z} up to chain homotopy equivalence, with no grading shifts necessary for Reidemeister moves. The differential raises



Figure 2: The full twist, denoted by \mathcal{F}_n (depicted here for $n = 4$).

homological grading by one (ie KC^* is a cochain complex) and respects the q -grading. The asterisk refers to homological grading.

- Shifts in homological and q -grading of a complex C^* will be denoted with h and q , respectively. Thus, the complex $h^a q^b KC^*(\mathcal{Z})$ indicates the Khovanov complex for \mathcal{Z} shifted up in homological degree by a , and in q -degree by b . The shifts take place before the use of the asterisk, so that the notation $h^a q^b KC^*(\mathcal{Z})$ should be thought of as implying $(h^a q^b KC)^*(\mathcal{Z})$.
- For a given chain complex C^* , the notation $C^*_{>a}$ will denote the truncated complex

$$C^*_{>a} := \begin{cases} C^* & \text{if } * > a \\ \emptyset & \text{if } * \leq a \end{cases}. \quad (1)$$

Note that this ensures that $C^*_{>b}$ is a subcomplex of $C^*_{>a}$ as long as $b \geq a$, with the inclusion

$$C^*_{>b} \hookrightarrow C^*_{>a}$$

inducing an isomorphism on homology in all homological degrees strictly greater than $b+1$. As with the use of the asterisk, any shifts indicated are meant to take place before the truncation, so that $h^a q^b KC^*_{>c}(\mathcal{Z})$ implies $(h^a q^b KC)^*_{>c}(\mathcal{Z})$.

- Single Temperley-Lieb diagrams within a complex C^* will typically be denoted by greek letters. We will use the notation $h_{C^*}(\delta)$ to denote the homological grading of δ within C^* . In many cases the complex will be clear from the context, and the subscript will be omitted.
- For a Temperley-Lieb diagram δ , the notation $\text{th}(\delta)$ will indicate the *through-degree* of δ . This is the number of strands within δ whose endpoints are on opposite ends of the diagram. See Figure 4 for clarification.
- Identity cobordisms will be denoted by I , together with a subscript if necessary for clarification. Dotted planar cobordisms between Temperley-Lieb diagrams will typically be written as $\phi_{i,j} : \delta_i \rightarrow \delta_j$. More general dotted tangle cobordisms will often appear via Reidemeister moves and be notated by ρ .

With the notations indicated above, we state the goal of this section here.

Theorem 2.2. *Fix an even integer $n = 2p$. Let \mathcal{F}_n denote an oriented full right-handed twist, and define $n_{\overline{\mathcal{F}}}$ and $N_{\mathcal{F}}$ as above. Then there exists a sequence of complexes $C^*(k)$ satisfying the following properties.*

2.2 Simplifying Khovanov complexes

We begin by recalling the defining aspect of $KC^*(\cdot)$. Given an oriented tangle diagram \mathcal{Z} , we construct $KC^*(\mathcal{Z})$ by finding crossings in \mathcal{Z} and defining

$$KC^*(\times) = h^{-n^-} q^{n^+ - 2n^-} (\underbrace{\quad} \rightarrow q \underbrace{\quad}) \quad (2)$$

where the underlined term is in homological grading zero, the map is a saddle cobordism, and n^+ and n^- are either 1 or 0 depending on whether the crossing was positively or negatively oriented. The full $KC^*(\mathcal{Z})$ is then a large tensor product over all of these two term complexes, with diagrams and cobordisms stitched together in the usual sense of planar algebras (see [BN05] for more details).

In order to simplify $KC^*(\mathcal{Z})$, we have several tools at our disposal. There is the obvious approach of breaking \mathcal{Z} up into separate tangles and trying to simplify their Khovanov complexes individually, before tensoring them all back together again. There is also the idea of using Equation 2 to view $KC^*(\mathcal{Z})$ as the cone on a chain map $KC^*(\underbrace{\quad}) \rightarrow KC^*(\underbrace{\quad})$, and attempting to simplify $KC^*(\underbrace{\quad})$ and/or $KC^*(\underbrace{\quad})$ separately. This idea can be expanded into viewing $KC^*(\mathcal{Z})$ as a large multicone of various cobordism maps in the hopes of simplifying various diagrams within the multicone. However, the presence of the degree shifts causes a slight bit of trouble because the orientation of the original crossing (and thus the entire diagram) cannot be maintained on both of its resolutions. Therefore we adopt the following convention, also adopted in the author's earlier related paper [IW18].

Definition 2.4. The symbol $\widetilde{KC}^*(\cdot)$ will stand for the *renormalized Khovanov complex*

$$\widetilde{KC}^*(\cdot) := h^{n^-} q^N KC(\cdot) \quad (3)$$

where the symbols n^- and $N := 2n^- - n^+$ will count positive and negative crossings in whatever tangle they are attached to. Thus we will write Equation 2 in the form

$$\widetilde{KC}^*(\times) = \text{Cone} \left(\widetilde{KC}^*(\underbrace{\quad}) \rightarrow q \widetilde{KC}^*(\underbrace{\quad}) \right) \quad (4)$$

and it will be understood that the various n^- and N terms that are implied by the notation are actually different numbers. With this convention in place, it will not matter what orientations are assigned to the resolved diagrams within the cone of Equation 4.

Notice that this convention ensures that, for any tangle \mathcal{Z} , $\widetilde{KC}^*(\mathcal{Z})$ has left-most term in homological grading zero (ie taking 0-resolutions at every crossing), and right-most term in homological grading equal to the number of crossings in \mathcal{Z} (ie taking 1-resolutions at every crossing). However, the trade-off for this normalizing convention is that, since the 'true' grading of $KC^*(\cdot)$ is invariant under Reidemeister moves, we must incur grading shifts when performing Reidemeister moves with $\widetilde{KC}^*(\cdot)$.

Lemma 2.5. *Suppose D_1 and D_2 are two tangle (or link) diagrams that are related by Reidemeister moves (ie the diagrams are tangle isotopic, representing the same tangle or link). Let n_1^- and n_2^- be the number of negative crossings in the diagrams D_1 and D_2 respectively, and similarly for the q -grading renormalizations N_1 and N_2 . Then using the convention of Definition 2.4,*

$$\widetilde{KC}^*(D_1) \simeq h^{n_1^- - n_2^-} q^{N_1 - N_2} \left(\widetilde{KC}^*(D_2) \right). \quad (5)$$

Proof.

$$\begin{aligned}
\widetilde{KC}^*(D_1) &= h^{n_1^-} q^{N_1} KC^*(D_1) \\
&= h^{n_1^- - n_2^- + n_2^-} q^{N_1 - N_2 + N_2} KC^*(D_1) \\
&\simeq h^{n_1^- - n_2^- + n_2^-} q^{N_1 - N_2 + N_2} KC^*(D_2) \\
&\simeq h^{n_1^- - n_2^-} q^{N_1 - N_2} \left(h^{n_2^-} q^{N_2} KC^*(D_2) \right) \\
&= h^{n_1^- - n_2^-} q^{N_1 - N_2} \left(\widetilde{KC}^*(D_2) \right)
\end{aligned}$$

□

In other words, Reidemeister moves shift the renormalized homological grading of $\widetilde{KC}^*(\cdot)$ by precisely the number of negative crossings that were removed. In particular, using negative Reidemeister 1 moves and Reidemeister 2 moves to eliminate crossings both shift homological degree by 1. Similar statements hold for shifting of q -grading, but we will be focusing on the homological grading for the most part here. Compare Lemma 2.5 with the various shifts described by Rozansky throughout [Roz], and also Proposition 2.19 in [AW].

With the notations of Equations 3 and 4 in place, we explore the notion of viewing Khovanov complexes as large multicones. If we are planning on simplifying individual pieces of such a multicone via chain homotopy equivalences, we will need a construction that can keep track of these homotopies. For this we recall some general homological algebra (compare to Section 8.1 in [Roz]) for complexes over additive categories.

Definition 2.6. Suppose we are given the following data in a fixed category of chain complexes over some additive category:

- A finite index set \mathcal{C} with a \mathbb{Z} -grading $h_{\mathcal{C}} : \mathcal{C} \rightarrow \mathbb{Z}$.
- For all $i \in \mathcal{C}$, a chain complex (A_i^*, d_i) .
- For all $i, j \in \mathcal{C}$, a map (not necessarily a chain map) $f_{ij}^* : A_i^* \rightarrow h^{\text{hc}(j) - \text{hc}(i) - 1} A_j^*$ satisfying
 - $f_{ii}^* := d_i$
 - For all $j \neq i$ in \mathcal{C} with $h_{\mathcal{C}}(j) \leq h_{\mathcal{C}}(i)$, $f_{ij}^* := 0$
 - For all $i, k \in \mathcal{C}$, $\sum_{j \in \mathcal{C}} f_{jk}^* f_{ij}^* = 0$.

Then we can form the *multicone*

$$M = \text{Multicone} \left(A_i^* \xrightarrow{f_{ij}^*} h^{\text{hc}(j) - \text{hc}(i) - 1} A_j^* \right) \quad (6)$$

which is a chain complex (M, d_M) whose terms are the direct sum of all of the terms of the complexes A_i

$$M := \bigoplus_{i \in \mathcal{C}} A_i$$

and whose differential is the sum of all of the maps f_{ij}

$$d_M := \sum_{i, j \in \mathcal{C}} f_{ij}.$$

For a term $\alpha \in A_i^* \subset M$, we determine the homological grading as the sum of the contributions of viewing α in A_i^* and viewing A_i^* in \mathcal{C}

$$h_M(\alpha) := h_{A_i}(\alpha) + h_{\mathcal{C}}(i).$$

The reader may verify that this definition gives a well defined chain complex. When $h_{\mathcal{C}}(j) - h_{\mathcal{C}}(i) = 1$, the maps f_{ij}^* assemble to define chain maps; when $h_{\mathcal{C}}(j) - h_{\mathcal{C}}(i) = 2$, the maps f_{ij}^* assemble to form null-homotopies for the compositions of any two of these chain maps; and so on. Because the original system \mathcal{C} was finite, this process must eventually end, and so of course the sum in the definition of d_M is finite. When $\mathcal{C} = \{0, 1\}$ and we have the single chain map $f_{01}^* : A_0 \rightarrow A_1$, this construction recovers the usual cone on f_{01}^* .

Remark 2.7. We employ the term ‘multicone’ in Definition 2.6 following [Roz]. A complex built in this manner is also often referred to as a *totalization* or *convolution* of a *twisted complex*. See for instance [BK91].

Note that *any* finite chain complex \mathcal{C}^* can be represented as a multicone by declaring that \mathcal{C} is indexed by the terms in \mathcal{C}^* while the maps $f_{i(i+1)}$ are given by the differentials of \mathcal{C}^* . Meanwhile all of the maps f_{ij}^* with $h_{\mathcal{C}}(j) - h_{\mathcal{C}}(i) \geq 2$ are zero maps (ie no homotopies are needed).

Proposition 2.8. *Given a chain complex presented as a multicone M as in Equation 6, and given chain homotopy equivalences $\iota_i : A_i^* \rightarrow (A'_i)^*$ for each $i \in \mathcal{C}$, there exist maps $(f'_{ij})^*$ such that we can form the multicone*

$$M' := \text{Multicone}_{i,j \in \mathcal{C}} \left((A'_i)^* \xrightarrow{(f'_{ij})^*} h^{\text{hc}(j) - \text{hc}(i) - 1} (A'_j)^* \right)$$

that is chain homotopy equivalent to M :

$$M \simeq M'.$$

Proof. This is a standard result generalizing the fact that the homotopy category of complexes over an additive category is triangulated (Proposition 2 in [BK91]). \square

Proposition 2.8 tells us that we can replace complexes within a multicone with chain homotopy equivalent ones, but it tells us nothing about the maps $(f'_{ij})^*$ that result. For that we need some stronger assumptions.

Definition 2.9. A chain map $\iota : A^* \rightarrow (A')^*$ will be called a *very strong deformation retract* if there are maps $\iota^{-1} : (A')^* \rightarrow A^*$ and $H : A^* \rightarrow h^{-1}A^*$ satisfying:

- (i) ι^{-1} is a chain map such that $\iota \circ \iota^{-1} = I_{A'}$ and $\iota^{-1} \circ \iota = I_A + dH + Hd$. In other words, ι is a strong deformation retract.
- (ii) The maps involved satisfy the following *side conditions*: $HH = 0$, $\iota H = 0$, $H\iota' = 0$.

Given a strong deformation retract ι satisfying only item (i) above, it is always possible to replace ι with a very strong deformation retract $\tilde{\iota}$ satisfying item (ii) as well (see [LS87], as well as [Mar01] for more considerations on such maps and constructions similar to the ones below). In the cases of interest in this paper, however, our deformation retracts will all start out very strong.

Proposition 2.10. *In the situation of Proposition 2.8, suppose all of the maps ι_i are very strong deformation retracts (with accompanying maps ι_i^{-1} and H_i). Then the maps $(f'_{ij})^*$ used to build M' (satisfying $M' \simeq M$) are sums of terms of the form $\iota(f + fHf + fHfHf + \dots)\iota^{-1}$ as indicated in slightly more detail below:*

$$f'_{i\ell} = \sum_{(j_1, \dots, j_k)} \iota_\ell f_{j_k \ell} H_{j_k} f_{j_{k-1} j_k} \cdots f_{j_2 j_3} H_{j_2} f_{j_1 j_2} H_{j_1} f_{i j_1} \iota_i^{-1}$$

where we sum over all sequences of j 's that 'partition the path' from index i to index ℓ (disallowing the differentials f_{jj}).

Proof. The finiteness of \mathcal{C} ensures that the sums above are finite. In this case, one can check explicitly that the maps $f'_{i\ell}$ satisfy the conditions needed to build the multicone M' . Then one can build explicit maps $\iota_{MM'} : M \rightarrow M'$ and $\iota_{M'M} : M' \rightarrow M$ written as follows:

$$\iota_{MM'} = \iota(I + fH + fHfH + \dots), \quad \iota_{M'M} = (I + Hf + HfHf + \dots)\iota^{-1}.$$

All of these maps are to be interpreted as sums over 'partitions of paths between various indices' as in the expansion of $\iota(f + fHf + fHfHf + \dots)\iota^{-1}$ above. Again, one can check explicitly that these are indeed chain maps (up to this point, the assumption that the various ι are very strong deformation retracts is not used). The composition $\iota_{MM'} \circ \iota_{M'M}$ is actually equal to identity thanks to the side conditions (ii) of Definition 2.9. The composition $\iota_{M'M} \circ \iota_{MM'}$ is only homotopic to identity, with a homotopy of the form $H_M = H + HfH + HfHfH + \dots$. The details of this computation are left to the energetic reader. \square

Note that, even if M^* required no non-zero homotopies f_{ij}^* for $h_{\mathcal{C}}(j) - h_{\mathcal{C}}(i) \geq 2$, the equivalent $(M')^*$ will normally require such homotopies within its multicone structure.

We now specialize towards our goal of simplifying Khovanov complexes of tangles. Let \mathcal{C}^* represent any chain complex in Bar-Natan's category of planar diagrams and dotted cobordisms.

Definition 2.11. The notation

$$\mathcal{C}^* = \text{Multicone}_{\mathcal{Z}_i, \mathcal{Z}_j \in \mathcal{C}^*} \left(\widetilde{KC}^*(\mathcal{Z}_i) \xrightarrow{\phi_{i,j}^*} h^{\text{hc}^*(\mathcal{Z}_j) - \text{hc}^*(\mathcal{Z}_i) - 1} \widetilde{KC}^*(\mathcal{Z}_j) \right) \quad (7)$$

indicates that the complex \mathcal{C}^* is a multicone over various chain maps of complexes, where each individual complex is the Khovanov complex of a given tangle diagram \mathcal{Z}_i , and each $\phi_{i,j}$ is a dotted tangle cobordism (more generally, an R -linear combination of such cobordisms) from \mathcal{Z}_i to \mathcal{Z}_j that determines a chain map of dotted cobordisms $\phi_{i,j}^* : \widetilde{KC}^*(\mathcal{Z}_i) \rightarrow \widetilde{KC}^*(\mathcal{Z}_j)$. Often the tangles \mathcal{Z}_i will be genuine Temperley-Lieb diagrams δ_i with maps $\phi_{i,j} = 0$ for $h_{\mathcal{C}^*}(\delta_j) - h_{\mathcal{C}^*}(\delta_i) \geq 2$, so that we will see the simpler

$$\mathcal{C}^* = \text{Multicone}_{h_{\mathcal{C}^*}(\delta_j) - h_{\mathcal{C}^*}(\delta_i) = 1} \left(\widetilde{KC}^*(\delta_i) \xrightarrow{\phi_{i,j}^*} \widetilde{KC}^*(\delta_j) \right). \quad (8)$$

This will be the case when we are taking a known chain complex and choosing to view it as a multicone over its constituent Temperley-Lieb diagrams.

If we are not concerned with the maps within such a multicone of cobordism maps, we have the following version of Proposition 2.8.

Corollary 2.12. *Let \mathcal{X} be some tangle. Suppose \mathcal{C}^* is a complex of dotted cobordisms $\phi_{i,j}$ between Temperley-Lieb diagrams δ_i, δ_j where each δ_i can be concatenated with \mathcal{X} . Suppose for each i we have a tangle isotopy*

$$\rho_i : \begin{array}{c} \text{|||||} \\ \boxed{\mathcal{X}} \\ \hline \boxed{\delta_i} \\ \text{|||||} \end{array} \xrightarrow{\cong} \begin{array}{c} \text{|||||} \\ \boxed{\mathcal{X}'_i} \\ \text{|||||} \end{array}.$$

Then there exist maps $(\phi'_{i,j})^*$ fitting into a multicone structure so that

$$M^* := \text{Multicone}_{\substack{\text{h}_{\mathcal{C}^*}(\delta_j) - \text{h}_{\mathcal{C}^*}(\delta_i) = 1 \\ \delta_i, \delta_j \in \mathcal{C}^*}} \left(\begin{array}{c} \widetilde{KC}^* \left(\begin{array}{c} \text{|||||} \\ \boxed{\mathcal{X}} \\ \hline \boxed{\delta_i} \\ \text{|||||} \end{array} \right) \xrightarrow{\left(\begin{array}{c} \text{|||||} \\ \boxed{I_{\mathcal{X}}} \\ \hline \boxed{\phi_{i,j}} \\ \text{|||||} \end{array} \right)^*} \widetilde{KC}^* \left(\begin{array}{c} \text{|||||} \\ \boxed{\mathcal{X}} \\ \hline \boxed{\delta_j} \\ \text{|||||} \end{array} \right) \end{array} \right) \quad (9)$$

$$\simeq \text{Multicone}_{\delta_i, \delta_j \in \mathcal{C}^*} \left(\text{h}^{a_i} \text{q}^{b_i} \widetilde{KC}^* (\mathcal{X}'_i) \xrightarrow{(\phi'_{i,j})^*} \text{h}^{\text{h}_{\mathcal{C}^*}(\delta_j) - \text{h}_{\mathcal{C}^*}(\delta_i) - 1} \text{h}^{a_j} \text{q}^{b_j} \widetilde{KC}^* (\mathcal{X}'_j) \right)$$

where the shifts a_i, b_i, a_j, b_j are determined by applying Lemma 2.5 to the isotopies ρ_i and ρ_j .

Moreover, for the homological degree of any diagram ϵ coming from some $\widetilde{KC}^* (\mathcal{X}'_i)$ within the multicone M^* , we have

$$\text{h}_{M^*}(\epsilon) = \text{h}_{\widetilde{KC}^* (\mathcal{X}'_i)}(\epsilon) + \text{h}_{\mathcal{C}^*}(\delta_i) + a_i \quad (10)$$

and similarly for the q -degree.

Proof. If we use Equation 8 to write the known complex \mathcal{C}^* as a multicone, this is Proposition 2.8 applied to the current situation since the isotopies ρ_i produce chain homotopy equivalences of shifted renormalized Khovanov complexes. The diagram to have in mind is, for all $\delta_i, \delta_j \in \mathcal{C}$,

$$\begin{array}{ccc} \widetilde{KC}^* \left(\begin{array}{c} \text{|||||} \\ \boxed{\mathcal{X}} \\ \hline \boxed{\delta_i} \\ \text{|||||} \end{array} \right) & \xrightarrow{\left(\begin{array}{c} \text{|||||} \\ \boxed{I_{\mathcal{X}}} \\ \hline \boxed{\phi_{i,j}} \\ \text{|||||} \end{array} \right)^*} & \text{h}^{\text{h}_{\mathcal{C}}(\delta_j) - \text{h}_{\mathcal{C}}(\delta_i) - 1} \widetilde{KC}^* \left(\begin{array}{c} \text{|||||} \\ \boxed{\mathcal{X}} \\ \hline \boxed{\delta_j} \\ \text{|||||} \end{array} \right) \\ \downarrow \rho_i^* & & \downarrow \rho_j^* \\ \text{h}^{a_i} \text{q}^{b_i} \widetilde{KC}^* \left(\begin{array}{c} \text{|||||} \\ \boxed{\mathcal{X}'_i} \\ \text{|||||} \end{array} \right) & \xrightarrow{(\phi'_{i,j})^*} & \text{h}^{\text{h}_{\mathcal{C}}(\delta_j) - \text{h}_{\mathcal{C}}(\delta_i) - 1} \text{h}^{a_j} \text{q}^{b_j} \widetilde{KC}^* \left(\begin{array}{c} \text{|||||} \\ \boxed{\mathcal{X}'_j} \\ \text{|||||} \end{array} \right) \end{array}$$

□

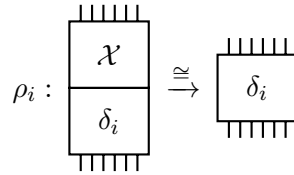
On the other hand, if we need to know something about the maps $(\phi'_{i,j})^*$, we will need a version of Proposition 2.10, and so we will need our maps to be very strong deformation retracts.

Lemma 2.13. *Suppose $\rho : \mathcal{Z} \rightarrow \mathcal{Z}'$ is a Reidemeister 1 or 2 move that eliminates crossings. Then the induced map ρ^* on the Khovanov complexes is a very strong deformation retract.*

Proof. This is easy to check using the definitions of the maps (given in Section 4 of [BN05]) and the fact that closed spheres evaluate to zero. Indeed, in that paper the fact that Reidemeister 2 moves are strong deformation retracts is remarked upon and utilized to prove invariance under Reidemeister 3 moves. \square

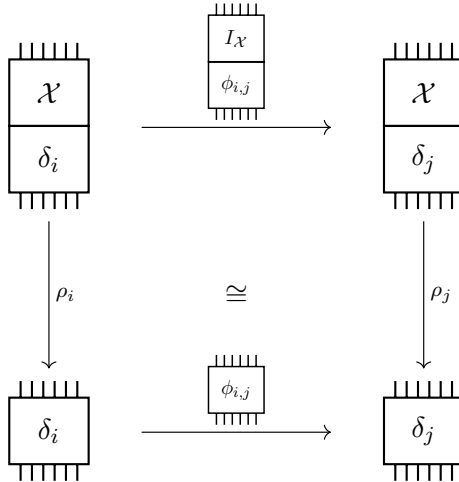
Although one could write down a general translation of Proposition 2.10 for various situations, we will only need the following corollary that describes the main case of interest in this paper.

Corollary 2.14. *Let \mathcal{X} be some tangle. Suppose \mathcal{C}^* is a complex of dotted cobordisms $\phi_{i,j}$ between Temperley-Lieb diagrams δ_i, δ_j where each δ_i can be concatenated with \mathcal{X} . Suppose for each $\delta_i \in \mathcal{C}^*$ we have a tangle isotopy*



consisting entirely of Reidemeister 1 and 2 moves that remove crossings, satisfying the following conditions.

- The grading shifts a_i, b_i for ρ_i^* (via applying Lemma 2.5) are equivalent for all i (that is, there exist constants a, b independent of i such that $a_i = a, b_i = b$ for all i).
- For each dotted cobordism $\phi_{i,j} : \delta_i \rightarrow \delta_j$, the compositions $\rho_j \circ (I_{\mathcal{X}} \cdot \phi_{i,j})$ and $\phi_{i,j} \circ \rho_i$ are isotopic as dotted tangle cobordisms in $B^3 \times [0, 1]$:



Then we have

$$M^* := \text{Multicone}_{\text{hc}^*(\delta_j) - \text{hc}^*(\delta_i) = 1} \left(\widetilde{KC}^* \left(\begin{array}{c} \text{|||||} \\ \mathcal{X} \\ \delta_i \\ \text{|||||} \end{array} \right) \xrightarrow{\left(\begin{array}{c} \text{|||||} \\ I_{\mathcal{X}} \\ \phi_{i,j} \\ \text{|||||} \end{array} \right)^*} \widetilde{KC}^* \left(\begin{array}{c} \text{|||||} \\ \mathcal{X} \\ \delta_j \\ \text{|||||} \end{array} \right) \right) \\ \simeq \text{Multicone}_{\text{hc}(\delta_j) - \text{hc}(\delta_i) = 1} \left(\text{h}^a \text{q}^b \widetilde{KC}^* (\delta_i) \xrightarrow{\pm \phi_{i,j}^*} \text{h}^a \text{q}^b \widetilde{KC}^* (\delta_j) \right).$$

If in addition the Reidemeister maps ρ_i^* can be given signs in a consistent manner to cancel with the \pm signs above, we actually have

$$M^* \simeq \text{h}^a \text{q}^b \mathcal{C}^*.$$

Proof. Lemma 2.13 tells us that all of our chain maps ρ_i^* are very strong deformation retracts, so that Proposition 2.10 ensures that the maps $(\phi'_{i,j})^*$ in the new multicone are originally defined as compositions

$$(\phi'_{i,j})^* := \rho_j^*(I_{\mathcal{X}} \cdot \phi_{i,j})^*(\rho_i^{-1})^*.$$

Maps involving larger compositions do not exist because the complexes $\text{h}^a \text{q}^b \widetilde{KC}^* (\delta_i)$ are all *single term* complexes, whereas the larger composition maps act as homotopies that need to reach lower homological gradings. Then the assumptions imply we have an isotopy of dotted cobordisms

$$\rho_j \circ (I_{\mathcal{X}} \cdot \phi_{i,j}) \circ \rho_i^{-1} \cong \phi_{i,j}$$

at which point we invoke the functoriality of Bar-Natan's constructions to conclude that we have a homotopy

$$(\phi'_{i,j})^* \sim \pm \phi_{i,j}^*.$$

Once again, since we are dealing with single term complexes, the homotopy is irrelevant and these maps must in fact be equal. Since (-1) is also a very strong deformation retract, we have the option to include signs with our maps ρ_i^* if necessary to cancel the \pm signs, assuming a consistent choice of such signs can be found. The proof is outlined by the commuting diagram of Figure 5. \square

In general, the majority of the theorems in this section are proved in a similar fashion. We take a given tangle \mathcal{Z} and view it as the concatenation of two tangles $\mathcal{Z} = \mathcal{X} \cdot \mathcal{Y}$ to analyze its renormalized Khovanov complex

$$\widetilde{KC}^*(\mathcal{Z}) = \widetilde{KC}^* \left(\begin{array}{c} \text{|||||} \\ \mathcal{X} \\ \mathcal{Y} \\ \text{|||||} \end{array} \right) = \begin{array}{c} \text{|||||} \\ \widetilde{KC}^*(\mathcal{X}) \\ \widetilde{KC}^*(\mathcal{Y}) \\ \text{|||||} \end{array}.$$

We then look to apply either Corollary 2.12 or 2.14 by treating the complex $\widetilde{KC}^*(\mathcal{Y})$ (or perhaps some simplification of it) as the required \mathcal{C}^* and finding tangle isotopies $\rho_i : \mathcal{X} \cdot \delta_i \xrightarrow{\cong} \mathcal{X}'_i$ for each

$\delta_i \in \mathcal{C}^*$. Under these conditions, Equation 9 becomes

$$\widetilde{KC}^*(\mathcal{Z}) \simeq \text{Multicone}_{\delta_i, \delta_j \in \mathcal{C}^*} \left(h^{a_i} q^{b_i} \widetilde{KC}^*(\mathcal{X}'_i) \xrightarrow{(\phi'_{i,j})^*} h^{\text{h}_{\mathcal{C}^*}(\delta_j) - \text{h}_{\mathcal{C}^*}(\delta_i) - 1} h^{a_j} q^{b_j} \widetilde{KC}^*(\mathcal{X}'_j) \right). \quad (11)$$

In some cases we will only be interested in the homological degrees of various diagrams in $\widetilde{KC}^*(\mathcal{Z})$ so that the maps $(\phi'_{i,j})^*$ will be irrelevant and we can use the relatively simple Corollary 2.12. In other cases we will actually want to claim that $\widetilde{KC}^*(\mathcal{Z})$ is chain homotopy equivalent to a shifted copy of $\widetilde{KC}^*(\mathcal{Y})$, which will require checking all of the various requirements of Corollary 2.14.

Remark 2.15. In [Roz], Rozansky does not make mention of the use of very strong deformation retracts, and instead collapses the tower of Figure 5 into two layers - the top and bottom only. In doing so, it is true that the resulting square can be arranged to commute up to homotopy, but this is not enough to guarantee the existence of a map from the top multicone to the bottom multicone. In addition, one needs these diagonal homotopies to commute with other ‘horizontal’ maps within the multicones up to higher homotopies, which then need to commute with further horizontal maps up to even higher homotopies, and so forth. Even then, it is not immediately clear what the homotopy inverse map should be. The multi-layer approach of Figure 5 avoids this problem by using very strong deformation retracts to build the equivalence between the first two layers (put another way, the top square commutes up to a very simplistic homotopy \tilde{H} which we can incorporate into both the vertical map and its inverse), while the lower layers all have one-term complexes where commuting up to homotopy is the same as commuting on the nose and the equivalence is clear.

2.3 A remark on dotted cobordisms

In [BN05] Bar-Natan asserts that the arguments for functoriality concerning undotted tangle cobordisms continue to hold for dotted tangle cobordisms. In rings where 2 is invertible, a dotted cobordism can be converted to an undotted cobordism with a coefficient of 2^{-1} and so the claim is obvious. Otherwise however, it is perhaps less clear to see precisely why this is the case. Here we present a quick argument to show why two isotopic dotted tangle cobordisms do indeed induce homotopic maps on Khovanov complexes, up to a sign. We begin with the following lemma which is well-known to experts.

Lemma 2.16. *The dotted identity cobordisms indicated below induce homotopic maps on Khovanov complexes up to a sign:*

$$\left(\begin{array}{c} \nearrow \\ \searrow \end{array} \right)^* \sim - \left(\begin{array}{c} \searrow \\ \nearrow \end{array} \right)^* \quad (12)$$

$$\left(\begin{array}{c} \searrow \\ \nearrow \end{array} \right)^* \sim - \left(\begin{array}{c} \nearrow \\ \searrow \end{array} \right)^*. \quad (13)$$

Proof. The homotopy is illustrated in the following diagram.

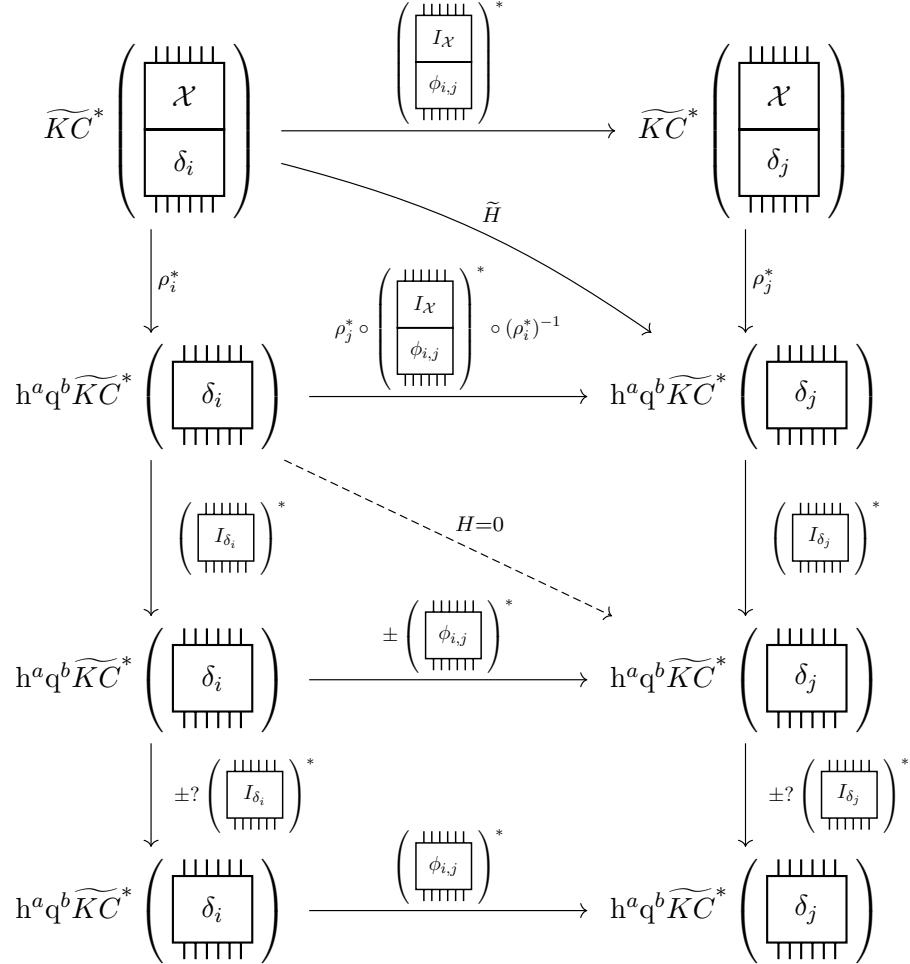
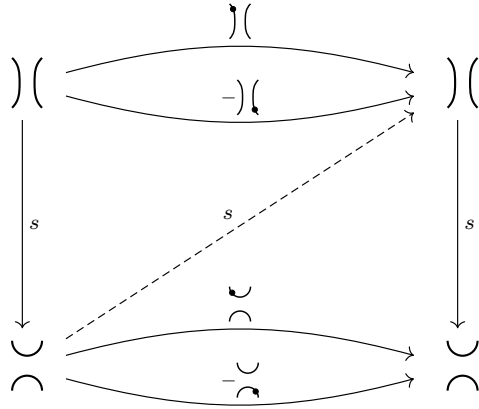


Figure 5: A diagram for Corollary 2.14. We envision a large system of these downward towers of maps, one for each pair of $\delta_i, \delta_j \in \mathcal{C}^*$ with $\mathrm{h}_{\mathcal{C}^*}(\delta_j) - \mathrm{h}_{\mathcal{C}^*}(\delta_i) = 1$. Because the terms $\widetilde{KC}^*(\delta_i)$ are one-term complexes, there is no need to account for higher degree maps. Similarly, although Bar-Natan's functoriality only guarantees that the top two squares commute up to some homotopies \widetilde{H} and H , the fact that our mid-layer complexes have only one term ensures that the central H is zero. The multicone of the top layer forms $\widetilde{KC}^*(\mathcal{Z})$, while the bottom layer forms a shifted copy of \mathcal{C}^* . If the various ρ maps involve only Reidemeister 1 and 2 simplifications (so the ρ^* maps are very strong deformation retracts), we can build an equivalence from the first layer down to the second layer. Since $H = 0$, we can continue to the third layer; however a further argument is needed to find a consistent choice of signs to reach the fourth and final layer.



The diagram shows the complex $\widetilde{KC}^*(\times)$ on the left and right, with the two chain maps $(\times)^*$ and $-(\times)^*$ drawn horizontally. The homotopy is drawn as a dashed line. The symbol s stands for the obvious saddle map, so that composing $s \circ s$ via the homotopy creates a tube that can be cut using the neck-cutting relation of [BN05]. The other homotopy is identical. \square

Proposition 2.17. *If ϕ_1 and ϕ_2 are two isotopic tangle cobordisms from tangle Z_1 to Z_2 in B^3 , then their induced chain maps $KC^*(Z_1) \rightarrow KC^*(Z_2)$ are homotopic up to a sign.*

Proof. An (un-dotted) tangle cobordism in $B^3 \times [0, 1]$ can be viewed as a ‘movie’ in B^3 , where $[0, 1]$ is tracking the time coordinate of the movie. Recall that any such movie can be decomposed into a sequence of elementary movies corresponding to Morse moves (saddle, birth, and death) and Reidemeister moves. If such cobordisms are isotopic, then their movies are linked via some sequence of so-called ‘movie moves’ (see Carter and Saito [CS98]), all of which are shown to produce homotopies between the corresponding cobordism maps up to a sign in [BN05].

For dotted tangle cobordisms, we must add one extra type of elementary movie: a single dotted identity cobordism. Then if two dotted tangle cobordisms are isotopic, their movies are linked by a sequence of movie moves as in [CS98] together with two new moves that correspond to sliding a dot along the cobordism in either the B^3 direction or the $[0, 1]$ direction. Sliding a dot in the B^3 direction clearly maintains the corresponding chain map, except possibly in the case where we move a dot past a crossing in our planar projection. This is precisely the case covered by Lemma 2.16.

Meanwhile, sliding a dot in the $[0, 1]$ direction gives rise to moves that swap the ordering of some elementary movie m with a dotted identity I_\bullet . With the help of Lemma 2.16, we can begin any such move by pushing the dot along the tangle in the B^3 direction until it is far from the portion of the tangle that is affected by m (all elementary movies are local in nature). Then the two orderings of movies $I_\bullet \circ m$ and $m \circ I_\bullet$ trivially must give the same cobordism map.

Finally, to ensure that these are all of the moves needed, we note that none of the movie moves of Carter-Saito involve a closed component of a cobordism, and thus there is never a need to consider a dot within one of their movie moves. The dot can always be slid to the beginning frame or ending frame (depending on which boundary the dotted component reaches) before performing the movie move. \square

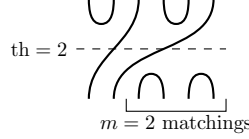


Figure 6: For this diagram δ with $n = 6$, $m = 2$ refers to the two matchings indicated (and of course, this implies that there are also $m = 2$ matchings on the top half of δ). Thus $\text{th}(\delta) = (6) - 2(2) = 2$.

Lemma 2.16 also leads to chain homotopy equivalences for standard mapping cones:

$$\text{Cone} \left(\widetilde{KC}^* (\times) \xrightarrow{\nearrow} \widetilde{KC}^* (\times) \right) \simeq \text{Cone} \left(\widetilde{KC}^* (\times) \xrightarrow{\nwarrow} \widetilde{KC}^* (\times) \right) \quad (14)$$

$$\text{Cone} \left(\widetilde{KC}^* (\times) \xrightarrow{\nearrow} \widetilde{KC}^* (\times) \right) \simeq \text{Cone} \left(\widetilde{KC}^* (\times) \xrightarrow{\nwarrow} \widetilde{KC}^* (\times) \right). \quad (15)$$

We will further analyze how this affects certain specific multicones in Section 6.

With Corollaries 2.12 and 2.14 at the ready, and Proposition 2.17 allowing us to make use of Bar-Natan's functoriality for our constructions, we can now turn towards proving Theorem 2.2 in earnest. Although much of the work from this point is equivalent to the similar arguments of Rozansky in [Roz], we present the proofs for completeness. The reader who is familiar with Rozansky's work may safely skim the remainder of this section.

2.4 A simplified complex for $KC^*(\mathcal{F}_n)$

The saddle map of Equation 2 increases homological grading, and so it appears likely that, for a tangle like \mathcal{F}_n made up entirely of right-handed crossings, higher homological gradings will correspond to diagrams with lower through-degrees. Of course, for any diagram $\delta \in KC^*(\mathcal{F}_n)$, the parity of $\text{th}(\delta)$ must match the parity of n . Compare the following theorem with Theorem 8.3 in [Roz].

Theorem 2.18. *For any $n \geq 1$, $\widetilde{KC}^*(\mathcal{F}_n)$ is chain homotopy equivalent to a complex $C^*(\mathcal{F}_n)$ where, for any $m \in \{0, 1, \dots, \lfloor \frac{n}{2} \rfloor\}$, diagrams $\delta \in C^*(\mathcal{F}_n)$ satisfy the following properties:*

1. *Diagrams $\delta \in C^*(\mathcal{F}_n)$ having through-degree $\text{th}(\delta) = n - 2m$ appear only in homological degrees $\text{h}(\delta) \leq 2m(n - m)$.*
2. *There exists at least one diagram $\delta \in C^*(\mathcal{F}_n)$ with through-degree $\text{th}(\delta) = n - 2m$ such that $\text{h}(\delta) = 2m(n - m)$.*
3. *No diagrams in $C^*(\mathcal{F}_n)$ contain disjoint circles.*

When n is even, the complex $C^*(\mathcal{F}_n)$ will form the 'base case' $C^*(1)$ required by Theorem 2.2 after some further shifts, but we refrain from that notation here since we will be inducting on n (including odd n). The symbol m in Theorem 2.18 refers to the number of *matchings* on either the top or bottom of the diagram δ . See Figure 6.

Although Theorem 2.18 can be strengthened to give relationships between $\text{th}(\delta)$ and $\text{q}(\delta)$ as well, we will not need those relationships here.

Before we can begin the proof, we need the following notations.

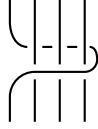


Figure 7: The right-handed Jucys-Murphy braid \mathcal{E}_n for $n = 4$.



Figure 8: The diagram δ of Figure 6 is decomposed as $\delta^{\text{top}} \cdot \iota_d \cdot \delta_{\text{bot}}$. Any Temperley-Lieb diagram can be decomposed in this way.

Definition 2.19. For any number of strands n , the symbol \mathcal{E}_n will denote the right-handed Jucys-Murphy element of the braid group pictured in Figure 7. In terms of the standard braid group generators, $\mathcal{E}_n := \sigma_1 \sigma_2 \cdots \sigma_{n-1} \sigma_{n-1} \cdots \sigma_2 \sigma_1$.

Note that \mathcal{E}_n has precisely $2(n - 1)$ crossings.

Definition 2.20. Let δ be a Temperley-Lieb diagram with through-degree $\text{th}(\delta) = d$. Any such diagram can be ‘pulled outward’ until it can be written as the vertical concatenation of three diagrams, which we denote as follows:

$$\delta = \delta^{\text{top}} \cdot \iota_d \cdot \delta_{\text{bot}}. \tag{16}$$

Here, ι_d is the vertical identity diagram on the d strands that pass from top to bottom of δ , contributing to the through-degree. Then δ^{top} and δ_{bot} refer to the upper and lower halves of δ that contain the upper and lower matchings. As long as δ has no disjoint circles, this decomposition is unique. See Figure 8 for clarification.

The most important aspect of these notations is the isotopy described by the following lemma.

Lemma 2.21. *For any n and any Temperley-Lieb diagram δ with $\text{th}(\delta) = d$, we have a braid isotopy*

$$\tag{17}$$

that uses only Reidemeister 2 moves which remove crossings.

Proof. See Figure 9, which illustrates the isotopy. This is one version of ‘cup sliding’ as it is referred to in [Roz]. If we always slide one ‘innermost’ cup at a time, only Reidemeister 2 simplifications are used. \square

presentation

$$\widetilde{KC}^*(\mathcal{F}_{n+1}) \simeq \text{Multicone}_{\delta_i, \delta_j \in C^*(\mathcal{F}_n)} \left(h^{a_i} q^{b_i} \widetilde{KC}^* \left(\mathcal{E}_{\delta_i}^{\delta_i} \right) \xrightarrow{(\phi'_{i,j})^*} h^{\text{h}_{C^*(\mathcal{F}_n)}(\delta_j) - \text{h}_{C^*(\mathcal{F}_n)}(\delta_i) - 1} h^{a_j} q^{b_j} \widetilde{KC}^* \left(\mathcal{E}_{\delta_j}^{\delta_j} \right) \right).$$

Here, if we want to estimate the homological degree of any diagram ϵ_i coming from some fixed $h^{a_i} q^{b_i} \widetilde{KC}^*(\mathcal{E}_{\delta_i}^{\delta_i})$ within the multicone, we will need to consider the three quantities (see Equation 10)

$$a_i, \quad \text{h}_{C^*(\mathcal{F}_n)}(\delta_i), \quad \text{h}_{\widetilde{KC}^*}(\mathcal{E}_{\delta_i}^{\delta_i})(\epsilon_i).$$

The homological shift a_i can be computed using Lemma 2.5 as applied to the isotopies ρ_i . As noted in the proof of Lemma 2.21, we use only Reidemeister 2 moves during the isotopy ρ_i , two for each matching. Each such move eliminates a pair of crossings, one positive and one negative, regardless of orientations of strands. Thus we eliminate precisely $2m_i$ negative crossings, and we have

$$a_i = 2m_i. \quad (18)$$

The induction hypothesis provides a homological bound for diagrams in $C^*(\mathcal{F}_n)$, giving

$$\text{h}_{C^*(\mathcal{F}_n)}(\delta_i) \leq 2m_i(n - m_i). \quad (19)$$

Finally, we consider diagrams in the complex $\widetilde{KC}^* \left(\mathcal{E}_{\delta_i}^{\delta_i} \right)$. The diagrams δ_i^{top} and δ_i^{bot} have no crossings, while \mathcal{E}_{n+1-2m_i} has precisely $2(n - 2m_i)$ crossings. The all-zero resolution of these crossings contributes a diagram $\epsilon_{i,0}$ with

$$\text{h}_{\widetilde{KC}^*}(\mathcal{E}_{\delta_i}^{\delta_i})(\epsilon_{i,0}) = 0, \quad \text{th}(\epsilon_{i,0}) = n + 1 - 2m_i \quad (20)$$

while the other resolutions contribute diagrams ϵ_i satisfying

$$\text{h}_{\widetilde{KC}^*}(\mathcal{E}_{\delta_i}^{\delta_i})(\epsilon_i) \leq 2(n - 2m_i), \quad \text{th}(\epsilon_i) = n + 1 - 2m \quad (21)$$

for some $m > m_i$.

Now to prove the theorem, we turn our arguments around and fix some $m \in \{0, 1, \dots, \lfloor \frac{n+1}{2} \rfloor\}$. Let $\hat{C}^*(\mathcal{F}_{n+1})$ denote the multicone

$$\hat{C}^*(\mathcal{F}_{n+1}) := \text{Multicone}_{\delta_i, \delta_j \in C^*(\mathcal{F}_n)} \left(h^{a_i} q^{b_i} \widetilde{KC}^* \left(\mathcal{E}_{\delta_i}^{\delta_i} \right) \xrightarrow{(\phi'_{i,j})^*} h^{\text{h}_{C^*(\mathcal{F}_n)}(\delta_j) - \text{h}_{C^*(\mathcal{F}_n)}(\delta_i) - 1} h^{a_j} q^{b_j} \widetilde{KC}^* \left(\mathcal{E}_{\delta_j}^{\delta_j} \right) \right).$$

Suppose that $\epsilon \in \hat{C}^*(\mathcal{F}_{n+1})$ with $\text{th}(\epsilon) = n + 1 - 2m$. By Equations 20 and 21, we see that ϵ must come from some complex $\widetilde{KC}^* \left(\mathcal{E}_{\delta_i}^{\delta_i} \right)$ with $\text{th}(\delta_i) = m_i \leq m$. In the case of equality $m_i = m$, Equations 18, 19, and 20 combine to give us the estimate

$$\begin{aligned} \text{h}_{\hat{C}^*(\mathcal{F}_{n+1})}(\epsilon) &= a_i + \text{h}_{C^*(\mathcal{F}_n)}(\delta_i) + \text{h}_{\widetilde{KC}^*}(\mathcal{E}_{\delta_i}^{\delta_i})(\epsilon) \\ &\leq 2m_i + 2m_i(n - m_i) + 0 \\ &= 2m(n + 1 - m). \end{aligned}$$

In the case $m_i < m$, we use Equation 21 in place of Equation 20, but the rest remains the same:

$$\begin{aligned}
h_{\hat{C}^*(\mathcal{F}_{n+1})}(\epsilon) &= a_i + h_{C^*(\mathcal{F}_n)}(\delta_i) + h_{\widetilde{KC}^*}(\mathcal{E}_{\delta_i}^{\delta_i})(\epsilon) \\
&\leq 2m_i + 2m_i(n - m_i) + 2(n - 2m_i) \\
&= 2(m_i + 1)(n + 1 - (m_i + 1)) \\
&\leq 2m(n + 1 - m)
\end{aligned}$$

where the final inequality uses the fact that $2x(n+1-x)$ is an increasing function of x for $x \in [0, \lfloor \frac{n}{2} \rfloor]$ together with the fact that $m_i < m$ (and so in particular $m_i + 1 \leq m$). Together, these two bounds show that the first condition of Theorem 2.18 is satisfied by $\hat{C}^*(\mathcal{F}_{n+1})$.

In order to find some diagram ϵ that satisfies the second condition of the theorem, we split into two cases. As long as we are not in the case of odd n with $m = \frac{n+1}{2}$, we can use the inductive assumption to find a diagram $\delta_i \in C^*(\mathcal{F}_n)$ with $\text{th}(\delta_i) = n - 2m$ and $h(\delta_i) = 2m(n - m)$ for our desired m . We then consider the diagram $\epsilon_{i,0}$ of Equation 20 for this choice of $\mathcal{E}_{\delta_i}^{\delta_i}$ with

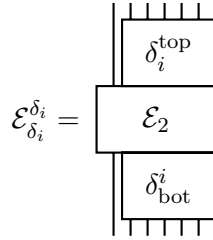
$$\text{th}(\epsilon_{i,0}) = n + 1 - 2m,$$

$$\begin{aligned}
h_{\hat{C}^*(\mathcal{F}_{n+1})}(\epsilon_{i,0}) &= 2m + 2m(n - m) + 0 \\
&= 2m(n + 1 - m)
\end{aligned}$$

as desired.

Finally, we consider the second condition of the theorem where n is odd and $m = \frac{n+1}{2}$. That is, we would like to find a diagram $\epsilon \in C^*(\mathcal{F}_{n+1})$ with $\text{th}(\epsilon) = 0$ and $h(\epsilon) = (n + 1) \left(\frac{n+1}{2} \right)$.

By the inductive assumption there exists some $\delta_i \in C^*(\mathcal{F}_n)$ with $m_i = \frac{n-1}{2}$ matchings, having $\text{th}(\delta_i) = 1$ and $h(\delta_i) = (n - 1) \left(\frac{n-1}{2} \right)$ (ie a term in $C^*(\mathcal{F}_n)$ of maximal homological degree and minimal through-degree). From this δ_i we arrive at a diagram $\mathcal{E}_{\delta_i}^{\delta_i}$ of the form



and it is well-known that $\mathcal{E}_2 = \mathcal{F}_2$ has a Khovanov complex having diagrams with through-degree zero in homological degrees one and two. The homological degree 2 term here contributes the required diagram $\epsilon \in \hat{C}^*(\mathcal{F}_{n+1})$, since it would have

$$h_{\hat{C}^*(\mathcal{F}_{n+1})}(\epsilon) = \left((n - 1) \left(\frac{n + 1}{2} \right) \right) + \left(2 \left(\frac{n - 1}{2} \right) \right) + (2) = (n + 1) \left(\frac{n + 1}{2} \right)$$

as desired.

This indicates that our multicone $\hat{C}^*(\mathcal{F}_{n+1})$ has the first two desired properties, and is chain homotopy equivalent to $\widetilde{KC}^*(\mathcal{F}_{n+1})$. Finally we can use Bar-Natan's local 'delooping' relations [BN07] to remove any disjoint circles from any of the diagrams in $\hat{C}^*(\mathcal{F}_{n+1})$ without altering homological gradings, arriving at our desired complex $C^*(\mathcal{F}_{n+1})$ and so we are done. \square

Corollary 2.22. *For even $n = 2p$, $C^*(\mathcal{F}_n)$ has its two maximal non-empty homological gradings $2p^2 - 1$ and $2p^2$ containing only diagrams δ with $\text{th}(\delta) = 0$.*

Proof. Note that the homological bound $2m(n - m)$ is an increasing function of $m \in \{0, 1, \dots, p\}$ (or equivalently, a decreasing function of through-degree).

$$\begin{aligned} \text{th}(\delta) = 0 = n - 2p &\implies \text{h}(\delta) \leq 2p(n - p) = 2p^2 \\ \text{th}(\delta) = 2 = n - 2(p - 1) &\implies \text{h}(\delta) \leq 2(p - 1)(n - p + 1) = 2p^2 - 2 \\ \text{th}(\delta) > 2 &\implies \text{h}(\delta) < 2p^2 - 2 \end{aligned}$$

□

2.5 Equivalence of $KC^*(\mathcal{F}_n^k)$ and $KC^*(\mathcal{F}_n^{k+1})$ in high homological degree for even n

Throughout this subsection (and indeed for the majority of the rest of this manuscript) we will focus on even $n = 2p$. In Section 2.4 we defined a complex $C^*(\mathcal{F}_n)$ which will play the role of $C^*(1)$ in Theorem 2.2. Corollary 2.22 shows how the top two degrees of $C^*(\mathcal{F}_n)$, which will play the role of $C^*_{>-2}(1)$, have special properties. Our goal in this section is to define complexes $C^*(\mathcal{F}_n^k)$ inductively to play the role of $C^*(k)$. The inductive definition will be tailored to allow for the inclusion of truncations demanded by Theorem 2.2.

Theorem 2.23. *Fix $n = 2p$. Then for all $k \in \mathbb{N}$ there exists a complex $C^*(\mathcal{F}_n^k)$ satisfying the following properties for each fixed k .*

(i) *We have a chain homotopy equivalence*

$$C^*(\mathcal{F}_n^k) \simeq \widetilde{KC}^*(\mathcal{F}_n^k).$$

(ii) *The shifted, truncated complex $\text{h}^{-2kp^2} \mathfrak{q}^{-2kp(p+1)} C^*_{>-2k}(\mathcal{F}_n^k)$ is comprised of diagrams δ having no disjoint circles, and satisfying $\text{h}(\delta) \leq 0$, $\text{th}(\delta) = 0$.*

(iii) *We have an equality of shifted, truncated complexes*

$$\text{h}^{-2kp^2} \mathfrak{q}^{-2kp(p+1)} C^*_{>-2k}(\mathcal{F}_n^k) = \text{h}^{-2(k+1)p^2} \mathfrak{q}^{-2(k+1)p(p+1)} C^*_{>-2k}(\mathcal{F}_n^{k+1}). \quad (22)$$

In other words, the top $2k$ degrees of $C^(\mathcal{F}_n^k)$ are precisely the same as the top $2k$ degrees of $C^*(\mathcal{F}_n^{k+1})$ (with a q -degree shift).*

We will prove Theorem 2.23 using a combination of Corollary 2.12 and Corollary 2.14. We begin with a simple lemma for presenting the necessary Reidemeister maps ρ related to concatenating with a full twist \mathcal{F}_n , together with their homological shifts.

Lemma 2.24. *If δ is a Temperley-Lieb diagram with m matchings, so that $\text{th}(\delta) = n - 2m$ and $\delta = \delta^{\text{top}} \cdot \iota_{n-2m} \cdot \delta_{\text{bot}}$ (as in Definition 2.20), we have*

$$\widetilde{KC}^* \left(\begin{array}{c} \text{|||||} \\ \mathcal{F}_n \\ \hline \delta \\ \text{|||||} \end{array} \right) \simeq \text{h}^{2m(n-m)} \mathfrak{q}^{2m(n+1-m)} \widetilde{KC}^* \left(\begin{array}{c} \text{|||||} \\ \delta^{\text{top}} \\ \hline \mathcal{F}_{n-2m} \\ \hline \delta_{\text{bot}} \\ \text{|||||} \end{array} \right) \quad (23)$$

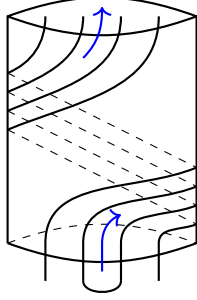


Figure 10: A matching can always be pulled through a full twist, as illustrated above. Each matching in δ can be pulled through in this way, ending up in precisely the same spot above \mathcal{F}_n as it was below it, but removing 2 strands from \mathcal{F}_n .

via a tangle isotopy utilizing only Reidemeister 1 and 2 moves which remove crossings.

Proof. We pull each ‘innermost’ matching of δ^{top} up through the full twist as shown in Figure 10 one at a time. Each such pull removes 2 strands from \mathcal{F}_n utilizing only Reidemeister 1 and 2 simplifications, so that we are left with \mathcal{F}_{n-2m} . To compute the grading shifts, we count positive and negative crossings. \mathcal{F}_n had $n(n-1)$ crossings, while \mathcal{F}_{n-2m} has $(n-2m)(n-2m-1)$ crossings, so we eliminated a total of $4m(n-m) - 2m$ crossings. Each matching pull removes precisely 2 crossings that are between the matched strands, which must be negative crossings (regardless of orientation). This means $2m$ of the eliminated crossings were negative. The other $4m(n-m-1)$ crossings occurred between unmatched strands, and thus must have occurred in positive and negative pairs (again regardless of orientation), and so we have removed $2m(n-m-1)$ positive crossings and $2m(n-m)$ negative crossings. Lemma 2.5 can then be used to complete the computation. \square

Our next construction is designed to allow for the full use of Corollary 2.14 by assigning signs to Reidemeister maps ρ_i coming from Lemma 2.24 in the case where $\text{th}(\delta_i) = 0$. This portion of the argument is based on Rozansky’s discussion on ‘quasi-trivial’ tangles (Section 7.3 in [Roz]), where the full twist is considered quasi-trivial without proof (the same claim is made for the Jucys-Murphy braid - see Remark 3.13). We will provide this proof for the full twist below (but will circumvent the corresponding claim for the Jucys-Murphy braid in Section 3.3).

Following [Roz], we begin by fixing a ‘closure’ diagram for our n strands

$$\gamma := \cap \cap \cdots \cap.$$

This allows us a consistent Reidemeister map

$$\rho_\gamma : \begin{array}{c} \boxed{\gamma} \\ \boxed{\mathcal{F}_n} \\ \text{|||||} \end{array} \xrightarrow{\cong} \begin{array}{c} \boxed{\gamma} \\ \text{|||||} \end{array}$$

via a reflection of the isotopy in Figure 10. This in turn gives us, for any δ_i with $\text{th}(\delta_i) = 0$, a pair of Reidemeister maps

(24)

Lemma 2.25. *The two maps of Equation 24 are isotopic as cobordisms embedded in $B^3 \times [0, 1]$ (ie the full twist is quasi-trivial in the language of [Roz]).*

Proof. We have the obvious isotopy

and it is clear in $B^3 \times [0, 1]$ that

$$\begin{array}{c} \rho_\gamma \circ \rho_\gamma^{-1} \\ \hline I_{\delta_i} \end{array} \circ \begin{array}{c} I_\gamma \\ \hline \rho_i \end{array} \cong \begin{array}{c} \rho_\gamma \\ \hline I_{\delta_i} \end{array} \circ \begin{array}{c} \rho_\gamma^{-1} \\ \hline \rho_i \end{array} .$$

Let $\rho_{2\pi}$ denote the cobordism $\rho_\gamma^{-1} \cdot \rho_i$, which is isotopic to rotating the disjoint link $\gamma \cdot \mathcal{F}_n \cdot \delta_i^{\text{top}}$ by a full 2π radians. The key point is to notice that the link $\gamma \cdot \mathcal{F}_n \cdot \delta_i^{\text{top}}$ is actually the *unlink* and so bounds disjoint discs that are maintained throughout the rotation $\rho_{2\pi}$. Thus $\rho_{2\pi}$ is isotopic to a cobordism that shrinks each component of $\gamma \cdot \mathcal{F}_n \cdot \delta_i^{\text{top}}$ to a small circle (roughly a point in B^3) before rotating and then expanding back to $\gamma \cdot \mathcal{F}_n \cdot \delta_i^{\text{top}}$, which is isotopic to identity since any two 1-dimensional cobordisms in $B^3 \times [0, 1]$ (with the same boundary and no closed components) are isotopic by dimension arguments. Thus $\rho_{2\pi} = \rho_\gamma^{-1} \cdot \rho_i \cong I$ and we are done. \square

With Lemma 2.25 in hand, the functoriality of Bar-Natan's construction tells us that the link cobordisms in Equation 24 must induce chain maps that are homotopic up to a sign which we will denote by σ_i . The reader can then verify that the following diagram is entirely commutative up to homotopy, with compositions homotopic to identity:

$$\begin{array}{ccc}
& & \sigma_i \left(\left(\begin{array}{c} I_\gamma \\ \rho_i \\ \text{|||||} \end{array} \right)^* \right)^{-1} \\
& & \swarrow \quad \searrow \\
\widetilde{KC}^* \left(\begin{array}{c} \gamma \\ \mathcal{F}_n \\ \delta_i \\ \text{|||||} \end{array} \right) & \begin{array}{c} \xrightarrow{\sigma_i \left(\begin{array}{c} I_\gamma \\ \rho_i \\ \text{|||||} \end{array} \right)^*} \\ \xrightarrow{\left(\begin{array}{c} \rho_\gamma \\ I_{\delta_i} \\ \text{|||||} \end{array} \right)^*} \\ \xleftarrow{\left(\begin{array}{c} \rho_\gamma \\ I_{\delta_i} \\ \text{|||||} \end{array} \right)^*} \\ \xleftarrow{\sigma_i \left(\begin{array}{c} I_\gamma \\ \rho_i \\ \text{|||||} \end{array} \right)^*} \end{array} & \widetilde{KC}^* \left(\begin{array}{c} \gamma \\ \delta_i \\ \text{|||||} \end{array} \right) \\
& & \left(\left(\begin{array}{c} \rho_\gamma \\ I_{\delta_i} \\ \text{|||||} \end{array} \right)^* \right)^{-1}
\end{array} \quad (25)$$

Lemma 2.26. Fix $n = 2p$. If \mathcal{C}^* is a chain complex made entirely of dotted cobordisms $\phi_{i,j}$ between diagrams δ_i, δ_j all having through-degree zero and having no disjoint circles, then

$$\text{Multicone}_{\text{h}_{\mathcal{C}^*}(\delta_j) - \text{h}_{\mathcal{C}^*}(\delta_i) = 1} \left(\widetilde{KC}^* \left(\begin{array}{c} \mathcal{F}_n \\ \delta_i \\ \text{|||||} \end{array} \right) \xrightarrow{\left(\begin{array}{c} I_{\mathcal{F}_n} \\ \phi_{i,j} \\ \text{|||||} \end{array} \right)^*} \widetilde{KC}^* \left(\begin{array}{c} \mathcal{F}_n \\ \delta_j \\ \text{|||||} \end{array} \right) \right) \simeq \text{h}^{2p^2} \text{q}^{2p(p+1)} \mathcal{C}^* \quad (26)$$

Proof. The braid isotopies of Lemma 2.24 provide the maps $\rho_i : \mathcal{F}_n \cdot \delta_i \xrightarrow{\cong} \delta_i$ which utilize only Reidemeister 1 and 2 simplifications, as required by Corollary 2.14. Since the δ_i, δ_j both have no disjoint circles, there is a consistent gap between their top and bottom matchings respected by the dotted cobordism $\phi_{i,j}$ allowing us to conclude that the tangle cobordisms $\rho_i, \rho_j, \phi_{i,j}$ commute up to isotopy, satisfying the second requirement of Corollary 2.14. The reader can quickly check that the grading shifts are precisely as indicated (note $\text{th}(\delta_i) = 0 \Rightarrow m_i = p$). We claim that the signs σ_i defined with the help of γ above provide the necessary consistency allowing us to collapse the bottom two layers of Figure 5 into the following single commuting diagram for all $\delta_i, \delta_j \in \mathcal{C}^*$:

$$\begin{array}{ccc}
\mathrm{h}^a \mathrm{q}^b \widetilde{KC}^* \left(\begin{array}{|c|} \hline \delta_i \\ \hline \end{array} \right) & \xrightarrow{\rho_j^* \circ \left(\begin{array}{|c|} \hline I_{\mathcal{F}_n} \\ \hline \phi_{i,j} \\ \hline \end{array} \right)^* \circ (\rho_i^*)^{-1}} & \mathrm{h}^a \mathrm{q}^b \widetilde{KC}^* \left(\begin{array}{|c|} \hline \delta_j \\ \hline \end{array} \right) \\
\downarrow \sigma_i \left(\begin{array}{|c|} \hline I_{\delta_i} \\ \hline \end{array} \right)^* & \dashrightarrow^{H=0} & \downarrow \sigma_j \left(\begin{array}{|c|} \hline I_{\delta_j} \\ \hline \end{array} \right)^* \\
\mathrm{h}^a \mathrm{q}^b \widetilde{KC}^* \left(\begin{array}{|c|} \hline \delta_i \\ \hline \end{array} \right) & \xrightarrow{\left(\begin{array}{|c|} \hline \phi_{i,j} \\ \hline \end{array} \right)^*} & \mathrm{h}^a \mathrm{q}^b \widetilde{KC}^* \left(\begin{array}{|c|} \hline \delta_j \\ \hline \end{array} \right)
\end{array} . \quad (27)$$

To prove that the maps of Equation 27 are indeed homotopic (and thus commute), we consider closing all of the diagrams present with our fixed closure γ (now omitting the trivial homotopy H):

$$\begin{array}{ccc}
\mathrm{h}^a \mathrm{q}^b \widetilde{KC}^* \left(\begin{array}{|c|} \hline \gamma \\ \hline \delta_i \\ \hline \end{array} \right) & \xrightarrow{\left(\begin{array}{|c|} \hline I_{\gamma} \\ \hline \rho_j \end{array} \right)^* \circ \left(\begin{array}{|c|} \hline I_{\mathcal{F}_n} \\ \hline \phi_{i,j} \\ \hline \end{array} \right)^* \circ \left(\left(\begin{array}{|c|} \hline I_{\gamma} \\ \hline \rho_i \end{array} \right)^* \right)^{-1}} & \mathrm{h}^a \mathrm{q}^b \widetilde{KC}^* \left(\begin{array}{|c|} \hline \gamma \\ \hline \delta_j \\ \hline \end{array} \right) \\
\downarrow \sigma_i \left(\begin{array}{|c|} \hline I_{\gamma} \\ \hline I_{\delta_i} \\ \hline \end{array} \right)^* & & \downarrow \sigma_j \left(\begin{array}{|c|} \hline I_{\gamma} \\ \hline I_{\delta_j} \\ \hline \end{array} \right)^* \\
\mathrm{h}^a \mathrm{q}^b \widetilde{KC}^* \left(\begin{array}{|c|} \hline \gamma \\ \hline \delta_i \\ \hline \end{array} \right) & \xrightarrow{\left(\begin{array}{|c|} \hline I_{\gamma} \\ \hline \phi_{i,j} \\ \hline \end{array} \right)^*} & \mathrm{h}^a \mathrm{q}^b \widetilde{KC}^* \left(\begin{array}{|c|} \hline \gamma \\ \hline \delta_j \\ \hline \end{array} \right)
\end{array} . \quad (28)$$

We claim that the commutativity of the maps in Equation 28 implies the same in Equation 27. Indeed since any planar cobordism $\phi_{i,j}$ can be decomposed into a sequence of saddles and single-dotted identity cobordisms, it is enough to note that both of these types of maps remain non-zero after ‘closing’ with I_{γ} . Thus any sign discrepancy in the commutativity of Equation 27 would persist in Equation 28, and so it is enough to show that the maps in Equation 28 commute.

If we allow a slight abuse of notation whereby we omit the presence of concatenated identity cobordisms, we utilize the homotopies of Equation 25 to see

$$\sigma_j(\rho_j)^*(\phi_{i,j})^*((\rho_i)^*)^{-1} \simeq \sigma_i(\rho_{\gamma})^*(\phi_{i,j})^*((\rho_{\gamma})^*)^{-1}.$$

Now we use the fact that, since $\phi_{i,j}$ and ρ_{γ} are tangle isotopies affecting disjoint parts of the planar diagrams involved ($\phi_{i,j}$ turns δ_i into δ_j , while ρ_{γ} untwists $\gamma \cdot \mathcal{F}_n$), $\phi_{i,j}^*$ and ρ_{γ}^* commute with no

sign issue and thus

$$\sigma_i(\rho_\gamma)^*(\phi_{i,j})^*((\rho_\gamma)^*)^{-1} \simeq \sigma_i(\phi_{i,j})^*(\rho_\gamma)^*((\rho_\gamma)^*)^{-1} \simeq \sigma_i\phi_{i,j}^*.$$

As in the proof of Corollary 2.14, the fact that these are all one-term complexes means that all of these chain homotopies are actually equalities, and so the maps of Equation 28 commute as desired. All of this was true for any δ_i, δ_j having $\text{th}(\delta_i) = \text{th}(\delta_j) = 0$, and so we are done. \square

Having Lemmas 2.24 and 2.26 at our disposal, we can turn to the proof of Theorem 2.23. The strategy is to induct on k as follows. We view \mathcal{F}_n^{k+1} as the concatenation $\mathcal{F}_n \cdot \mathcal{F}_n^k$ to view $\widetilde{KC}^*(\mathcal{F}_n^{k+1})$ as a multicone over the complex $C^*(\mathcal{F}_n^k)$. We then use Corollary 2.12 to further simplify this multicone, resulting in our desired complex $C^*(\mathcal{F}_n^{k+1})$. The homological degree formulas of Equation 10 will allow us to conclude that the top $2k$ degrees of $C^*(\mathcal{F}_n^{k+1})$ are determined by the top $2k$ degrees of $C^*(\mathcal{F}_n^k)$ alone, which are inductively guaranteed to fit the requirements of the complex \mathcal{C}^* in Lemma 2.26.

Proof of Theorem 2.23. We define the complex $C^*(\mathcal{F}_n^k)$ inductively. The base case of $k = 1$ is already defined in Theorem 2.18. Viewing \mathcal{F}_n^{k+1} as the concatenation $\mathcal{F}_n \cdot \mathcal{F}_n^k$, we inductively simplify $\widetilde{KC}^*(\mathcal{F}_n^{k+1})$ into $C^*(\mathcal{F}_n^k)$, which plays the role of \mathcal{C}^* from the statement of Corollary 2.12:

$$\widetilde{KC}^*(\mathcal{F}_n^{k+1}) \simeq \text{Multicone}_{h_{C^*(\mathcal{F}_n^k)}(\delta_j) - h_{C^*(\mathcal{F}_n^k)}(\delta_i) = 1} \left(\widetilde{KC}^* \left(\begin{array}{c} \text{|||||} \\ \mathcal{F}_n \\ \text{|||||} \\ \delta_i \\ \text{|||||} \end{array} \right) \xrightarrow{\left(\begin{array}{c} \text{|||||} \\ I_{\mathcal{F}_n} \\ \phi_{i,j} \\ \text{|||||} \end{array} \right)^*} \widetilde{KC}^* \left(\begin{array}{c} \text{|||||} \\ \mathcal{F}_n \\ \text{|||||} \\ \delta_j \\ \text{|||||} \end{array} \right) \right). \quad (29)$$

The isotopies $\rho_i : (\mathcal{F}_n \cdot \delta_i) \xrightarrow{\cong} (\mathcal{X}'_i)$ are provided by Lemma 2.24 and so Corollary 2.12 gives

$$\widetilde{KC}^*(\mathcal{F}_n^{k+1}) \simeq \text{Multicone}_{\delta_i, \delta_j \in C^*(\mathcal{F}_n^k)} \left(h^{a_i} q^{b_i} \widetilde{KC}^* \left(\begin{array}{c} \text{|||||} \\ \delta_i^{\text{top}} \\ \mathcal{F}_{n-2m_i} \\ \delta_i^{\text{bot}} \\ \text{|||||} \end{array} \right) \xrightarrow{(\phi'_{i,j})^*} h^{a_j} q^{b_j} \widetilde{KC}^* \left(\begin{array}{c} \text{|||||} \\ \delta_j^{\text{top}} \\ \mathcal{F}_{n-2m_j} \\ \delta_j^{\text{bot}} \\ \text{|||||} \end{array} \right) \right)$$

where the shifts a_i, b_i, a_j, b_j can be computed from Lemma 2.24 depending on m_i, m_j . We now utilize Theorem 2.18, which tells us that $\widetilde{KC}^*(\mathcal{F}_{n-2m_i}) \simeq C^*(\mathcal{F}_{n-2m_i})$, to simplify our multicone further. The resulting complex is our definition for $C^*(\mathcal{F}_n^{k+1})$ which satisfies item (i) of Theorem 2.23 by construction. If we allow a slight abuse of notation, the general statement of Proposition

2.8 allows us to write $C^*(\mathcal{F}_n^{k+1})$ as

$$\widetilde{KC}^*(\mathcal{F}_n^{k+1}) \simeq C^*(\mathcal{F}_n^{k+1}) :=$$

$$\text{Multicone}_{\delta_i, \delta_j \in C^*(\mathcal{F}_n^k)} \left(h^{a_i} q^{b_i} \left(\begin{array}{c} \delta_i^{\text{top}} \\ C^*(\mathcal{F}_{n-2m_i}) \\ \delta_{\text{bot}}^i \end{array} \right) \xrightarrow{(\phi''_{i,j})^*} h^{\text{h}_{C^*(\mathcal{F}_n^k)}(\delta_j) - \text{h}_{C^*(\mathcal{F}_n^k)}(\delta_i) - 1} h^{a_j} q^{b_j} \left(\begin{array}{c} \delta_j^{\text{top}} \\ C^*(\mathcal{F}_{n-2m_j}) \\ \delta_{\text{bot}}^j \end{array} \right) \right)$$

where we have written $\phi''_{i,j}$ to indicate that our maps $\phi'_{i,j}$ may have changed yet again while utilizing the homotopy equivalences $\widetilde{KC}^*(\mathcal{F}_{n-2m_i}) \simeq C^*(\mathcal{F}_{n-2m_i})$.

Now we investigate the homological grading in this multicone. Since δ_i^{top} and δ_{bot}^i have no crossings, any diagram $\epsilon \in C^*(\mathcal{F}_n^{k+1})$ coming from $\delta_i \in C^*(\mathcal{F}_n^k)$ with $\text{th}(\delta_i) = m_i$ can actually be viewed as coming from the corresponding $C^*(\mathcal{F}_{n-2m_i})$ in the simplified multicone. In this way the homological degree of such an ϵ can be computed (with the help of Lemma 2.24) as

$$\text{h}_{C^*(\mathcal{F}_n^{k+1})}(\epsilon) = \text{h}_{C^*(\mathcal{F}_{n-2m_i})}(\epsilon) + \text{h}_{C^*(\mathcal{F}_n^k)}(\delta_i) + 2m_i(n - m_i).$$

Theorem 2.18 tells us that such an ϵ must be a diagram with $\text{th}(\epsilon) = (n - 2m_i) - 2\ell$ for some number of ‘new’ matchings ℓ , and with homological degree

$$\text{h}_{C^*(\mathcal{F}_{n-2m_i})}(\epsilon) \leq 2\ell((n - 2m_i) - \ell)$$

which quickly yields the inequality

$$\text{h}_{C^*(\mathcal{F}_n^{k+1})}(\epsilon) \leq \text{h}_{C^*(\mathcal{F}_n^k)}(\delta_i) + 2(m_i + \ell)(2p - (m_i + \ell)). \quad (30)$$

We first show that $C^*(\mathcal{F}_n^{k+1})$ satisfies item (ii) of the statement of the theorem. Taking the shifts into account, this is equivalent to showing that $\text{h}_{C^*(\mathcal{F}_n^{k+1})}(\epsilon) \leq 2(k+1)p^2$ and that $\text{th}(\epsilon) \geq 2$ implies $\text{h}_{C^*(\mathcal{F}_n^{k+1})}(\epsilon) \leq 2(k+1)(p^2 - 1)$.

The first of these two inequalities follows from Equation 30 almost immediately using the inductive hypothesis together with the fact that $x(2p - x)$ is maximized when $x = p$:

$$\begin{aligned} \text{h}_{C^*(\mathcal{F}_n^{k+1})}(\epsilon) &\leq 2kp^2 + 2p^2 \\ &= 2(k+1)p^2. \end{aligned}$$

The second inequality follows by recognizing that $\text{th}(\epsilon) \geq 2 \implies \text{th}(\delta_i) \geq 2$, so that we may inductively conclude that $\text{h}_{C^*(\mathcal{F}_n^k)}(\delta_i) \leq 2k(p^2 - 1)$ in this case. From here, we note that $\text{th}(\epsilon) \geq 2$ also indicates $x = m_i + \ell \leq p - 1$ in our analysis of $x(2p - x)$, giving us

$$\begin{aligned} \text{th}(\epsilon) \geq 2 \implies \text{h}_{C^*(\mathcal{F}_n^{k+1})}(\epsilon) &\leq 2k(p^2 - 1) + 2(p - 1)(p + 1) \\ &= 2(kp^2 - k + p^2 - 1) \\ &= 2(k+1)(p^2 - 1). \end{aligned}$$

Finally, to verify item (iii), we begin by considering the case when δ_i was *not* in the top $2k$ homological degrees of $C^*(\mathcal{F}_n^k)$, ie

$$h_{C^*(\mathcal{F}_n^k)}(\delta_i) \leq 2kp^2 - 2k.$$

In this case, Equation 30 quickly yields

$$\begin{aligned} h_{C^*(\mathcal{F}_n^{k+1})}(\epsilon) &\leq 2kp^2 - 2k + 2p^2 \\ &= 2(k+1)p^2 - 2k \end{aligned} \quad (31)$$

where we've again used the fact that $x(2p-x)$ is maximized when $x=p$.

The homological bound in Equation 31 applies only to the terms in the multicone coming from $\delta \in C^*(\mathcal{F}_n^k)$ with $h_{C^*(\mathcal{F}_n^k)}(\delta) \leq 2kp^2 - 2k$. As such, if we are interested in the truncated complex $C_{>2(k+1)p^2-2k}^*(\mathcal{F}_n^{k+1})$, it is enough to consider the multicone of Equation 29 only for $\delta_i, \delta_j \in C_{>2kp^2-2k}^*(\mathcal{F}_n^k)$. By inductive assumption, the complex $\bar{C}^* := C_{>2kp^2-2k}^*(\mathcal{F}_n^k)$ consists of only diagrams δ with $\text{th}(\delta) = 0$ and no disjoint circles. For this reason, Lemma 2.26 applies when we simplify the truncated Equation 29:

$$\begin{aligned} \widetilde{KC}_{>2(k+1)p^2-2k}^*(\mathcal{F}_n^{k+1}) &\simeq \text{Multicone}_{h_{\bar{C}^*}(\delta_j) - h_{\bar{C}^*}(\delta_i) = 1} \left(\widetilde{KC}^* \left(\begin{array}{c} \text{|||||} \\ \boxed{\mathcal{F}_n} \\ \hline \boxed{\delta_i} \\ \text{|||||} \end{array} \right) \xrightarrow{\left(\begin{array}{c} \text{|||||} \\ \boxed{I_{\mathcal{F}_n}} \\ \hline \boxed{\phi_{i,j}} \\ \text{|||||} \end{array} \right)^*} \widetilde{KC}^* \left(\begin{array}{c} \text{|||||} \\ \boxed{\mathcal{F}_n} \\ \hline \boxed{\delta_j} \\ \text{|||||} \end{array} \right) \right) \\ &\simeq h^{2p^2} q^{2p(p+1)} \bar{C}^* \end{aligned}$$

implying that

$$C_{>2(k+1)p^2-2k}^*(\mathcal{F}_n^{k+1}) = h^{2p^2} q^{2p(p+1)} \bar{C}^*.$$

We then apply an overall shift of $h^{-2(k+1)p^2} q^{-2(k+1)p(p+1)}$ to both sides of this equivalence, shifting the designated homological truncation points according to our notational convention (see Definition 2.1), to verify item (iii) in the statement of the theorem. \square

2.6 Proof of Theorem 2.2

Proof of Theorem 2.2. We define the complexes $C^*(k)$ to be shifted copies of the complexes $C^*(\mathcal{F}_n^k)$ of Theorem 2.23:

$$C^*(k) := h^{-2kp^2} q^{-2kp(p+1)} C^*(\mathcal{F}_n^k),$$

which are then chain homotopy equivalent to further shifts of the Khovanov complexes $KC^*(\mathcal{F}_n^k)$ as required (see the renormalization of Definition 2.4). Item (iii) of Theorem 2.23 then guarantees that our truncated complexes include into each other

$$C_{>-2}^*(1) \hookrightarrow C_{>-4}^*(2) \hookrightarrow \cdots \hookrightarrow C_{>-2k}^*(k) \hookrightarrow \cdots$$

as required. Each complex in this sequence of inclusions satisfies item (ii) of Theorem 2.23, and therefore the limiting complex does as well. Because the maps are inclusions, any truncation of the limiting complex matches the corresponding truncation in the sequence of inclusions, and so can be computed by simplifying and truncating a Khovanov complex of finite twists. \square

Theorem 2.2 gives us access to a well-defined chain complex in Bar-Natan’s categorification of the Temperley-Lieb algebra to assign to an infinite twist on $n = 2p$ strands. Any finite set of chain terms and differentials for this complex can be computed, up to a grading shift, as the upper-most homological degrees of (a chain homotopy equivalent simplification of) $KC^*(\mathcal{F}_n^k)$ for large enough k . If we imagine that our infinite twist (or perhaps, many infinite twists on various sets of strands) are closed up in some way as in Figure 1, then in fact we have Khovanov complexes of genuine links (with high but *finite* amounts of twisting), and we can pass to actual Khovanov chain groups and homology groups purely from Bar-Natan’s setting (ie, without recourse to Khovanov’s invariant for tangles [Kho02]). This is the plan for the following sections.

Remark 2.27. As described in Section 5.2, our complex $C^*(\mathcal{F}_n^\infty)$ has graded Euler characteristic recovering the zero-weight Jones-Wenzl projector $P_{n,0}$. One can also show that $C^*(\mathcal{F}_n^\infty)$ is an idempotent complex by an argument similar to the proof of Theorem 2.23: one copy of $C^*(\mathcal{F}_n^\infty)$ is comprised of through-degree zero terms, all of which unwind any finite approximation of the second copy of $C^*(\mathcal{F}_n^\infty)$. However, following [Roz] we hesitate to call this complex a categorified projector without a similar construction for the other $P_{n,m}$ and a categorical analogue of how the various projectors give a decomposition of identity.

On the other hand, Ben Elias and Matt Hogancamp have a separate construction in [EHb] for categorifying all of the Jones-Wenzl projectors together via categorical diagonalization [EHa] of the full twist operator in the category of Soergel bimodules, and it seems likely that our construction here matches theirs for a specific choice of eigenmap. See also [CH15].

3 Defining Khovanov homology for links in $\#^r(S^2 \times S^1)$

3.1 Links in $\#^r(S^2 \times S^1)$

Let $M^r = \#^r(S^2 \times S^1)$. A link \mathcal{L} in M^r with ℓ components is a (smooth) embedding $\coprod_\ell S^1 \hookrightarrow M^r$. As discussed in the intro, we build M^r by performing r S^0 -surgeries on S^3 . We then draw M^r as a copy of S^3 together with its embedded attaching spheres $(S^0 \times S^2)_i$ for $i = 1, \dots, r$. Each single pair $(S^0 \times S^2)_i$ is drawn as two oppositely oriented spheres with a dashed line (called a *surgery line*, and denoted by sl_i) drawn between them. Rather than trying to envision the handle $(D^1 \times S^2)_i$ that connects these two spheres in M^r , we imagine the spheres as teleportation points - a traveler in our diagram for M^r who touches one sphere is immediately teleported to the ‘mirror image’ point on the corresponding sphere (coordinates (x, y, z) from the center of one sphere correspond to coordinates $(x, y, -z)$ from the center of the other). In this way, an oriented link $\mathcal{L} \subset M^r$ can be drawn as a planar diagram L with crossings as usual, except that the link is allowed to intersect any of the $(S^0 \times S^2)_i$ in mirrored points.

To analyze such link diagrams in detail, we fix our diagram for M^r by placing our attaching spheres $(S^0 \times S^2)_i$ and surgery lines sl_i so that the planar projection P' of M^r is as shown in Figure 11.

Definition 3.1. We say a link $\mathcal{L} \subset M^r$ is in *standard position* if the following conditions are satisfied for each $i = 1, \dots, r$:

- $\mathcal{L} \cap sl_i = \emptyset$, that is, \mathcal{L} does not intersect any of the surgery lines.
- $\mathcal{L} \pitchfork (S^0 \times S^2)_i$, that is, \mathcal{L} intersects each attaching sphere $(S^0 \times S^2)_i$ transversely.

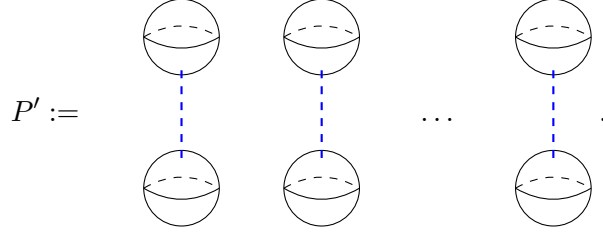


Figure 11: P' denotes the fixed diagram for the planar projection of M^r . Our diagrams for links in M^r will be drawn in P' .

- The intersection points $\mathcal{L} \cap (S^0 \times S^2)_i$ are arranged in a ‘straight’ line on each sphere as indicated in the far right diagram of Figure 12. This arrangement shall also be referred to as *standard position* for the intersection points.

Given such an \mathcal{L} , we let n_i denote the geometric intersection number of \mathcal{L} with the belt sphere of the handle $(D^1 \times S^2)$, so that $\mathcal{L} \cap (S^0 \times S^2)_i$ is the collection of n_i pairs of mirrored points on the two spheres.

The first two conditions of Definition 3.1 are clearly generic. Furthermore, Figure 12 shows how we can further isotope any generic \mathcal{L} into standard position by moving the intersection points of $\mathcal{L} \cap (S^0 \times S^2)_i$ one at a time towards their chosen targets (generically missing the other intersection points). Of course, this involves choices that we will consider further below.

Given a link $\mathcal{L} \subset M^r$, we first isotope \mathcal{L} so that it is in standard position, and then we project down to P' and call the resulting diagram $L \subset P'$. We then further isotope \mathcal{L} as needed so that L is also in general position. That is, strands of L miss the projections of the intersection points $(S^0 \times S^2)_i \cap \mathcal{L}$ and $(S^0 \times S^2)_i \cap sl_i$, and the entire diagram contains no cusps or triple points of intersection involving any combination of strands of L , surgery lines sl_i , and ‘borders’ of attaching spheres $(S^0 \times S^2)_i$. We record over- and under-crossing data between strands of L and/or surgery lines sl_i in the usual way; we also record whether or not strands of L are ‘over’ (respectively ‘under’) any attaching sphere with solid (respectively dashed) lines. Then L is called a *link diagram* for \mathcal{L} .

Proposition 3.2. *Two link diagrams L_1 and L_2 drawn in P' depict isotopic links in M^r if and only if L_1 and L_2 are related by planar isotopies in P' , together with the following types of moves:*

- Reidemeister moves in P' , involving crossings of L alone or crossings of L with the fixed surgery lines and sphere borders. See Figures 13 and especially 14.
- Mirror moves - given any element β in the braid group on n_i strands, a copy of β can be inserted adjacent to one sphere in the pair $(S^0 \times S^2)_i$, together with a copy of β^{-1} adjacent to the other sphere (see Figure 15).
- Finger moves - see the local picture of Figure 16; finger moves at other points of the sphere can be moved to this point, up to possible braid group elements as described above.
- Point-pass moves - see the local picture of Figure 17, where strands can pass either above or below any intersection point $\mathcal{L} \cap (S^0 \times S^2)_i$ or $sl_i \cap (S^0 \times S^2)_i$ in accordance with whether the strand is above or below the sphere.

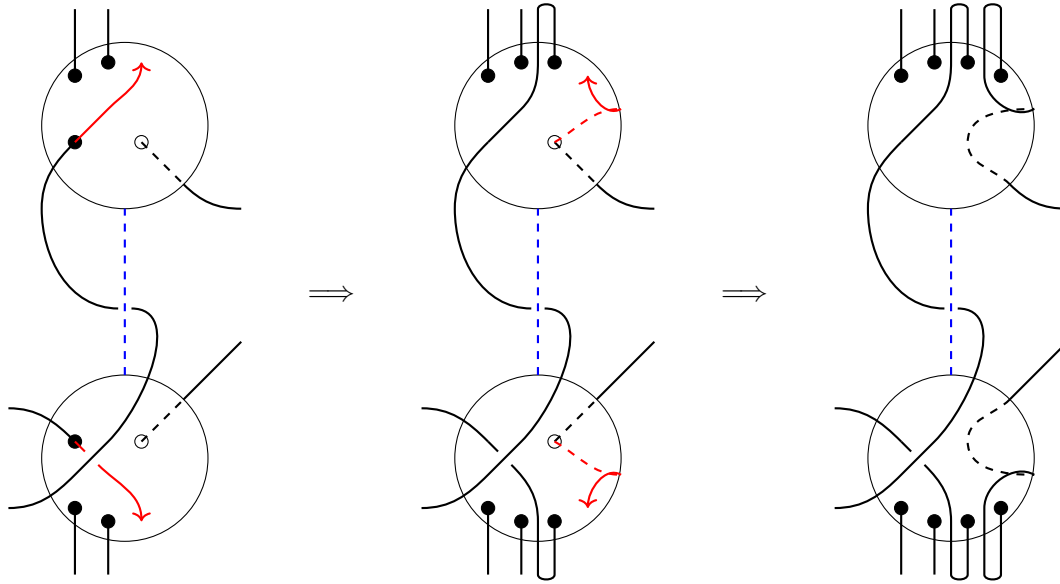


Figure 12: We choose a path for each intersection point to follow along the sphere so that the mirrored points occur in a ‘straight’ line, which we refer to as standard position for the points. We then isotope \mathcal{L} near each $(S^0 \times S^2)_i$ by following along these paths, one at a time, and ‘tugging’ the strand outward once the point has reached standard position, as illustrated in the sequence above. The depths of the spheres are omitted for clarity. The open circle indicates an intersection point on the ‘back’ side of the sphere. Note that there are many ordered sets of paths to arrange such points into standard position, but the resulting diagrams are all connected by isotopies of \mathcal{L} in M^r generated by the mapping class group of the n_i -punctured sphere.

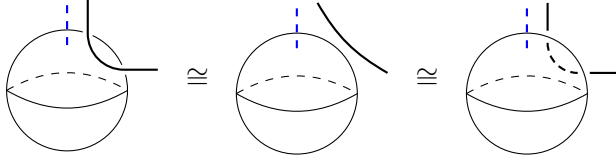


Figure 13: Reidemeister 2 moves involving L and sphere borders. The intersection points $\mathcal{L} \cap (S^0 \times S^2)_i$ are omitted for clarity.

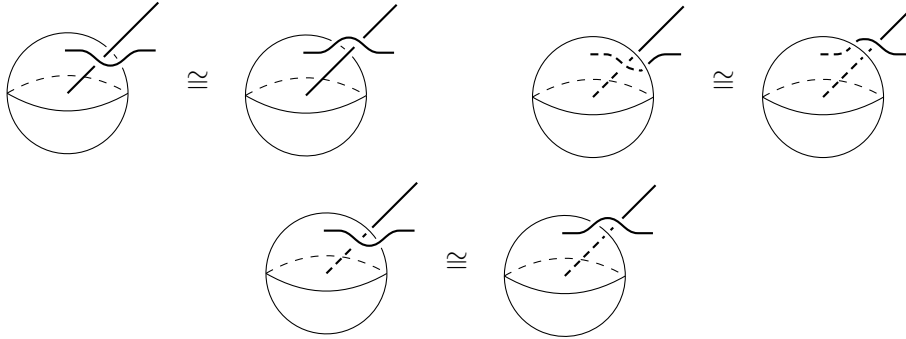


Figure 14: Some examples of Reidemeister 3 moves involving L and sphere borders are shown here. The intersection points $\mathcal{L} \cap (S^0 \times S^2)_i$ and the surgery line sl_i are omitted. Note that, since Reidemeister 3 moves always involve moving an ‘entire crossing’ either above or below a third strand, we will always maintain which strands are over/under the sphere.

- The surgery-wrap move - we allow a disjoint nearby strand of L to ‘wrap around’ any dashed surgery-line, as illustrated in Figure 18.

Proof. As usual, all of our choices in producing L from \mathcal{L} involved isotopies. We begin with our choice of putting \mathcal{L} into standard position, starting from the ‘linear’ requirement for the intersection points. This involves a choice of a path for each point of intersection towards a designated point on the sphere (missing the other intersection points). Any two such choices are connected by an element of the mapping class group of the sphere. Thus there are isotopies which miss the north pole which correspond to the braid group acting on the n_i strands entering $(S^0 \times S^2)_i$, and there are isotopies which ‘cross’ the north pole and correspond to a wrapping-like move creating a Jucys-Murphy element $\mathcal{E}_{n_i}^{\pm 1}$. Of course, such elements are themselves generated by the braid group, and so we need only consider braid-like isotopies of the n_i strands. These are generated by the mirror moves (since any isotopy on the surface of one sphere of the pair $(S^0 \times S^2)_i$ must be mirrored on the other).

Tangencies of \mathcal{L} with some $(S^0 \times S^2)_i$ correspond to pushing a strand ‘through’ the attaching sphere and out to the other side, which can be realized by a finger move up to a new choice of arranging the intersection points into standard position (so, up to further mirror moves). Meanwhile, points of intersection of $\mathcal{L} \cap sl_i$ correspond to passing a strand of L ‘through’ a surgery line sl_i . This move is generated by the surgery wrap move together with a Reidemeister 2 move as

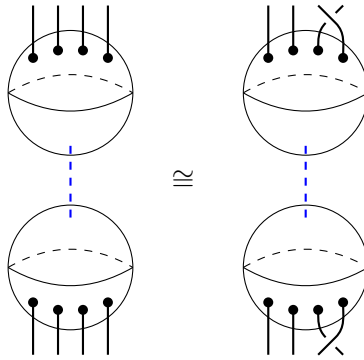


Figure 15: An example of a mirror move, with $\beta = \sigma_3$.

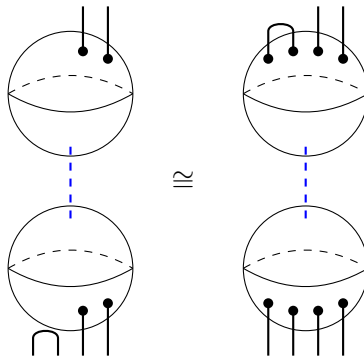


Figure 16: The finger move, by definition. We envision pushing the matching through the attaching sphere and out to the other side. Naturally, there is a similar move given by reflecting this picture about the horizontal axis.



Figure 17: The point-pass moves for $\mathcal{L} \cap (S^0 \times S^2)_i$, by definition. A strand over (respectively under) the sphere can pass over (respectively under) any intersection point in $\mathcal{L} \cap (S^0 \times S^2)_i$. There are similar moves for L passing over or under the points $sl_i \cap (S^0 \times S^2)_i$, as well as for the horizontal reflections of these pictures.



Figure 18: The surgery-wrap move, by definition.

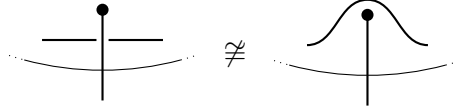
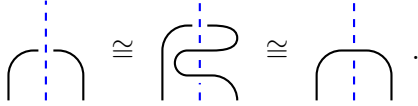
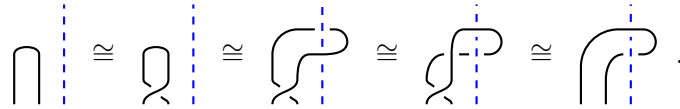


Figure 19: This move, which may look similar to a point-pass move, is not allowed for link diagrams L in P' . It would require \mathcal{L} to either pass through itself, or pass through the attaching sphere and appear on the corresponding mirrored sphere. There is a similar disallowed move for a strand over the sphere passing ‘under’ the point $sl_i \cap (S^0 \times S^2)_i$.

illustrated below:



We now analyze possible singularities in the planar diagram during an isotopy of \mathcal{L} . Cusps, tangencies, and triple points of intersections of L correspond to Reidemeister moves. Having fixed our $(S^0 \times S^2)_i$ and sl_i , there are no cusps of sphere borders or surgery lines. A triple point involving strand(s) of L , a sphere border, and/or a surgery line corresponds to a Reidemeister 3 move involving those objects. A tangency between a strand of L and a sphere border corresponds to a Reidemeister 2 move between them. A tangency between a strand of L and a single sl_i can correspond to either a Reidemeister 2 move, or a surgery-wrap move. One might worry that there should be two versions of the surgery-wrap move corresponding to right-handed or left-handed twisting, but in fact in our unoriented diagrams these are equivalent via other Reidemeister moves:



Of course this leads to two different versions once orientations are considered, which will lead to slightly different effects on the Khovanov homology further below.

Finally, the possibility of a strand of L passing through an intersection point of $\mathcal{L} \cap (S^0 \times S^2)_i$ or $sl_i \cap (S^0 \times S^2)_i$ corresponds to a point-pass move. Notice that, since \mathcal{L} may not pass through the sphere without appearing on the corresponding mirrored sphere, the move illustrated in Figure 19 is disallowed (and similarly for the corresponding picture involving the point $sl_i \cap (S^0 \times S^2)_i$). \square

Remark 3.3. Note that the moves listed in Proposition 3.2 allow for some perhaps more conventional moves that one might expect, such as various forms of ‘sphere-wrapping’ that are combinations of point-passing and surgery-wrapping. See Figure 20.

3.2 Defining the Khovanov homology $Kh(L)$ of a link diagram $L \subset P'$

Given an oriented link $\mathcal{L} \subset M^r$, we can derive an oriented link diagram $L \subset P'$ as described in the previous section. In order to ease the notation of some grading shifts later, we (arbitrarily) orient our surgery lines. When reading over the following notations, it is useful to remember that our goal is to convert our diagram L into the diagram $L(\vec{k})$ containing many full twists in place of the surgery lines (see Figure 1).

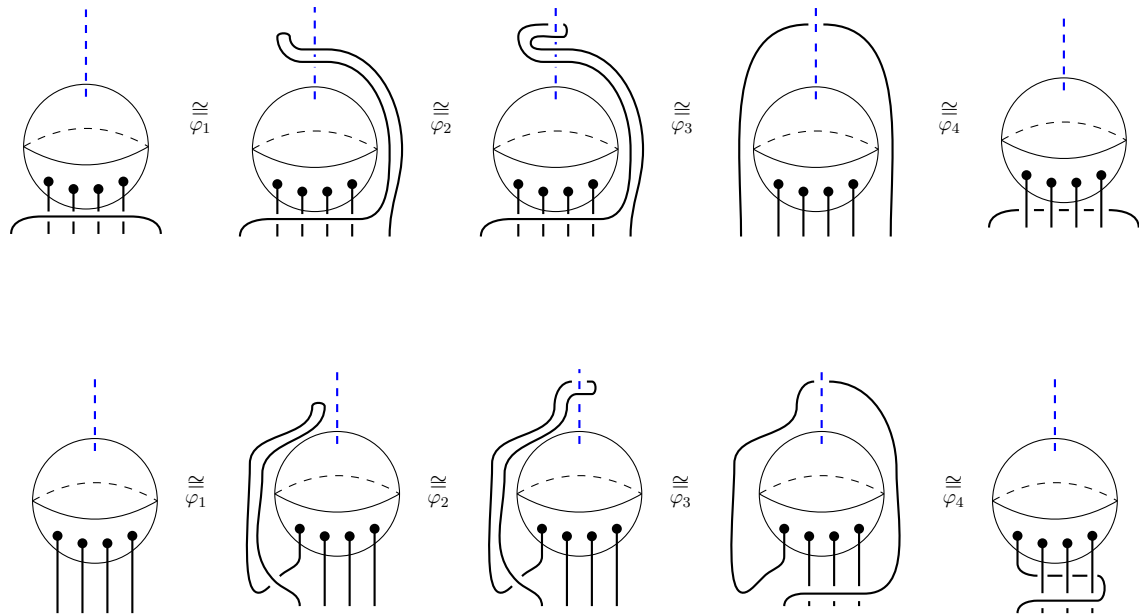


Figure 20: Some other ‘wrapping-style’ moves that are allowable using combinations of the moves listed in Proposition 3.2. In both sequences above, the isotopy φ_1 is accomplished with basic Reidemeister moves, while φ_2 is a surgery-wrap move. φ_3 uses further Reidemeister moves and point-pass moves for passing over the sphere, and finally φ_4 uses Reidemeister moves and point-pass moves for passing under the sphere. Note the ability to create a single, non-mirrored Jucys-Murphy element \mathcal{E}_{n_i} , which is the version Rozansky considers in [Roz].

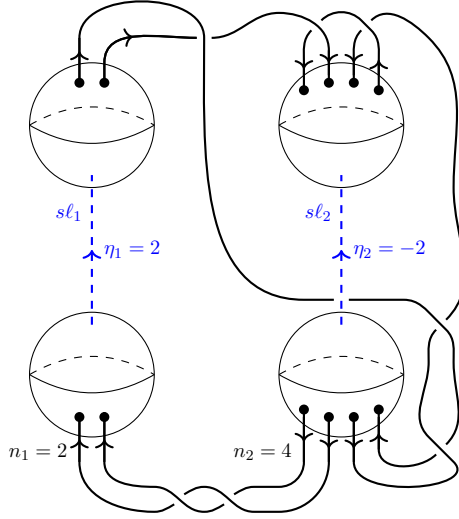


Figure 21: The example of Figure 1 has been oriented, and the basic notations of Definition 3.4 are included. The orientations of the sl_i are arbitrary; swapping such an orientation would swap the sign of the corresponding η_i . The reader can consider oriented full twists in place of the surgery lines to verify that we have $n_1^+ = 2$ and $n_1^- = 0$ so that $N_1 = -2$, while $n_2^+ = 6$ and $n_2^- = 6$ so that $N_2 = 6$.

Definition 3.4. We collect the following notations for quantities involving the various attaching spheres and surgery lines here as a single definition. All of the following definitions are taken over $i = 1, \dots, r$, and assume that we are given a specific link diagram $L \subset P'$ representing $\mathcal{L} \subset M^r$.

- sl_i will denote the i^{th} surgery line.
- $n_i = 2p_i$ is the geometric intersection number between L and the belt sphere in the i^{th} handle $(D^1 \times S^2)_i$.
- n_i^+ and n_i^- denote the number of positive (respectively negative) crossings in a *single copy of the full twist* on n_i strands, assuming they are oriented in the same way as the strands of L entering the attaching spheres $(S^0 \times S^2)_i$. In the notation of Section 2 (see Definition 2.1), $n_i^- := n_{\mathcal{F}n_i^-}$.
- $N_i := 2n_i^- - n_i^+$.
- η_i will denote the difference between the number of strands of L that enter $(S^0 \times S^2)_i$ with the same orientation as that of sl_i , and the number of strands that enter with the opposite orientation as sl_i . Thus η_i is the algebraic intersection number of L with the i^{th} belt sphere, oriented according to the orientation of sl_i .

See Figure 21 for clarification. Note that swapping the orientation of sl_i also swaps the sign of η_i .

Definition 3.5. Given a link diagram $L \subset P'$ and a vector $\vec{k} = (k_1, \dots, k_r) \in \mathbb{Z}^r$, the symbol $L(\vec{k})$ denotes the oriented planar link diagram obtained from L by performing the following steps:

1. Replace each sl_i with n_i parallel copies of sl_i attached to L at the intersection points of L with $(S^0 \times S^2)_i$. These new strands are oriented to match the orientation of L .
2. Over/under crossing data for the new strands is inherited from the corresponding data from the sl_i and $(S^0 \times S^2)_i$. That is to say, if a strand of L intersects a new strand at a point formerly along sl_i , then L is drawn over (respectively under) the new strand if L was originally drawn over (respectively under) that point along sl_i . Similarly, if L intersects a new strand at a point within the projection of $(S^0 \times S^2)_i$, then L is drawn over (respectively under) the new strand if L was originally drawn over (respectively under) that sphere.
3. For each $i = 1, \dots, r$ choose a point along sl_i that is not a crossing point, and insert the braid $\mathcal{F}_{n_i}^{k_i}$ into the set of n_i parallel strands at that point. Note that, in the case of $\vec{k} = \vec{0}$, this step does nothing.
4. Replace P' with the standard plane P (ie, erase or ignore the surgery spheres in the diagram).

See Figure 1 for clarification. We view $L(\vec{k}) \subset P$ as a planar diagram for a link in S^3 .

Definition 3.6. Given a link diagram $L \subset P'$, we construct the *Khovanov complex of L* , denoted $KC^*(L)$, using the following steps:

1. Replace L by the planar diagram $L(\vec{0})$, viewed as a link in S^3 .
2. For each $i = 1, \dots, r$ choose a point along sl_i that is not a crossing point, and insert the complex $C^*(\mathcal{F}_{n_i}^\infty)$ of Theorem 2.2 at that point.
3. Take the planar algebraic tensor product of these complexes, together with the Khovanov complexes coming from the crossings already present in the diagram $L(\vec{0})$, in the sense of the tangle canopolies of [BN05].

See Figure 22 for clarification. In a slight abuse of notation via Definition 3.5, we can think of this complex as $C^*(L(\infty))$. Analogously, we define the *finite approximation complex* $C^*(L(\vec{k}))$ to be the (finite) complex obtained by following the same procedure, but placing the finite complex $C^*(k_i)$ at each insertion point instead of $C^*(\mathcal{F}_{n_i}^\infty)$.

From here we define the *Khovanov homology of L* $Kh(L)$ from $KC^*(L)$ by applying Khovanov's functor to complexes of modules over the ground ring and taking homology as usual.

Proposition 3.7. *Given a link diagram $L \subset P'$ and an arbitrary homological lower bound a , there exists some finite \vec{k} such that the truncated Khovanov complex $KC_{\geq a}^*(L) = C_{\geq a}^*(L(\infty))$ is equal to the truncation of the finite approximation complex $C_{\geq a}^*(L(\vec{k}))$. In other words, $KC^*(L)$ can be approximated by the truncation of a finite complex in any given homological range. See Figure 22 for clarification.*

Recall that $C^*(k_i)$ is chain homotopy equivalent to the shifted Khovanov complex of k_i full twists. In particular, we can use Proposition 3.7 to prove:

Corollary 3.8. *Given a link diagram $L \subset P'$, the Khovanov homology $Kh^*(L)$ can be approximated in any finite range of homological degrees by the shifted Khovanov homology of a genuine link*

$$\begin{aligned}
& KC_{\geq a}^* \left(\text{Diagram 1} \right) := KC_{\geq a}^* \left(\text{Diagram 2} \right) \\
& = KC_{\geq a}^* \left(\text{Diagram 3} \right) \\
& \simeq h^{-2k_1-2k_2} q^{-6k_1-6k_2} KC_{\geq b}^* \left(\text{Diagram 4} \right)
\end{aligned}$$

Figure 22: A diagrammatic example illustrating Definition 3.6 (the first line) and Proposition 3.7 (the second line is the truncated finite approximation complex $C_{\geq a}^*$ by definition) for the oriented link diagram L of Figure 21. The third line unpacks the homological shifts inherent in the definitions of the $C^*(k_i)$ for this figure; note that such shifts also affect the truncation point.

diagram $L(\vec{k})$ for some finite \vec{k} . More precisely, given any homological bound a , there exists some \vec{k} that depends on a such that

$$Kh^*(L) \cong H^* \left(\mathfrak{h}^{\sum_i k_i(n_i^- - 2p_i^2)} \mathfrak{q}^{\sum_i k_i(N_i - 2p_i(p_i + 1))} KC(L(\vec{k})) \right) \quad (32)$$

in all homological gradings $* \geq a$.

Proof of both Proposition 3.7 and Corollary 3.8. By definition, $KC^*(L)$ is a planar tensor product of homotopy colimits of inclusions of truncated complexes, which can be viewed as a large stable homotopy colimit of truncations of the tensor products. That is to say, there must exist some starting value \vec{k}_0 and truncation points $c_i \rightarrow -\infty$ allowing us to build $KC^*(L)$ via a limit of inclusions

$$C_{>c_0}^*(L(\vec{k}_0)) \hookrightarrow C_{>c_1}^*(L(\vec{k}_0 + \vec{1})) \hookrightarrow \dots$$

where we are choosing to take the colimit ‘diagonally’ increasing each entry of \vec{k} by one at each step (this is only for ease of notation). Thus, given the finite homological bound a , we can find $c_i < a$ allowing $\vec{k}_0 + \vec{i}$ to satisfy the requirements of Proposition 3.7.

In this way we have $Kh^*(L) = H^*(C^*(L(\vec{k})))$ for $* > a$. Since each $C^*(k_i)$ within $C^*(L(\vec{k}))$ is chain homotopy equivalent to $\mathfrak{h}^{k_i(n_i^- - 2p_i^2)} \mathfrak{q}^{k_i(N_i - 2p_i(p_i + 1))} KC^*(\mathcal{F}_{n_i}^{k_i})$ (Theorem 2.2), we have for the full tensor product

$$C^*(L(\vec{k})) \simeq \mathfrak{h}^{\sum_i k_i(n_i^- - 2p_i^2)} \mathfrak{q}^{\sum_i k_i(N_i - 2p_i(p_i + 1))} KC^*(L(\vec{k})).$$

Although these complexes may no longer be chain homotopic after truncation, their homology groups beyond the truncation point must remain isomorphic, which proves Corollary 3.8. \square

3.3 Invariance of $Kh(\mathcal{L})$ for links in M^r

The goal of this section is to prove the following theorem.

Theorem 3.9. *Suppose L_1 and L_2 are two link diagrams in P' representing isotopic links in M^r . Then, up to grading shifts that depend only on the quantities η_i for each surgery line, $Kh(L_1) \cong Kh(L_2)$.*

According to Proposition 3.2, it is enough to show the isomorphism whenever L_1 and L_2 are related by one of the move types listed there (together with showing invariance of our choice of insertion points along the $s\ell_i$). According to Corollary 3.8, the isomorphism can be checked in any finite homological range for shifted Khovanov complexes of genuine links $L_1(\vec{k})$ and $L_2(\vec{k})$ in S^3 . Note that, although any given required k_i may be different for the diagrams L_1 and L_2 , we can always take the maximum and thus assume that the vector \vec{k} is the same for $L_1(\vec{k})$ and $L_2(\vec{k})$. Thanks to this viewpoint, many of the move types of Proposition 3.2 are nearly immediate consequences of isotopies of links in S^3 . The only type of move that requires closer examination is the surgery-wrap move. Perhaps unsurprisingly, it is this type of move that causes the grading shifts as we will see below. The strategy for proving invariance under this move is very similar to the strategy for proving Theorem 2.23. Compare the following lemma to Lemma 2.24 from Section 2.5.

Lemma 3.10. *If δ is a Temperley-Lieb diagram with $\text{th}(\delta) = 0$, we have*

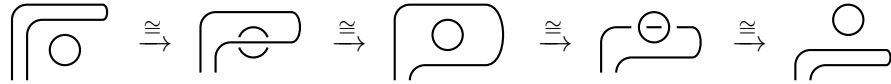
$$\widetilde{KC}^* \left(\begin{array}{c} \boxed{\delta} \\ \vdots \\ \text{---} \\ \vdots \\ \text{---} \\ \vdots \\ n_i \end{array} \right) \simeq h^{n_i} q^{n_i} \widetilde{KC}^* \left(\begin{array}{c} \boxed{\delta} \\ \vdots \\ \text{---} \\ \vdots \\ \text{---} \\ \vdots \\ n_i \end{array} \right) \quad (33)$$

regardless of the orientation of any of the strands. The tangle isotopy that accomplishes this utilizes only Reidemeister 2 moves that remove crossings.

Proof. Since $\text{th}(\delta) = 0$, there is a clear innermost cup sliding isotopy of Reidemeister 2 simplifications as in Lemma 2.21 and the blue strands coming down from δ must come in oppositely oriented pairs. From here, we count crossings as usual. The details are left to the reader. \square

In Section 2.5, Lemma 2.25 provided an isotopy between two link cobordisms, implying that the chain maps induced by those two cobordisms were homotopic up to a sign. This time around our two link cobordisms will not necessarily be isotopic as far as we can tell, but their ‘difference’ up to isotopy will be a special sort of link cobordism whose induced chain map will be ignorable via the following lemma.

Lemma 3.11. *Let ρ_\circ denote the tangle cobordism (embedded in $B^3 \times [0, 1]$) illustrated by the following movie of Reidemeister moves:*



Then $\rho_\circ^* = I^*$, the identity map (ie the product cobordism in Bar-Natan’s category of dotted cobordisms between planar diagrams) sending the disjoint circle to itself and the ‘wrapping strand’ to itself.

Proof. We write out the chain maps corresponding to the sequence of Reidemeister 2 moves indicated by ρ_\circ in Figure 23 (see [BN05] where these maps are defined and shown to be chain homotopy equivalences). Utilizing the notation in that figure, together with the \cdot notation for vertical concatenation as usual, the overall map ρ_\circ^* can be computed as

$$\begin{aligned} \rho_\circ^* &= (a - b) \cdot (c - d) \\ &= a \cdot c - a \cdot d - b \cdot c + b \cdot d. \end{aligned}$$

The birth and death in $a \cdot d$ create a disjoint sphere, so that $a \cdot d = 0$. The other compositions are

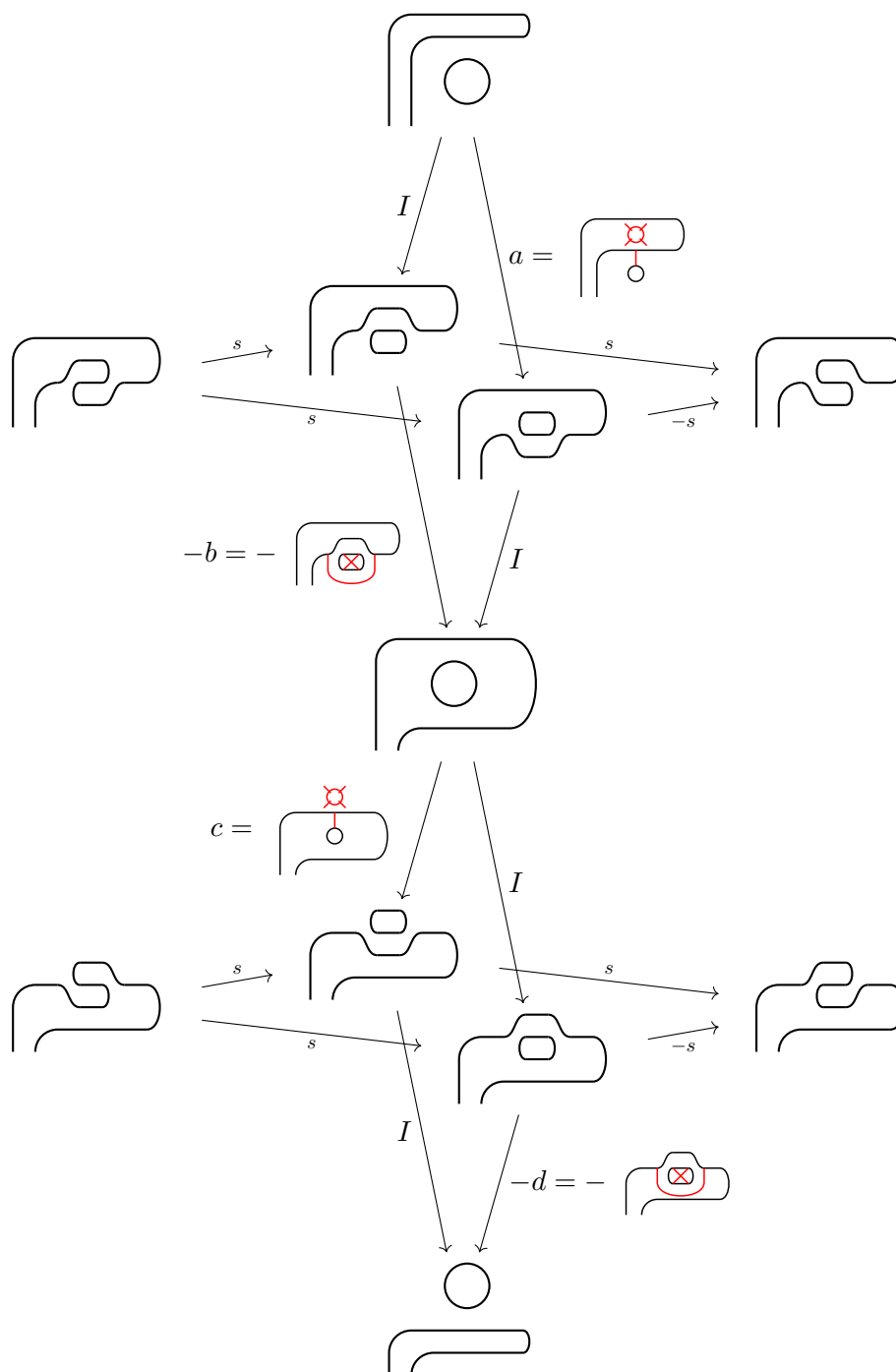


Figure 23: The chain maps corresponding to the Reidemeister movie ρ_o of Lemma 3.11. Identity maps are labelled I . Saddle cobordisms are marked with red lines. The maps a and c have circle births, while the maps b and d have circle deaths.

described below and expanded utilizing Bar-Natan's neck-cutting relation.

$$\begin{aligned}
 a \cdot c &= \text{[Diagram: A box with a folded curtain on the left and a dot on the right. A strand enters from the bottom left, loops around the curtain, and exits at the top left.]} = \text{[Diagram: A box with a folded curtain on the left and a dot on the right. A strand enters from the bottom left and exits at the top left.]} + \text{[Diagram: A box with a folded curtain on the left and a dot on the right. A strand enters from the bottom left and exits at the top right.]} \\
 -b \cdot c &= - \text{[Diagram: A box with a folded curtain on the left and a dot on the right. A strand enters from the bottom left, loops around the curtain, and exits at the top right.]} = -2 \text{[Diagram: A box with a folded curtain on the left and a dot on the right. A strand enters from the bottom left and exits at the top right.]} \\
 b \cdot d &= \text{[Diagram: A box with a folded curtain on the left and a dot on the right. A strand enters from the bottom left, loops around the curtain, and exits at the top right.]} = \text{[Diagram: A box with a folded curtain on the left and a dot on the right. A strand enters from the bottom left and exits at the top right.]} + \text{[Diagram: A box with a folded curtain on the left and a dot on the right. A strand enters from the bottom left and exits at the top right.]}
 \end{aligned}$$

After combining, the terms with a dot on the 'folded curtain' all cancel, leaving a sum of two terms that is clearly equivalent (again via a neck-cutting relation) to an identity morphism taking the disjoint circle around to the other side of the curtain. \square

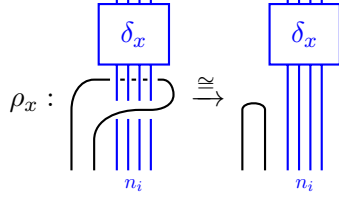
Lemma 3.12. *If \mathcal{C}^* is a chain complex made entirely of dotted cobordisms $\phi_{x,y}$ between diagrams δ_x, δ_y all having through-degree zero and having no disjoint circles, then abusing notation slightly we have*

$$\text{Multicone}_{h_{\mathcal{C}^*}(\delta_y) - h_{\mathcal{C}^*}(\delta_x) = 1} \left(\widetilde{KC}^* \left(\begin{array}{c} \boxed{\delta_x} \\ \vdots \\ \text{[Strands]} \\ n_i \end{array} \right) \xrightarrow{\left(\begin{array}{c} \boxed{\phi_{x,y}} \\ \vdots \\ \text{[Strands]} \end{array} \right)^*} \widetilde{KC}^* \left(\begin{array}{c} \boxed{\delta_y} \\ \vdots \\ \text{[Strands]} \\ n_i \end{array} \right) \right) \simeq h^{n_i} q^{n_i} \left(\begin{array}{c} \boxed{\mathcal{C}^*} \\ \vdots \\ \text{[Strands]} \\ n_i \end{array} \right) \tag{34}$$

regardless of the orientation of any of the strands.

Proof. The proof is identical in form to the proof of Lemma 2.26, so we will be brief. Because each

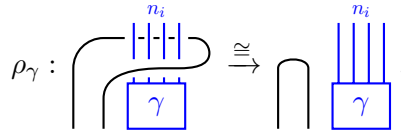
of the δ_x have $\text{th}(\delta_x) = 0$ and no disjoint circles, Lemma 3.10 gives tangle isotopies



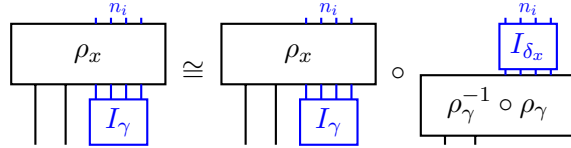
which satisfy the requirements of Corollary 2.14. Meanwhile, after choosing a closure

$$\gamma := \cup \dots \cup$$

to concatenate on the *bottom* of the strands coming from the sl_i , we also have a consistent tangle isotopy



Just as in the proof of Lemma 2.25, there is an isotopy of cobordisms



where we consider the composition $(\rho_x \cdot I_\gamma) \circ (I_{\delta_x} \cdot \rho_\gamma^{-1})$ separately. The reader can verify that, since this cobordism is taking place after $(I_{\delta_x} \cdot \rho_\gamma)$ which effectively removes any crossings from the local picture, our composition $(\rho_x \cdot I_\gamma) \circ (I_{\delta_x} \cdot \rho_\gamma^{-1})$ is isotopic to a sequence of tangle cobordisms of the form ρ_\circ as in Lemma 3.11, all of which induce identity maps on the chain level. This allows us to use functoriality to select a consistent choice of signs σ_x such that

$$\sigma_x \left(\left(\begin{array}{c} \rho_x \\ I_\gamma \end{array} \right)^* \right) \simeq \left(\begin{array}{c} I_{\delta_x} \\ \rho_\gamma \end{array} \right)^*$$

leading to a corresponding version of Equation 25 for use in the bottom two layers of Figure 5. Just as in the proof of Lemma 2.26, we have ρ_γ and $\phi_{x,y}$ commuting because they affect disjoint parts of the tangle diagram, and the fact that we are dealing with only one-term complexes ensures that the homotopies between maps are trivial. \square

Note that we have adjusted the subscript notation of the diagrams to involve x and y instead of i and j as in Section 2 because i is now being used to track which surgery line sl_i we are considering.

Remark 3.13. In [Roz], Rozansky's version of this proof using quasi-triviality boils down to the assertion that the two cobordisms $(\rho_x \cdot I_\gamma)$ and $(I_{\delta_x} \cdot \rho_\gamma)$ are themselves isotopic. It seems unclear whether or not this is the case for these cobordisms in $B^3 \times [0, 1]$, which is where functoriality for Bar-Natan's construction has been established (even if we close the other strands and view our

cobordisms in $S^3 \times [0, 1]$, this isotopy seems unclear to the author; the 2-sphere swept out by the ‘wrapping strand’ would split S^3 into two 3-balls, but both 3-balls contain other strands of the link). The computation of Lemma 3.11 here provides the work-around: although ρ_\circ may not be isotopic to identity as an embedded cobordism in $B^3 \times [0, 1]$, it still induces an identity map on the chain level.

Definition 3.14. We call a surgery-wrap *positive* (respectively *negative*) if the crossings involved between L and the surgery-line are positive (respectively negative).

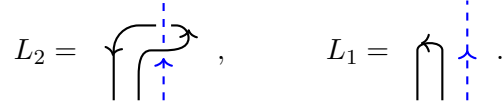
Theorem 3.15. Suppose a link diagram L_2 is obtained from another link diagram L_1 in P' by introducing a positive surgery wrap along sl_i . Then

$$Kh^*(L_2) \cong h^{\eta_i} q^{3\eta_i} Kh^*(L_1). \quad (35)$$

Similarly, if L_3 is obtained from L_1 by introducing a negative surgery wrap along sl_i , we have

$$Kh^*(L_3) \cong h^{-\eta_i} q^{-3\eta_i} Kh^*(L_1). \quad (36)$$

Proof. L_1 and L_2 are the same diagram everywhere except near a specific surgery line sl_i , where we have the following local pictures:



According to Proposition 3.7, it is enough to produce a chain homotopy equivalence between all of the truncated complexes which approximate $KC^*(L_1)$ and $KC^*(L_2)$. Allowing a slight abuse of notation once again, we must locally show that

$$KC^* \left(\begin{array}{c} \boxed{C_{>-2k_i}^*(k_i)} \\ \vdots \\ \text{crossing} \\ \vdots \\ n_i \end{array} \right) \stackrel{?}{\simeq} h^{\eta_i} q^{3\eta_i} \left(\begin{array}{c} \boxed{C_{>-2k_i}^*(k_i)} \\ \vdots \\ \text{parallel strands} \\ \vdots \\ n_i \end{array} \right)$$

for any $k_i > 0$. We know from Theorem 2.2 that the complexes $C_{>-2k_i}^*(k_i)$ satisfy the conditions of Lemma 3.12, allowing us to write

$$\widetilde{KC}^* \left(\begin{array}{c} \boxed{C_{>-2k_i}^*(k_i)} \\ \vdots \\ \text{crossing} \\ \vdots \\ n_i \end{array} \right) \simeq h^{\eta_i} q^{\eta_i} \left(\begin{array}{c} \boxed{C_{>-2k_i}^*(k_i)} \\ \vdots \\ \text{parallel strands} \\ \vdots \\ n_i \end{array} \right).$$

Recalling Definition 2.4, this is equivalent to writing

$$KC^* \left(\begin{array}{c} \boxed{C_{>-2k_i}^*(k_i)} \\ \vdots \\ \text{crossing} \\ \vdots \\ n_i \end{array} \right) \simeq h^{\eta_i - \eta^-} q^{\eta_i - N} \left(\begin{array}{c} \boxed{C_{>-2k_i}^*(k_i)} \\ \vdots \\ \text{parallel strands} \\ \vdots \\ n_i \end{array} \right)$$

where n^- and N count positive and negative crossings in the diagram on the left. Notice that any blue strand that agrees with the orientation assigned to sl_i will contribute two positive crossings to this diagram by definition, while the disagreeing strands will contribute two negative crossings. From here it is a simple exercise to verify that $n_i - n^- = \eta_i$ and $n_i - N = 3\eta_i$. The proof for the negative wrapping move is similar, except the roles of agreement and disagreement are reversed and so we negate η_i .

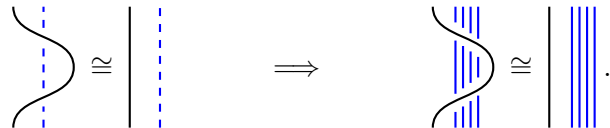
Notice that if we had chosen the opposite orientation for sl_i , our positive and negative surgery wrap moves would swap, but we would also negate our η_i . Thus our shifts are well-defined. \square

Proof of Theorem 3.9. We need to check invariance with respect to the move types listed in Proposition 3.2, as well as changing the insertion point along any sl_i . Surgery-wrap moves have already been considered in Theorem 3.15, causing chain homotopy equivalences on truncations up to grading shifts depending on the η_i . For all of the other moves, we utilize Corollary 3.8 and check for chain homotopy equivalences between complexes of genuine links. That is to say, if L_2 is obtained from L_1 by performing either a Reidemeister move, a mirror move, a finger move, or a point-pass move, then we wish to show that

$$\begin{aligned} & \mathfrak{h}^{\sum_i k_i(n_i^- - 2p_i^2)} \mathfrak{q}^{\sum_i k_i(N_i - 2p_i(p_i+1))} KC^*(L_1(\vec{k})) \\ & \stackrel{?}{\cong} \mathfrak{h}^{\sum_i k_i(n_i^- - 2p_i^2)} \mathfrak{q}^{\sum_i k_i(N_i - 2p_i(p_i+1))} KC^*(L_2(\vec{k})) \end{aligned} \quad (37)$$

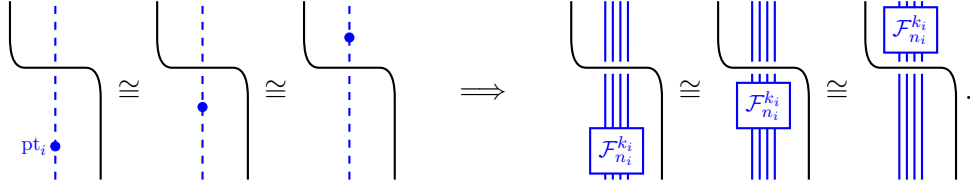
for any \vec{k} . Notice that in Equation 37 we do not truncate the complexes. Isotopies $L_1(\vec{k}) \cong L_2(\vec{k})$ in S^3 will allow us to prove Equation 37 which implies isomorphisms of homology groups even after truncation, despite the fact that the truncated complexes may no longer be chain homotopy equivalent. However, the shifts p_i, n_i^-, N_i are somewhat deceptive here since each is taken to apply to its respective diagram (ie, in the first line $n_i^- = n_i^-(L_1(\vec{k}))$, while in the second line $n_i^- = n_i^-(L_2(\vec{k}))$). The basic idea of the proof is to ensure that the overall shifts remain consistent during any necessary isotopy in S^3 of $L_1(\vec{k})$ into $L_2(\vec{k})$. It is also necessary to ensure that the various η_i remain constant as well, since the grading shift from surgery-wrapping uses this. We will collectively refer to the set $\{p_i, n_i^-, N_i, \eta_i\}$ as the *shifting data* for a given sl_i in a diagram.

We first note that, since we are now viewing $L_1(\vec{k})$ and $L_2(\vec{k})$ in S^3 and are ignoring the spheres $(S^0 \times S^2)_i$, Reidemeister moves involving sphere borders are completely ignorable and correspond to simple planar isotopies. In the case of Reidemeister moves involving crossings of L_1 , we immediately get corresponding Reidemeister moves for $L_1(\vec{k})$ in S^3 that do not affect any of the shifting data for any of the sl_i . Similarly, a Reidemeister move involving crossings of L_1 with some sl_i leads to corresponding ‘parallel’ Reidemeister moves for $L_1(\vec{k})$ in S^3 which again do not affect any of the shifting data. Such a Reidemeister 2 move is illustrated below:

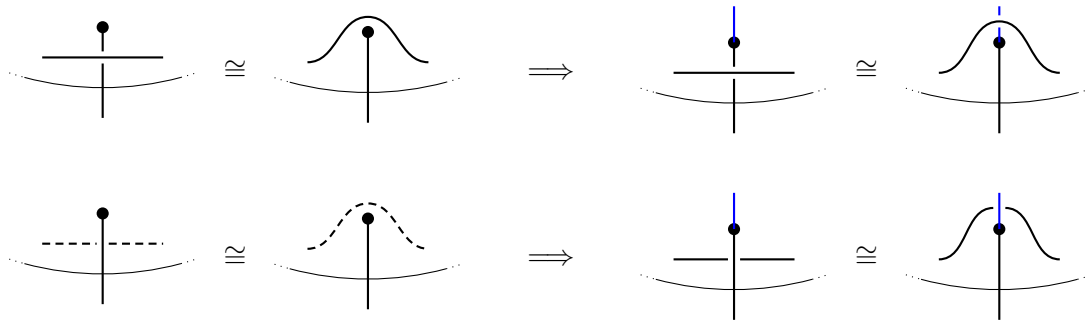


Moving an insertion point pt_i along sl_i leads to obvious isotopies in S^3 that ‘slide’ the full twisting along the parallel strands, possibly over or under some other strands via many Reidemeister 3

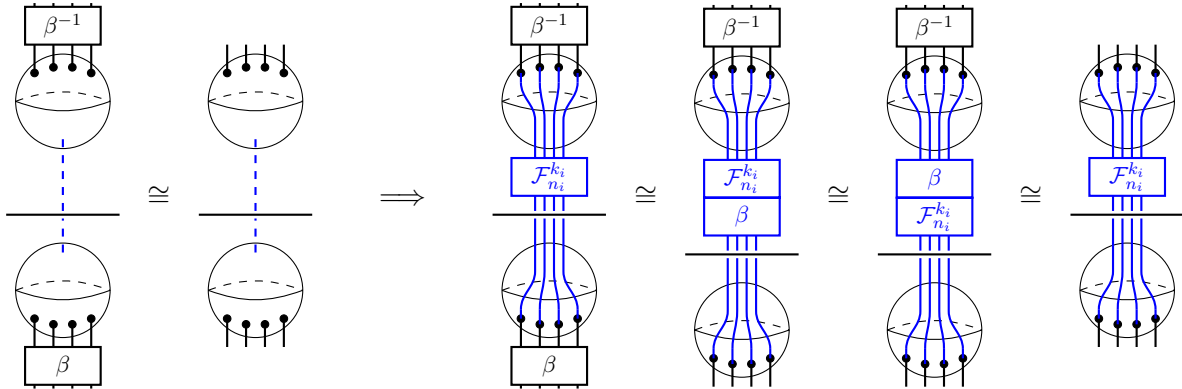
moves:



Again it is clear that the shifting data remain constant between such diagrams. A point-pass move likewise corresponds to a simple isotopy that maintains all shifting data where we slide a strand over or under the ‘gluing point’ of the black and blue strands according to whether the strand was over or under the sphere. Note that since we are ignoring the spheres in our diagrams for $L_1(\vec{k})$ and $L_2(\vec{k})$, we no longer draw the strands under the sphere as dashed lines.

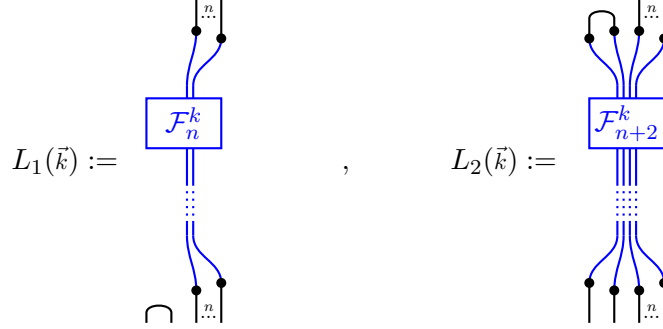


Mirror moves utilize the fact that the full twist is a central element of the braid group. Thus any braid β inserted adjacent to a surgery sphere can be ‘slid’ upwards along the surgery line sl_i , above or below any other crossings with L , passing through the full twists $\mathcal{F}_{n_i}^{k_i}$, until it meets its inverse braid β^{-1} that was also inserted adjacent to the other sphere. Once again, the shifting data clearly remains constant. We illustrate the case below with one strand of L crossing over the given sl_i .



The remaining move, which is slightly more interesting than the previous moves, is the finger move where some of the shifting data can change. We present the invariance under this move in slightly more detail than the others. First, it is clear from Figure 16 that, although the number of strands n_i changes by two during a finger move, the two new strands must be oppositely oriented so that η_i remains unchanged. Next, we demonstrate the S^3 isotopy that performs the finger move

on $L(\vec{k})$. Let $L_1(\vec{k})$ and $L_2(\vec{k})$ be as indicated by the local pictures below, corresponding to the left and right diagrams from Figure 16 after inserting our full twists into a ‘topmost’ point on the surgery line $s\ell_i$:



where we have fixed $k := k_i$ and $n := n_i(L_1(\vec{k}))$, so that $n_i(L_2(\vec{k})) = n + 2$. The symbols \cdot are to indicate that there can be any (even) number of strands n to start with. The dotted lines in place of the blue strands are there to indicate that the link may have strands crossing over or under the parallel blue strands in that area.

There is a clear isotopy in S^3 from $L_2(\vec{k})$ to $L_1(\vec{k})$ by first pulling the matching through the full twist as in Figure 10, and then ‘sliding’ the matching further down along the path of the surgery line (perhaps passing over or under other stands of L , similarly to the braid β in a mirror move) until we arrive at $L_1(\vec{k})$. To find relationships in the shifting data before and after the isotopy, we count crossings in the same way as we did during the proof of Lemma 2.24. Letting $n_{i,j}^- := n_i^-(L_j(\vec{k}))$, and similarly for the other shifting data, we find the following conversions (recall from Definition 3.4 that $n_{i,j}^-$ denotes the number of negative crossings that occur in a *single* copy of \mathcal{F}_{n_i} in $L_j(\vec{k})$, and similarly for $N_{i,j}$):

$$\begin{aligned} p_{i,2} &= p_{i,1} + 1 \\ n_{i,2}^- &= n_{i,1}^- + 2n + 2 \\ N_{i,2} &= N_{i,1} + 2n + 4 \\ \eta_{i,2} &= \eta_{i,1}. \end{aligned}$$

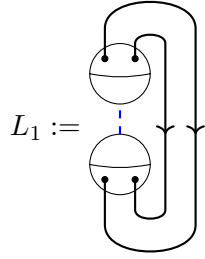
Compare this to the shifts of $2m(n - m)$ and $2m(n - m + 1)$ of Lemma 2.24 in the case of $m = 1$ matching, but with $n + 1$ used in place of n . The reader can check that these shifts result in *no* overall shift in either grading when checking Equation 37, ie

$$\begin{aligned} n_{i,2}^- - 2p_{i,2}^2 &= n_{i,1}^- - 2p_{i,1}^2 \\ N_{i,2} - 2p_{i,2}(p_{i,2} + 1) &= N_{i,1} - 2p_{i,1}(p_{i,1} + 1) \end{aligned}$$

and so the isotopy described above gives the required chain homotopy equivalence between complexes.

This finishes all of the moves required by Proposition 3.2, and so we are done. \square

Proof of Theorem 1.1. For a link $\mathcal{L} \subset M^r$ with diagram L in P^r , we have Khovanov homology groups $Kh(L)$ (Definition 3.6) which are well-defined up to grading shifts by Theorem 3.9 allowing us to use the notation $Kh(\mathcal{L})$. In the case when $r = 0$ and there are no attaching spheres or surgery lines to replace with infinite twists, our definition is clearly equivalent to that of the usual Khovanov homology of $\mathcal{L} \subset S^3$. \square



\cdots					\vdots
	\mathbb{Z}_2				-8
	\mathbb{Z}	\mathbb{Z}			-6
			\mathbb{Z}_2		-4
			\mathbb{Z}	\mathbb{Z}	-2
				\mathbb{Z}	0
\cdots	-3	-2	-1	0	$\begin{array}{c} q \\ h \end{array}$

Figure 24: The diagram L_1 along with the Khovanov homology groups $Kh(L_1)$ presented in a table with horizontal axis denoting homological grading and vertical axis denoting q -grading. Because we are forming complexes that are ‘infinite on the left’, the axes are drawn ‘backwards’. The pattern of groups is 2-periodic for h -grading below 0 and for q -grading ‘below’ 0.

Remark 3.16. Our constructions and proofs have used a fixed projection $M^r \rightarrow P'$, with isotopies that fix the ambient M^r while isotoping the link. This is enough to construct a well-defined $Kh(\mathcal{L})$ for links in a fixed copy of M^r , proving Theorem 1.1. It is also possible to show that the construction is invariant under moves that alter the projection, corresponding to moving the attaching spheres and surgery lines in the planar diagram P' . The proofs are similar in spirit to the proof of Theorem 3.9. We will investigate this further in Section 6.1 where knotifications for r -component links in S^3 naturally lead to a different planar projection of M^r .

4 Examples in $M^1 = S^2 \times S^1$ and M^2

In this section we present some computations of $Kh^*(L)$ over \mathbb{Z} for some simple diagrams L for links in M^r . Throughout this section we will make use of the well-known complex for the infinite full twist on two strands:

$$C^*(\mathcal{F}_2^\infty) \simeq \left(\cdots \rightarrow q^{-5} \begin{array}{c} \overline{\smile} \\ \underline{\smile} \end{array} \xrightarrow{\begin{array}{c} \overline{\smile} + \underline{\smile} \\ \overline{\smile} - \underline{\smile} \end{array}} q^{-3} \begin{array}{c} \overline{\smile} \\ \underline{\smile} \end{array} \xrightarrow{\begin{array}{c} \overline{\smile} - \underline{\smile} \\ \overline{\smile} + \underline{\smile} \end{array}} \underline{q^{-1} \begin{array}{c} \overline{\smile} \\ \underline{\smile} \end{array}} \right) \quad (38)$$

where the pair of maps $(\overline{\smile} + \underline{\smile})$ and $(\overline{\smile} - \underline{\smile})$ repeat ad infinitum to the left and we have underlined the term in homological degree zero. (Compare to the 2-strand projector in [CK12], which has a fixed identity term on the far left; here, this term is pushed out to $-\infty$ since we are fixing the terms in maximal homological degree instead.)

4.1 Two unlinked longitudes in $S^2 \times S^1$

Let L_1 denote the diagram of Figure 24 for the link in $M^1 = S^2 \times S^1$ formed by taking two longitudes in $D^2 \times S^1$. Inserting the complex (38) in place of the surgery line results in a simple

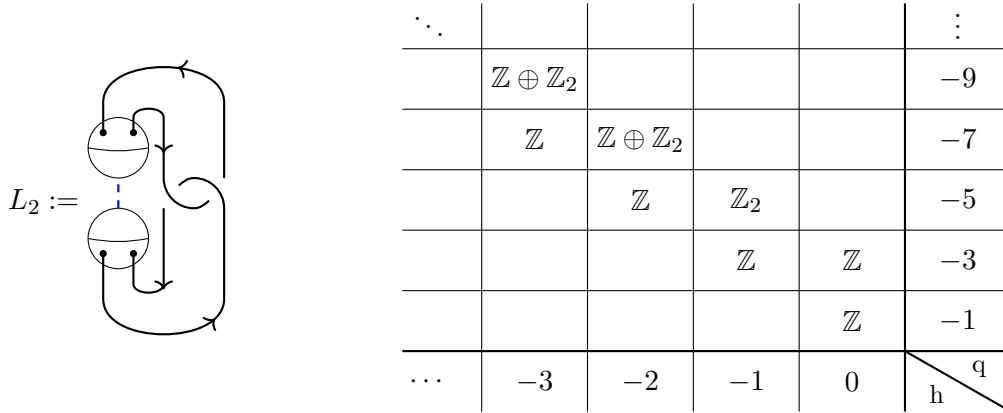


Figure 25: The diagram L_2 along with the Khovanov homology groups $Kh(L_2)$ presented in a table with horizontal axis denoting homological grading and vertical axis denoting q -grading. The pattern of groups is 1-periodic for h -grading below -1 and for q -grading ‘below’ -5 .

complex of the form

$$\dots \longrightarrow q^{-9} \bigcirc \xrightarrow{2 \bigcirc} q^{-7} \bigcirc \xrightarrow{0} q^{-5} \bigcirc \xrightarrow{2 \bigcirc} q^{-3} \bigcirc \xrightarrow{0} \underline{q^{-1} \bigcirc}.$$

Bar-Natan’s delooping isomorphism converts this to

$$\begin{array}{cccccc} & q^{-10}\mathbb{Z} & & q^{-8}\mathbb{Z} & & q^{-6}\mathbb{Z} & & q^{-4}\mathbb{Z} & & \underline{q^{-2}\mathbb{Z}} \\ \dots & \oplus & \nearrow 2 & \oplus & & \oplus & \nearrow 2 & \oplus & & \oplus \\ & q^{-8}\mathbb{Z} & & q^{-6}\mathbb{Z} & & q^{-4}\mathbb{Z} & & q^{-2}\mathbb{Z} & & \underline{q^0\mathbb{Z}} \end{array}$$

from which we can quickly compute the homology to be:

$$Kh^{i,j}(L_1) \cong \begin{cases} \mathbb{Z} & \text{if } (i, j) = (0, 0) \\ \mathbb{Z} & \text{if } (i, j) = (-2k + \epsilon, -2 - 4k) \text{ for } k \geq 0, \epsilon \in \{0, 1\} \\ \mathbb{Z}_2 & \text{if } (i, j) = (-1 - 2k, -4 - 4k) \text{ for } k \geq 0 \end{cases}$$

The table is presented in Figure 24. Note that this is precisely the stable homology of the torus links $T(2, k)$ as $k \rightarrow \infty$.

4.2 The Whitehead knot in $S^2 \times S^1$

Let L_2 denote the diagram of Figure 25 for the knot in $M^1 = S^2 \times S^1$ resulting from performing 0-surgery on one component of the Whitehead link in S^3 (L_2 can also be viewed as the knotification of the properly oriented Hopf link; see Section 6.1). We tensor the complex (38) along the surgery

line together with the complex

$$h^{-2}q^{-4} \left(\begin{array}{c} \text{---} \\ \text{---} \end{array} \xrightarrow{s} q \right) \left(\begin{array}{c} \downarrow (-) \uparrow \\ \text{---} \end{array} \xrightarrow{\quad} q^3 \right) \left(\quad \right)$$

(here s denotes the usual saddle cobordism) coming from the two crossings already present in the diagram to arrive at the following complex

$$\begin{array}{ccccccccc}
 \dots & \longrightarrow & q^{-13} & \begin{array}{c} \bigcirc \\ \bigcirc \end{array} & \xrightarrow{w^+} & q^{-11} & \begin{array}{c} \bigcirc \\ \bigcirc \end{array} & \xrightarrow{w^-} & q^{-9} & \begin{array}{c} \bigcirc \\ \bigcirc \end{array} & \xrightarrow{w^+} & q^{-7} & \begin{array}{c} \bigcirc \\ \bigcirc \end{array} & \xrightarrow{w^-} & q^{-5} & \begin{array}{c} \bigcirc \\ \bigcirc \end{array} \\
 & & & \downarrow s & & & \downarrow s & & & & \downarrow s & & & \downarrow s & & & \downarrow s \\
 \dots & \longrightarrow & q^{-12} & \begin{array}{c} \bigcirc \\ \bigcirc \end{array} & \xrightarrow{-2 \begin{array}{c} \bigcirc \\ \bigcirc \end{array}} & q^{-10} & \begin{array}{c} \bigcirc \\ \bigcirc \end{array} & \xrightarrow{0} & q^{-8} & \begin{array}{c} \bigcirc \\ \bigcirc \end{array} & \xrightarrow{-2 \begin{array}{c} \bigcirc \\ \bigcirc \end{array}} & q^{-6} & \begin{array}{c} \bigcirc \\ \bigcirc \end{array} & \xrightarrow{0} & q^{-4} & \begin{array}{c} \bigcirc \\ \bigcirc \end{array} \\
 & & & \downarrow 0 & & & \downarrow 0 & & & & \downarrow 0 & & & \downarrow 0 & & & \downarrow 0 \\
 \dots & \longrightarrow & q^{-10} & \begin{array}{c} \bigcirc \\ \bigcirc \end{array} & \xrightarrow{2 \begin{array}{c} \bigcirc \\ \bigcirc \end{array}} & q^{-8} & \begin{array}{c} \bigcirc \\ \bigcirc \end{array} & \xrightarrow{0} & q^{-6} & \begin{array}{c} \bigcirc \\ \bigcirc \end{array} & \xrightarrow{2 \begin{array}{c} \bigcirc \\ \bigcirc \end{array}} & q^{-4} & \begin{array}{c} \bigcirc \\ \bigcirc \end{array} & \xrightarrow{0} & \underline{q^{-2}} & \begin{array}{c} \bigcirc \\ \bigcirc \end{array}
 \end{array}$$

where w^\pm denotes the map

$$w^\pm := \begin{array}{c} \bigcirc \\ \bigcirc \end{array} \pm \begin{array}{c} \bigcirc \\ \bigcirc \end{array}.$$

If we use Bar-Natan's delooping isomorphism and split this complex in terms of q -degree, we see the following collection of complexes:

- In q -degree -1 there is a single-term complex \mathbb{Z} in homological grading zero whose homology is the same.
- In q -degree -3 there is a complex of the form (still arranged as a tensor product of two complexes, with homological gradings constant along diagonals in the usual way)

$$\left(\begin{array}{cc} & \mathbb{Z} \\ & \downarrow 1 \\ & \mathbb{Z} \\ \mathbb{Z} & \underline{\mathbb{Z}} \end{array} \right).$$

The homology is then easily computed to be

$$Kh^{i,-3}(L_2) \cong \begin{cases} \mathbb{Z} & \text{if } i = -1, 0 \\ 0 & \text{else} \end{cases}.$$

- In q -degree -5 we have a complex of the form

$$\left(\begin{array}{ccc} & \begin{pmatrix} 1 \\ -1 \end{pmatrix} \\ & \mathbb{Z} \xrightarrow{\quad} \mathbb{Z} \oplus \mathbb{Z} \\ \downarrow 1 & & \downarrow \begin{pmatrix} 1 & 1 \end{pmatrix} \\ \mathbb{Z} & & \mathbb{Z} \\ \\ \mathbb{Z} \xrightarrow{2} \mathbb{Z} & & \end{array} \right)$$

where the lower right (empty) corner has homological degree zero. The homology can be computed after a Gaussian elimination of the vertical identity map to be

$$Kh^{i,-5}(L_2) \cong \begin{cases} \mathbb{Z} & \text{if } i = -2 \\ \mathbb{Z}_2 & \text{if } i = -1. \\ 0 & \text{else} \end{cases}$$

- In q -degrees $-4k - 3$ for $k \geq 1$, we have complexes of the form

$$\left(\begin{array}{ccccc} & \begin{pmatrix} 1 \\ 1 \end{pmatrix} & & & \\ & \mathbb{Z} \xrightarrow{\quad} \mathbb{Z} \oplus \mathbb{Z} \xrightarrow{\begin{pmatrix} -1 & 1 \end{pmatrix}} \mathbb{Z} \\ \downarrow 1 & & \downarrow \begin{pmatrix} 1 & 1 \end{pmatrix} & & \\ \mathbb{Z} & \xrightarrow{-2} & \mathbb{Z} & & \\ \\ \mathbb{Z} & & \mathbb{Z} & & \end{array} \right)$$

where the lower right (empty) corner has homological degree $-2(k - 1)$. The homology can be computed after Gaussian elimination of the vertical identity and one of the right-most horizontal identities to be

$$Kh^{i,-4k-3}(L_2) \cong \begin{cases} \mathbb{Z} \oplus \mathbb{Z}_2 & \text{if } i = -2k \\ \mathbb{Z} & \text{if } i = -2k - 1. \\ 0 & \text{else} \end{cases}$$

- In q -degrees $-4k - 1$ for $k \geq 2$, we have complexes of the form

$$\left(\begin{array}{ccccc} & & \mathbb{Z} & \xrightarrow{\begin{pmatrix} 1 \\ -1 \end{pmatrix}} & \mathbb{Z} \oplus \mathbb{Z} & \xrightarrow{\begin{pmatrix} 1 & 1 \end{pmatrix}} & \mathbb{Z} \\ & & \downarrow 1 & & \downarrow \begin{pmatrix} 1 & 1 \end{pmatrix} & & \\ & & \mathbb{Z} & & \mathbb{Z} & & \\ & & & & & & \\ \mathbb{Z} & \xrightarrow{2} & \mathbb{Z} & & & & \end{array} \right)$$

where the lower right (empty) corner has homological degree $-2k + 3$. The homology can be computed after similar Gaussian eliminations to the previous case, giving the same homology

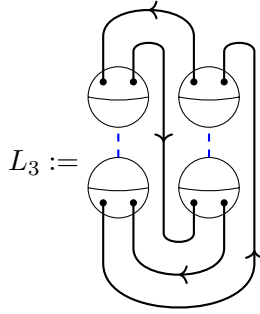
$$Kh^{i, -4k-1}(L_2) \cong \begin{cases} \mathbb{Z} \oplus \mathbb{Z}_2 & \text{if } i = -2k + 1 \\ \mathbb{Z} & \text{if } i = -2k \\ 0 & \text{else} \end{cases} .$$

All of these homology groups are summarized neatly in the table of Figure 25.

4.3 A crossingless knot in M^2

Let L_3 denote the diagram of Figure 26 for the corresponding knot in M^2 . We tensor together two copies of the complex (38) along the two surgery lines together, noting that all resolutions available create a single circle, to build an infinite complex of the form

$$\begin{array}{cccccccc} & & & & & & & \vdots \\ & & & & & & & \downarrow \\ & & & & & & & q^{-10} \bigcirc \\ & & & & & & & \downarrow 2 \bigcirc \\ & & & & & & & q^{-10} \bigcirc \xrightarrow{0} q^{-8} \bigcirc \\ & & & & & & & \downarrow 0 \qquad \downarrow 0 \\ & & & & & & & q^{-10} \bigcirc \xrightarrow{2 \bigcirc} q^{-8} \bigcirc \xrightarrow{0} q^{-6} \bigcirc \\ & & & & & & & \downarrow 2 \bigcirc \qquad \downarrow 2 \bigcirc \qquad \downarrow 2 \bigcirc \\ & & & & & & & q^{-10} \bigcirc \xrightarrow{0} q^{-8} \bigcirc \xrightarrow{-2 \bigcirc} q^{-6} \bigcirc \xrightarrow{0} q^{-4} \bigcirc \\ & & & & & & & \downarrow 0 \qquad \downarrow 0 \qquad \downarrow 0 \qquad \downarrow 0 \\ \dots \longrightarrow & q^{-10} \bigcirc & \xrightarrow{2 \bigcirc} & q^{-8} \bigcirc & \xrightarrow{0} & q^{-6} \bigcirc & \xrightarrow{2 \bigcirc} & q^{-4} \bigcirc & \xrightarrow{0} & \underline{q^{-2} \bigcirc} \end{array}$$



	\ddots						\vdots
	\mathbb{Z}^4	$\mathbb{Z}^3 \oplus \mathbb{Z}_2^2$					-11
		\mathbb{Z}^2	$\mathbb{Z} \oplus \mathbb{Z}_2^3$				-9
			\mathbb{Z}^3	$\mathbb{Z}^2 \oplus \mathbb{Z}_2$			-7
				\mathbb{Z}	\mathbb{Z}_2^2		-5
					\mathbb{Z}^2	\mathbb{Z}	-3
						\mathbb{Z}	-1
\dots	-5	-4	-3	-2	-1	0	$\begin{array}{l} q \\ h \end{array}$

$$Kh^{i,j}(L_3) \cong \begin{cases} \mathbb{Z} & \text{if } (i, j) = (0, -1) \\ \mathbb{Z}^{k+2} & \text{if } (i, j) = (-1 - 2k, -3 - 4k) \text{ for } k \geq 0 \\ \mathbb{Z}^k & \text{if } (i, j) = (-2k, -1 - 4k) \text{ for } k \geq 1 \\ \mathbb{Z}^k \oplus \mathbb{Z}_2^{k+2} & \text{if } (i, j) = (-1 - 2k, -5 - 4k) \text{ for } k \geq 0 \\ \mathbb{Z}^{k+1} \oplus \mathbb{Z}_2^k & \text{if } (i, j) = (-2k, -3 - 4k) \text{ for } k \geq 0 \\ 0 & \text{else} \end{cases}$$

Figure 26: The diagram L_3 along with the Khovanov homology groups $Kh(L_3)$ presented in a table with horizontal axis denoting homological grading and vertical axis denoting q -grading. The pattern is harder to see in this table, so the concrete formulas have been provided. The second and third cases describe the diagonal $2i - j = 1$, while the third and fourth cases describe the diagonal $2i - j = 3$.

The reader may verify that, after delooping, there are no non-zero compositions of maps, so that the signs are irrelevant. If we split the complex according to q-degree as in the example with L_2 , we find that the complex in any given q-degree (other than the easy case of q-degree -1) is supported in precisely two homological degrees, with a simple format that depends on the congruence class of the q-degree modulo 4:

- For q-degree $-1 - 4k$ with $k \geq 1$, $KC^*(L_3)$ is equivalent to a complex $\mathbb{Z}^{2k+1} \xrightarrow{d_{-1}} \mathbb{Z}^{2k}$ where d_{-1} is a matrix of the form

$$d_{-1} = \begin{pmatrix} 2 & 0 & 0 & 0 & 0 & \cdots & 0 \\ 0 & \vdots & 2 & \vdots & 0 & & \vdots \\ \vdots & & 2 & 0 & & & \\ & & 0 & 2 & & & \\ & & \vdots & 2 & & & \\ & & & 0 & & \vdots & \\ \vdots & & & \vdots & \ddots & 0 & \\ 0 & \cdots & & & & & 2 \end{pmatrix}$$

where each odd column (other than the first and last) has a 2 on and directly above the ‘diagonal’ as shown, and the rest of the entries are 0.

- For q-degree $-3 - 4k$ with $k \geq 0$, $KC^*(L_3)$ is equivalent to a complex $\mathbb{Z}^{2(k+1)} \xrightarrow{d_{-3}} \mathbb{Z}^{2k+1}$ where d_{-3} is a matrix of the form

$$d_{-3} = \begin{pmatrix} 0 & \cdots & & & \cdots & 0 \\ 0 & 2 & 2 & 0 & \cdots & \vdots \\ 0 & \cdots & & & & \\ 0 & 0 & 0 & 2 & 2 & 0 & \cdots \\ \vdots & & & & & \ddots & \\ 0 & \cdots & & & & \cdots & 0 \end{pmatrix}$$

where each even row has a 2 on and directly to the right of the ‘diagonal’ as shown, and the rest of the entries are 0.

From here, it is a simple computation to show that the homology of such complexes fits into the formula and table of Figure 26.

5 Decategorification and odd intersection numbers with belt spheres

5.1 The Kauffman bracket skein module

Given a 3-manifold M , Hoste and Przytycki (see the survey [HP92] on this topic) study the skein module $\mathcal{S}(M)$ generated over $R[q, q^{-1}]$ by isotopy classes of framed links in M , subject to local relations based on the Kauffman bracket $\langle \cdot \rangle$ (up to a renormalization depending on the orientation of the link):

$$\langle \times \rangle = \langle \rangle \langle \rangle - q \langle \text{---} \rangle, \quad \langle L \sqcup U \rangle = (q + q^{-1}) \langle L \rangle. \quad (39)$$

In the case of $M = M^r$, our definition for Khovanov homology requires the use of semi-infinite complexes. As such, in order to relate this to the skein module $\mathcal{S}(M^r)$, we must allow for power series in our ground ring. We let $\mathcal{S}_\ell(M^r)$ denote the skein module taken over the ring $R[q, q^{-1}]$ of formal Laurent series in q , with corresponding Kauffman bracket $\langle \cdot \rangle_\ell$.

In the following theorem, we call an oriented link $\mathcal{L} \subset M^r$ *null-homologous* if $[\mathcal{L}] = 0$ in $H_1(M^r)$. Note that this is equivalent to all of the algebraic intersection numbers η_i being zero, so our Khovanov homology groups are well-defined with no shifts incurred for performing surgery-wrap moves.

Theorem 5.1. *Given a framed, null-homologous link $\mathcal{L} \subset M^r$, with Khovanov homology groups $Kh^*(\mathcal{L})$ as defined in Section 3, the graded Euler characteristic $\chi_q(Kh^*(\mathcal{L}))$ recovers the Kauffman bracket skein module element $\langle \mathcal{L} \rangle_\ell \in \mathcal{S}_\ell(M^r)$ over the formal Laurent series ring $R[q, q^{-1}]$ up to a renormalization depending on the orientation of \mathcal{L} .*

Proof. Let L be a diagram for the link \mathcal{L} . Our definition for the Khovanov complex of a link in M^r is based on the usual Khovanov complex away from the inserted full twists, while allowing for complexes that are infinite ‘to the left’ whose graded Euler characteristic can give power series in q^{-1} . The Kauffman bracket relations of Equation 39 are precisely the relations categorified by the usual Khovanov complex via the exact triangle implied by Equation 4 and Bar-Natan’s delooping isomorphism [BN05]. It follows that, after adding kinks to L as necessary to equate the given framing for \mathcal{L} with the blackboard framing, $\chi_q(KC^*(L))$ satisfies all of the exact same relations as the Kauffman bracket and thus must match $\langle L \rangle_\ell$. \square

Since our categorified construction passes through complexes of diagrams in S^3 , which may be delooped into diagrams between empty links, we may rephrase Theorem 5.1 as follows.

Corollary 5.2. *The skein module $\mathcal{S}_\ell^0(M^r)$ of isotopy classes of null-homologous framed links in M^r (over $R[q, q^{-1}]$) is isomorphic to a single free summand $R[q, q^{-1}]$ generated by the empty link.*

In the case of $M^1 = S^2 \times S^1$, Hoste and Przytycki show [HP95] that the $\mathcal{S}(M^1)$ over $R[q, q^{-1}]$ is also isomorphic to a single free summand $R[q, q^{-1}]$ generated by the empty link, together with infinitely many torsion summands. For a link \mathcal{L} , let $\langle \mathcal{L} \rangle_{free} \in R[q, q^{-1}]$ denote the free part of $\langle \mathcal{L} \rangle \in \mathcal{S}(M^1)$.

Corollary 5.3. *For a null-homologous $\mathcal{L} \subset M^1$, the graded Euler characteristic $\chi_q(Kh^*(\mathcal{L}))$ recovers the polynomial $\langle \mathcal{L} \rangle_{free} \in R[q, q^{-1}]$.*

Proof. The arguments in [HP95] show that, over $R[q, q^{-1}]$,

$$\langle \mathcal{L} \rangle = \langle \mathcal{L} \rangle_{free} + \text{torsion}$$

where all of the torsion terms are annihilated by quantities of the form $(1 - q^{2a})$. The exact same arguments can be run in $\mathcal{S}_\ell(M^1)$ over $R[q, q^{-1}]$ but now the annihilators are all units, so that $\langle \mathcal{L} \rangle_\ell = \langle \mathcal{L} \rangle_{free}$. \square

The computations in Sections 4.1 and 4.2 provide examples of this behavior (note that in Section 4.1, we would get the same answer if the strands were oppositely oriented so that \mathcal{L} were null-homologous).

Remark 5.4. The computation in Section 4.3 provides a link $\mathcal{L} \subset M^2$ with $\chi_q(Kh^*(\mathcal{L})) \notin R[q, q^{-1}]$, showing that Corollary 5.3 does not hold there. This indicates that some aspect of Hoste's and Przytycki's argument must be altered in $\mathcal{S}(M^r)$ over $R[q, q^{-1}]$: either there is more than one free summand (corresponding to some non-empty, null-homologous links, perhaps similar to the one in Figure 26), or the torsion elements are annihilated by quantities that do not become units in $R[q, q^{-1}]$ (most likely corresponding to performing combinations of surgery wrap moves on differing surgery lines).

For links $\mathcal{L} \subset M^r$ with non-zero algebraic intersection numbers η_i , our Khovanov homology groups are only well-defined up to grading shifts depending on the η_i . From one point of view this would make the corresponding version of Theorem 5.1 unsatisfactory, since $\chi_q(Kh^*(\mathcal{L}))$ would only recover $\langle \mathcal{L} \rangle_\ell$ up to multiples of q^{3g} , where $g = \gcd(\eta_1, \dots, \eta_r)$. On the other hand, one could speculate that this ambiguity represents a naive categorical analogue of some aspect of the torsion in $\mathcal{S}(M^r)$, whereby we lose a notion of absolute gradings on our homology groups, but do retain some notion of relative gradings which are wholly invisible on the decategorified level.

Remark 5.5. In [HP95], Hoste and Przytycki provide computations in $\mathcal{S}(S^2 \times S^1)$ that show that any \mathcal{L} having odd intersection number with the belt sphere represents a trivial element in the skein module. Their methods generalize immediately to M^r for any r , so we are tempted to define

$$Kh^*(\mathcal{L}) := 0$$

for all \mathcal{L} having belt sphere intersection number n_i odd for some i . We will see another justification for this extension in what follows.

5.2 The WRT invariant

In this section we describe how, for a link $\mathcal{L} \subset M^r$, the graded Euler characteristic $\chi_q(Kh^*(\mathcal{L}))$ (evaluated at certain roots of unity) recovers the corresponding WRT invariant of \mathcal{L} in M^r . All of this material is a straightforward generalization of the arguments in the appendix of [Roz].

We begin by recalling some of the basic definitions (see [KL94] for a detailed account of these topics). Fixing an integer n , there exist in the Temperley-Lieb algebra TL_n certain idempotent elements $P_{n,d}$ for each d such that $n - d \in 2\mathbb{Z}_{\geq 0}$. These are the Jones-Wenzl projectors [Wen87], and they involve *rational* functions of q as their coefficients in TL_n . These projectors satisfy the following properties:

- $P_n := P_{n,n}$ is the usual Jones-Wenzl projector satisfying, for any Temperley-Lieb diagram δ ,

$$P_n \cdot \langle \delta \rangle = \langle \delta \rangle \cdot P_n = \begin{cases} P_n & \text{if } \delta = \iota_n, \text{ the identity diagram;} \\ 0 & \text{otherwise} \end{cases};$$

- $P_{n,d} \cdot \langle \delta \rangle = 0$ if $\text{th}(\delta) < d$;
- $P_{n,d}$ is a linear combination of terms of the form $\langle \delta^{\text{top}} \rangle \cdot P_d \cdot \langle \delta^{\text{bot}} \rangle$ for $\text{th}(\delta) = d$ (see Definition 2.20);
- $\sum_d P_{n,d} = \langle \iota_d \rangle$, the identity element in TL_n .

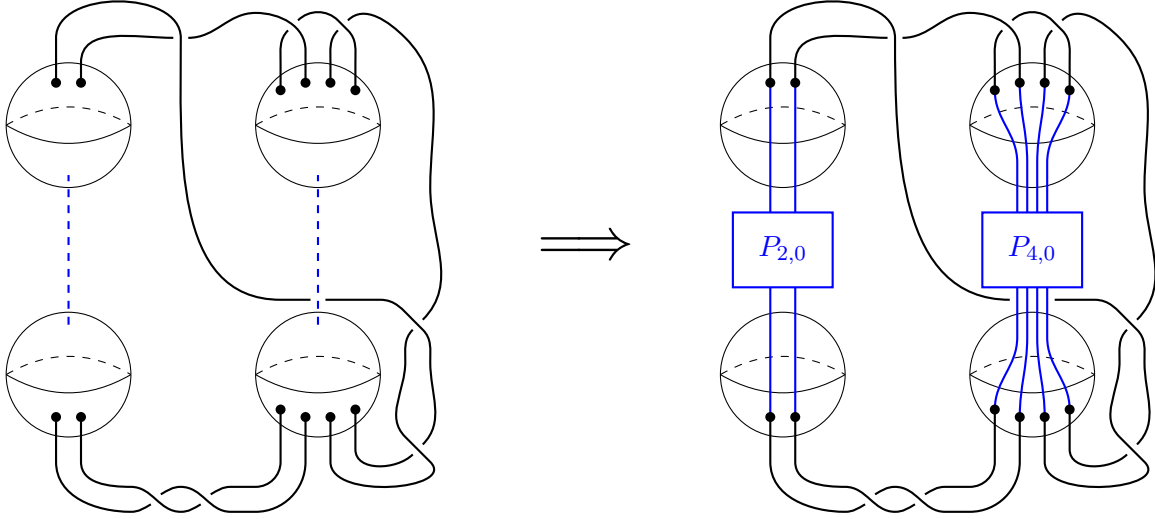


Figure 27: To compute the WRT invariant $Z_\rho(\mathcal{L}, M^r)$, it is enough to use the diagram $L(\vec{0})$ and insert $P_{n_i,0}$ instead of full twists into the cabled surgery lines, before taking the Kauffman bracket and evaluating at $q = e^{i\pi/\rho}$ (so long as $n_i \leq \rho - 2$ for each i).

Here we are using the notation $\langle \delta \rangle$ to indicate the element in TL_n corresponding to the isotopy class of δ .

With the help of the various $P_{n,d}$ we can define the WRT invariants [RT91, Wit89] of a link \mathcal{L} in a 3-manifold M . Suppose M can be obtained by performing surgery on a fixed (framed) link $\mathcal{L}_M \subset S^3$ (with diagram L_M). Let \mathcal{L}' be the link in S^3 (with diagram L'), disjoint from \mathcal{L}_M , that gives rise to $\mathcal{L} \subset M$ after the surgery is performed. Then the ρ^{th} WRT invariant of \mathcal{L} in M , denoted by $Z_\rho(\mathcal{L}, M)$, can be computed as a sum of terms involving the Kauffman brackets of diagrams formed from $L' \cup L_M \subset S^3$ by cabling the surgery link L_M and inserting Jones-Wenzl projectors into each component. The sum is taken over various cablings from a 0-cabling (deleting the link L_M) through to a $(\rho - 2)$ -cabling. After summing together these various Kauffman brackets, the expression is evaluated at $q = e^{i\pi/\rho}$ to arrive at the complex number $Z_\rho(\mathcal{L}, M)$.

For the case of $\mathcal{L} \subset M = M^r$ as illustrated in the previous sections, the links \mathcal{L}' and \mathcal{L}_M are clear. Given $\mathcal{L} \subset M^r$, the preimage link diagram L' is precisely what we have called $L(\vec{0})$ in Section 3.2, and the surgery link diagram L_{M^r} is just the unlink formed by placing 0-framed meridians encircling each surgery line. In the case of such meridian surgeries, it can be shown (see the appendix in [Roz]) that, so long as each intersection number n_i of \mathcal{L} with each belt sphere is even and satisfies $n_i \leq \rho - 2$, the majority of the terms in the sum of Kauffman brackets for $Z_\rho(\mathcal{L}, M^r)$ disappear and the result is equivalent to *deleting* the meridians and instead placing the projector $P_{n_i,0}$ along the cabling of what we have called the surgery lines sl_i . See Figure 27. Furthermore, if any of the intersection numbers n_i is odd, the resulting WRT invariant is zero.

This gives a further justification for simply defining $Kh^*(\mathcal{L}) := 0$ for links having odd intersection number with any of the belt spheres. Then in order to confirm that our homology $Kh^*(\mathcal{L})$ ‘categorifies’ the WRT invariants (in the sense that evaluating the graded Euler characteristic of $Kh^*(\mathcal{L})$ at $e^{i\pi/\rho}$ recovers Z_ρ), it is enough to show that the stable limiting complex associated to the infinite full twist as in Section 2 categorifies $P_{n_i,0}$ in this same sense. This is shown in the appendix to [Roz], but we repeat the argument here in our normalization.

We continue to use the notation $\langle \cdot \rangle$ to denote the unnormalized Kauffman bracket, which in S^3 is the same as the graded Euler characteristic of $\widetilde{KC}^*(\cdot)$ and satisfies equivalent formulas for shifts due to Reidemeister moves. In particular, for any term $\langle \delta^{\text{top}} \cdot P_d \cdot \delta_{\text{bot}} \rangle$ (allowing a slight abuse in the use of the notation $\langle \cdot \rangle$) in the linear combination for $P_{n,d}$, we must have δ^{top} having $\frac{n-d}{2}$ matchings. If we concatenate with a full twist \mathcal{F}_n , these matchings can be pulled through the twist giving (see Lemma 2.24; all homological shifts are even, and so have no effect on the Euler characteristic):

$$\langle \mathcal{F}_n \cdot \delta^{\text{top}} \cdot P_d \cdot \delta_{\text{bot}} \rangle = q^{(n-d)(n+1-\frac{n-d}{2})} \langle \delta^{\text{top}} \cdot \mathcal{F}_d \cdot P_d \cdot \delta_{\text{bot}} \rangle. \quad (40)$$

Now we consider the graded Euler characteristic of our limiting complex of Theorem 2.2 for the infinite twist on $n = 2p$ strands.

$$\begin{aligned} \lim_{k \rightarrow \infty} \chi_q(C^*(k)) &= \lim_{k \rightarrow \infty} \chi_q \left(h^{-2kp^2} q^{-2kp(p+1)} \widetilde{KC}_{\geq -(2k-1)}^*(\mathcal{F}_n^k) \right) \\ &= \lim_{k \rightarrow \infty} q^{-2kp(p+1)} \langle \mathcal{F}_n^k \rangle \end{aligned}$$

where we have discarded the truncation ($* \geq -(2k-1)$) since we are taking the stable limit of each coefficient in these (growing) polynomials, and any error terms get eliminated in this process. We now multiply by the identity written as a sum of projectors, and then write each projector as a linear combination $P_{2p,2m} = \sum_{\delta} a_{\delta} \langle \delta^{\text{top}} \cdot P_{2m} \cdot \delta_{\text{bot}} \rangle$ before using Equation 40:

$$\begin{aligned} \lim_{k \rightarrow \infty} q^{-2kp(p+1)} \langle \mathcal{F}_n^k \rangle &= \lim_{k \rightarrow \infty} q^{-2kp(p+1)} \langle \mathcal{F}_n^k \rangle \cdot \left(\sum_{m=0}^p P_{2p,2m} \right) \\ &= \lim_{k \rightarrow \infty} q^{-2kp(p+1)} \sum_{m=0}^p \langle \mathcal{F}_n^k \rangle \cdot P_{2p,2m} \\ &= \lim_{k \rightarrow \infty} q^{-2kp(p+1)} \sum_m \sum_{\delta} a_{\delta} \langle \mathcal{F}_n^k \cdot \delta^{\text{top}} \cdot P_{2m} \cdot \delta_{\text{bot}} \rangle \\ &= \lim_{k \rightarrow \infty} q^{-2kp(p+1)} \sum_m \sum_{\delta} a_{\delta} q^{2k(p-m)(p+m+1)} \langle \delta^{\text{top}} \cdot \mathcal{F}_{2m}^k \cdot P_{2m} \cdot \delta_{\text{bot}} \rangle \\ &= \lim_{k \rightarrow \infty} \sum_m \sum_{\delta} a_{\delta} q^{-2k(m^2+m)} \langle \delta^{\text{top}} \cdot \mathcal{F}_{2m}^k \cdot P_{2m} \cdot \delta_{\text{bot}} \rangle \\ &= \lim_{k \rightarrow \infty} \sum_m q^{-2k(m^2+m)} P_{2p,2m} \end{aligned}$$

where in the last line we have used the fact that $\langle \mathcal{F}_{2m} \rangle \cdot P_{2m} = P_{2m}$, which can be derived from the condition that P_{2m} kills all turnbacks. It is clear that, as $k \rightarrow \infty$, all terms for which $m \neq 0$ cannot contribute to a stable limit for any coefficient of the series, and so only the term $P_{2p,0}$ remains.

6 Khovanov homology for the knotification of a link in S^3

We now change our viewpoint slightly. Given a link $\mathcal{L} \subset S^3$ with $r+1$ components, there is a well-defined procedure to construct a *knot* $\mathcal{K}_{\mathcal{L}} \subset M^r$ which will be called the *knotification* of \mathcal{L} . This can be used, for instance, to define knot Floer invariants for \mathcal{L} [OS04]. Although the construction of Section 3 provides a corresponding Khovanov homology theory for $\mathcal{K}_{\mathcal{L}}$, we wish to augment the construction to allow for direct computation from the diagram L for $\mathcal{L} \subset S^3$, rather than first rearranging M^r (and $\mathcal{K}_{\mathcal{L}}$ within it) into the standard position of Section 3.

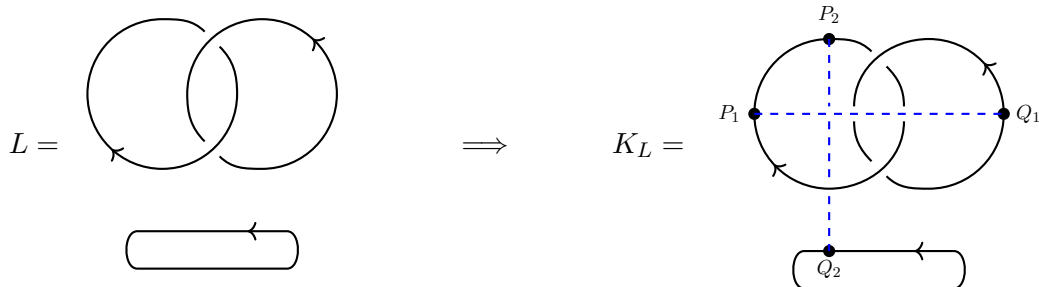


Figure 28: The oriented link diagram L for $\mathcal{L} \subset S^3$ has three components. We choose two pairs of points (P_i, Q_i) to act as attaching spheres and draw surgery lines between each pair. The resulting diagram K_L represents a well-defined knot $\mathcal{K}_{\mathcal{L}} \subset M^2$.

6.1 The knotification of a link in S^3

Given an oriented link diagram L for a link $\mathcal{L} \subset S^3$ with $r + 1$ components, we describe the process that produces a diagram K_L for the knotification $\mathcal{K}_{\mathcal{L}} \subset M^r$ (see Section 2.1 in [OS04] for further discussion).

First we focus on constructing $\mathcal{K}_{\mathcal{L}}$. We choose r pairs of points $(P_1, Q_1), (P_2, Q_2), \dots, (P_r, Q_r)$ along \mathcal{L} in such a way that the graph formed by identifying the points $P_i \cong Q_i$ on \mathcal{L} is connected. We view any pair (P_i, Q_i) as an embedding of $(S^0 \times S^2)_i$ into S^3 at the points P_i and Q_i , on which we perform S^0 surgery. The two strands of \mathcal{L} that intersect these spheres are connected in an orientation preserving manner by a band running along the handle $(D^1 \times S^2)_i$ (with an arbitrary amount of twisting), so that \mathcal{L} has geometric intersection number $n_i = 2$ with the belt sphere of the handle. This gives us the knot $\mathcal{K}_{\mathcal{L}}$.

To construct the planar diagram, we begin by drawing straight surgery lines in S^3 connecting each P_i to Q_i . After a small isotopy as necessary, we can assume our link, our choices of points, and our surgery lines are in general position so that the surgery lines did not intersect, and after projecting down to the plane, we have no points of triple intersection (this precludes the placement of a point P_i/Q_i at a crossing), no tangencies, and no cusps. As usual, we keep track of over and under crossing data in this process, and we draw our surgery lines sl_i as dashed lines in blue. We leave the sl_i unoriented, since L intersects each attaching sphere in two oppositely oriented points, ensuring that $\eta_i = 0$ for all i (see Definition 3.4, which can easily be adapted to our new situation). The resulting diagram is denoted K_L , representing the knot $\mathcal{K}_{\mathcal{L}} \subset M^r$. As before, we do not attempt to draw the handle. See Figure 28 for an example.

It is proven in [OS04] that this process gives a well-defined function taking a link $\mathcal{L} \subset S^3$ to a knot $\mathcal{K}_{\mathcal{L}} \subset M^r$. In particular, isotopies of \mathcal{L} and alternative choices of the data result in isotopic knots in M^r . Of particular interest here is the possibility of a handle-slide type of move which takes a chosen attaching point on one component of \mathcal{L} and passes it through the handle attached to some other point on that same component of \mathcal{L} , as illustrated for a diagram K_L in Figure 29.

6.2 The Khovanov homology of the knotification

We construct a Khovanov complex for our diagram K_L in a manner analogous to the construction of Section 3. First, we delete P_i and Q_i from our link diagram L . Then we replace each surgery line

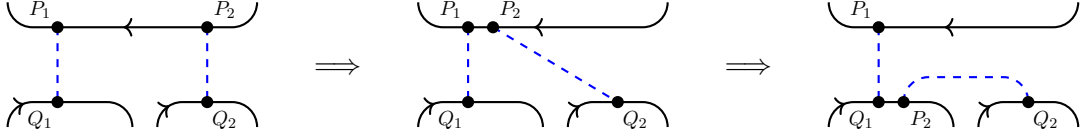


Figure 29: A handle-slide move that lets one point, representing an attaching sphere, pass through the surgered handle corresponding to another point. Note the orientations - with the ability to perform Reidemeister 1 moves on L before a handle-slide, all such moves are diagrammatically equivalent to the one illustrated here.

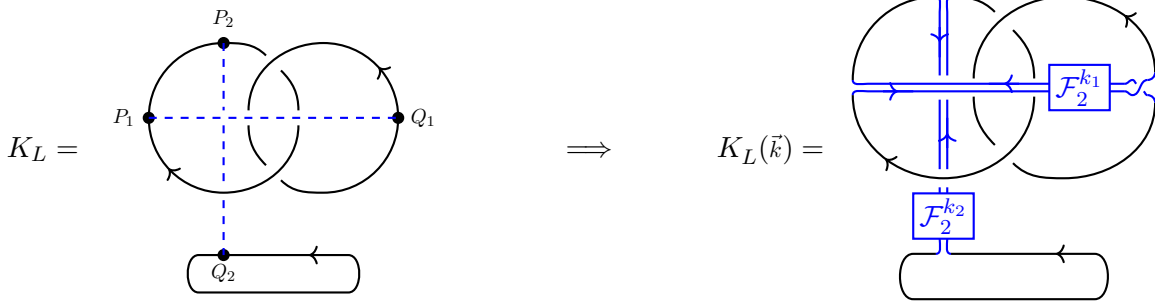


Figure 30: Continuing the example of Figure 28, we build a genuine knot diagram $K_L(\vec{k})$ from the oriented diagram K_L (which itself came from the diagram L for $\mathcal{L} \subset S^3$). $K_L(\vec{\infty})$ can be pictured similarly, with the complexes $C^*(\mathcal{F}_2^\infty)$ in place of the twists $\mathcal{F}_2^{k_i}$.

sl_i in our planar diagram K_L with two parallel copies of the line (maintaining crossing data with other strands), and then orient the strands to match with the strands of L at P_i . If necessary, we add a half twist (ie a positive crossing) near Q_i to allow these orientated strands to attach to L at Q_i . The resulting diagram could be denoted $K_L(\vec{0})$. We then choose a point on each sl_i (that is not a crossing point) at which to insert the complex $C^*(\mathcal{F}_2^\infty)$, and tensor this in the planar algebraic sense with the Khovanov complex for the rest of the diagram just as in Section 3, and define the result as the *Khovanov complex* of the diagram K_L . Again we allow ourselves the abuse of notation to think of this as defining

$$KC^*(K_L) := KC^*(K_L(\vec{\infty})). \quad (41)$$

The *Khovanov homology* $Kh^*(K_L)$ of the diagram K_L is then the homology of this complex $KC^*(K_L)$.

Meanwhile for any vector $\vec{k} = (k_1, \dots, k_r)$ we use the notation $K_L(\vec{k})$ to denote the genuine knot diagram formed by inserting $\mathcal{F}_2^{k_i}$ at each insertion point along sl_i . See Figure 30 for clarification. We also use the notation $C^*(K_L(\vec{k}))$ to denote the simplification of $\widetilde{KC}^*(K_L(\vec{k}))$ where the complexes $\widetilde{KC}^*(\mathcal{F}_2^{k_i})$ have been simplified to approximate Equation 38. This allows us to state the following versions of Proposition 3.7 and Corollary 3.8 whose proofs are identical to the earlier versions and are omitted here.

Proposition 6.1. *Given an $r + 1$ component link diagram L for $\mathcal{L} \subset S^3$ and an arbitrary homological lower bound a , there exists some finite \vec{k} such that the truncated Khovanov com-*

plex $KC_{\geq a}^*(K_L) = C_{\geq a}^*(K_L(\infty))$ is equal to the truncation of the finite approximation complex $C_{\geq a}^*(K_L(\vec{k}))$. In other words, $KC^*(K_L)$ can be approximated by a finite complex in any given homological range.

Corollary 6.2. *Given an $r + 1$ component link diagram L for $\mathcal{L} \subset S^3$, the Khovanov homology $Kh^*(K_L)$ can be approximated in any finite range of homological degrees by the Khovanov homology of a genuine link diagram $K_L(\vec{k})$ for finite \vec{k} . More precisely, given any homological bound a , there exists some \vec{k} that depends on a such that*

$$Kh^*(K_L) \cong Kh^*(K_L(\vec{k})) \tag{42}$$

in all homological gradings $* \geq a$.

Proof. Notice that in the case where all of the $\eta_i = 0$ (so all of the crossings in \mathcal{F}_2 are negative), all of the grading shifts cancel. \square

6.3 Invariance of $Kh^*(K_L)$

The goal of this section is two-fold. On the one hand, we wish to show that our definition for $Kh^*(K_L)$ is indeed an invariant of $\mathcal{K}_L \subset M^r$. Secondly, we expect our new construction to give the same homology as we would get by applying the results of Section 3 to our knot \mathcal{K}_L . Fortunately, these two goals are related since our new construction can be related to our old one by planar isotopies corresponding to changing the projection $M^r \rightarrow \mathbb{R}^2$ (see Remark 3.16).

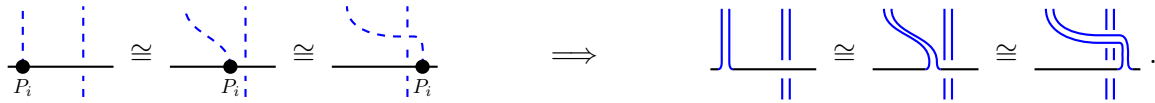
Theorem 6.3. *$Kh^*(K_L)$ is invariant under any of the relevant moves from Proposition 3.2 and Theorem 3.9. Specifically, any planar isotopies, Reidemeister moves, point-pass moves (better thought of now as ‘ P_i -pass’ or ‘ Q_i -pass’ moves), and surgery-wrap moves which fix the surgery data P_i, Q_i, sl_i induce an isomorphism on $Kh^*(K_L)$ with no grading shifts. $Kh^*(K_L)$ is also invariant under choice of insertion points for the $C^*(\mathcal{F}_2^\infty)$ along each sl_i .*

Proof. The proof works exactly the same way as in Theorem 3.15 (utilizing the through-degree zero property of the terms in $C^*(\mathcal{F}_2^\infty)$) and Theorem 3.9 (utilizing isotopies of genuine knots in S^3 now with the help of Corollary 6.2). The grading shifts all depended on η_i , which are all zero in the case of K_L . If we truly blow up the points P_i, Q_i into genuine spheres and arrange the intersections of them with the link properly, we can also arrange for mirror moves and finger moves, but these are unnecessary for our arguments in this section. \square

Theorem 6.4. *$Kh^*(K_L)$ is invariant under any planar isotopy, Reidemeister move, P_i/Q_i -pass move, and surgery-wrap move that affects the surgery data P_i, Q_i, sl_i . See the various figures in the proof below for clarification.*

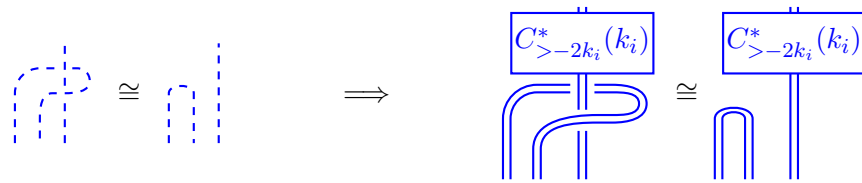
Proof. The proofs for planar isotopies and Reidemeister 2 and 3 moves work precisely the same as before. We use Corollary 6.2 and seek simple isotopies of genuine knots. A version of Reidemeister 2 is illustrated below:

We can use the same approach for P_i/Q_i -pass moves and any isotopies involving them, as illustrated below:



Note that we can always move insertion points so that the twists $\mathcal{F}_2^{k_i}$ do not need to be included in these local pictures (although clearly they would not cause problems if they were present).

Similarly, surgery-wrap moves involving a second surgery line (which in turn allow surgery lines to pass through each other or through themselves) are handled in the exact same way as they were in Theorem 3.15, where here it is important that we begin by moving the insertion points for the complexes $C^*(\mathcal{F}_2^\infty)$ so that only one is visible in the diagram. Rather than going through the details again, we simply show the diagrammatic version and refer the reader back to the proof of Theorem 3.15.



The essential idea is that, since $C_{>-2k_i}^*(k_i)$ is a complex made up of nothing but through-degree zero diagrams δ , we have cup-sliding isotopies giving very strong deformation retracts throughout the multicone expansion for $C_{>-2k_i}^*(k_i)$ that result in a multicone of single-term complexes. An additional argument is needed to ensure that we can give consistent signs to the resulting maps in order to keep our multicone truly unaltered - this is handled by choosing a consistent bottom closure γ for the diagram at hand, and noting that the isotopies could involve sliding the matchings of γ instead. These two choices are isotopic as tangle cobordisms up to a sequence of cobordisms of the form ρ_\circ which induce identity maps on the complexes (see Lemma 3.11). The projective functoriality of Bar-Natan's constructions then tell us that the two choices for each isotopy induce homotopic maps up to a sign, producing our set of consistent signs for our maps. The grading shifts work exactly the same as before.

Finally, we note that a Reidemeister 1 move on a surgery line creates a framing twist, which is equivalent to adding a full twist along blue strands in K_L . However, in the case of having only two parallel strands, a full twist is equivalent to a Jucys-Murphy element which can be added by a surgery wrap with one of the incoming strands as in Figure 20, and we have already checked general surgery wrapping moves. So we are done. \square

Corollary 6.5. *Given the knotification $\mathcal{K}_L \subset M^r$ of a link $\mathcal{L} \subset S^3$, the homology groups $Kh^*(K_L)$ constructed in this section are isomorphic to the homology groups $Kh^*(\mathcal{K}_L)$ constructed in Section 3.*

Proof. With the ability to isotope the link and the surgery data P_i, Q_i, sl_i , it is not hard to see that any diagram K_L can be isotoped into a diagram which matches the format of the diagrams of Section 3, at which point the constructions are precisely the same. See Figure 31 for an illustration using our previous example diagram. \square

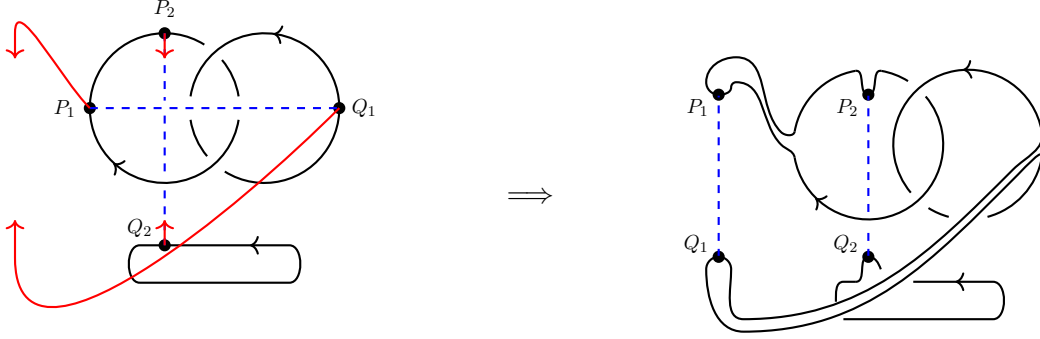


Figure 31: The isotopy moving K_L from Figure 28 into the standard position of Section 3, from which point the two constructions are equivalent (after replacing the points P_i, Q_i with small attaching spheres). Recall that surgery lines can pass through any strands of the link and each other, so there is no trouble in isotoping them into the desired position.

Finally, we turn to the question of invariance under the genuinely new diagrammatic move available in this section, the handle-slide. This move requires an extension of Lemma 2.16 from Section 2.3 for moving dots past crossings in a diagram. That lemma focused on changing a single dotted cobordism near a crossing. The following lemma concerns the case where we have many copies of the same dotted cobordisms, and we would like to change them all.

Lemma 6.6. *Consider a multicone of the form*

$$\mathcal{C}^* := \text{Multicone}_{\text{hc}^*(\mathcal{Z}_y) - \text{hc}^*(\mathcal{Z}_x) = 1} \left(\widetilde{KC}^*(\mathcal{Z}_x) \xrightarrow{\phi_{x,y}^*} \widetilde{KC}^*(\mathcal{Z}_y) \right)$$

where we have:

- All of the diagrams are the same tangle: $\mathcal{Z}_x = \mathcal{Z}_y = \mathcal{Z}$ for all x and y .
- There is a single crossing in \mathcal{Z} such that, for all x, y , $\phi_{x,y} = \text{crossing} + (-1)^{\text{hc}^*(\mathcal{Z}_x)} \tilde{\phi}$ for some fixed $\tilde{\phi}$ that is a sum of dotted cobordisms that are identity near the crossing. In other words, every map $\phi_{x,y}$ includes the same dotted identity cobordism near a crossing as one of its summands, while the other summands alternate as we traverse the multicone.

Then we have

$$\mathcal{C}^* \simeq \text{Multicone}_{\text{hc}^*(\mathcal{Z}_y) - \text{hc}^*(\mathcal{Z}_x) = 1} \left(\widetilde{KC}^*(\mathcal{Z}_x) \xrightarrow{(\phi'_{x,y})^*} \widetilde{KC}^*(\mathcal{Z}_y) \right)$$

where

$$\phi'_{x,y} = - \text{crossing} + (-1)^{\text{hc}^*(\mathcal{Z}_x)} \tilde{\phi}.$$

In other words, we are free to apply Lemma 2.16 to the entire multicone at once.

Of course, there is a similar statement for passing a dot along an over-crossing throughout a multicone as well.

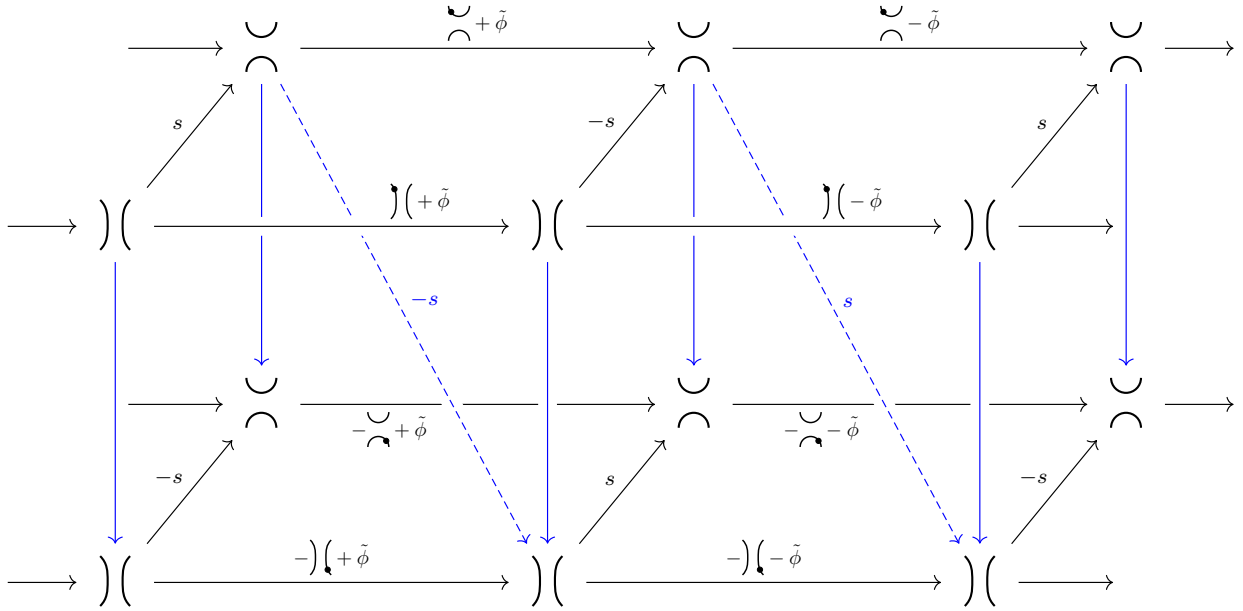


Figure 32: The diagram illustrating Lemma 6.6. The top faces, which we imagine continuing on in either direction (but not indefinitely), represent the multicone expansion of \mathcal{C}^* , while the bottom faces are the same but replacing ϕ with ϕ' by changing the sign of the specified dotted identity cobordism. The blue maps combine to provide the chain homotopy equivalence between these two multicones. The unmarked maps are identity maps, while the s stands for the obvious saddle cobordism.

Proof. The simplistic form of the diagrams and maps involved means that the homotopy of Lemma 2.16 can be repeated throughout the mapping cone, and the resulting diagram will commute as necessary giving a chain homotopy equivalence between the two multicones. See Figure 32. Note that the alternating signs of the ‘extra’ summands $\tilde{\phi}$ allow the diagonal homotopies to commute with the other maps as needed (ie there are no higher homotopies required). The details are left to the reader. □

Theorem 6.7. *Given a link diagram L for $\mathcal{L} \subset S^3$, let K_L^1 and K_L^2 be two knotification diagrams coming from L such that one is obtained from the other by a handle-slide move as in Figure 29. Then we have an isomorphism*

$$Kh^*(K_L^1) \cong Kh^*(K_L^2).$$

Proof. Call the two surgery lines involved sl_1 (running between P_1 and Q_1) and sl_2 (running between P_2 and Q_2), where P_2 is the point that is slid through the handle of sl_1 from P_1 to Q_1 (this is the case illustrated in Figure 29). Thus sl_1 is unchanged by the handle-slide but sl_2 is changed.

Having the ability to perform isotopies with the surgery lines, we begin by isotoping the local picture for K_{L_1} so that P_2 is very close to P_1 (this alone gives the second diagram in Figure 29). Next we isotope sl_2 further so that, starting from P_2 , it runs parallel along sl_1 until it reaches a

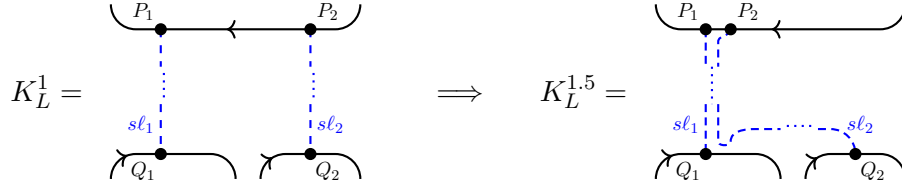


Figure 33: The local diagram for K_L^1 can be isotoped to the new local diagram $K_L^{1.5}$ where sl_2 runs parallel along sl_1 before reaching Q_2 . The dotted lines indicate places where there could be more crossings with other strands and surgery lines, but this crossing data is the same for sl_1 and sl_2 while they are running parallel.

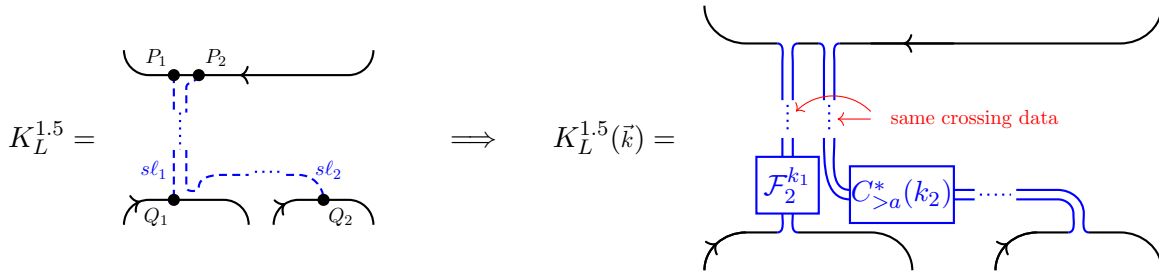


Figure 34: The diagram $K_L^{1.5}$ leads to the diagram $K_L^{1.5}(\vec{k})$ built by choosing insertion points near the point Q_1 . Again, the dotted lines indicate places where there could be more crossings with other strands and surgery lines, but this crossing data is the same for the strands coming from sl_1 and sl_2 while they are running parallel.

point near Q_1 before turning away and going towards Q_2 . The ability to have sl_2 pass through any other strands of L and/or other surgery lines ensures that we can accomplish this in such a way that the over/under crossing data of sl_2 matches that of sl_1 while running alongside it. Call this new diagram $K_L^{1.5}$ (See Figure 33 for clarification). Clearly we have $Kh^*(K_L^1) \cong Kh^*(K_L^{1.5})$. We wish to show that $Kh^*(K_L^{1.5}) \cong Kh^*(K_L^2)$.

In order to do this, we choose insertion points near the point Q_1 and insert a genuine twist $\mathcal{F}_2^{k_1}$ along sl_1 , but the truncated complex $C_{>a}^*(k_2)$ along sl_2 (here we set $a := -2k_2$ to avoid clutter in our diagrams). For all surgery lines away from this local picture, we choose arbitrary insertion points and insert $\mathcal{F}_2^{k_i}$ as usual. Allowing the usual abuse of notation, we will consider this as a diagram denoted $K_L^{1.5}(\vec{k})$. See Figure 34.

Now we use the complex for $C_{>a}^*(k_2)$ described in Section 4, notated in such a way as to fit into the diagram $K_L^{1.5}(\vec{k})$ in Figure 34:

$$\boxed{C_{>a}^*(k_2)} \simeq \left(\supset \subset \xrightarrow{\mathfrak{D}(\+) \mathfrak{C}} \supset \subset \xrightarrow{\mathfrak{D}(-) \mathfrak{C}} \supset \subset \rightarrow \dots \rightarrow \supset \subset \right). \quad (43)$$

In Equation 43, the pair of maps $(\mathfrak{D}(\+) \mathfrak{C})$ and $(\mathfrak{D}(-) \mathfrak{C})$ repeat in sequence for a total of k_2 such pairs. The q -degree shifts in this complex are omitted for simplicity.

If we imagine inserting Equation 43 into the diagram for $K_L^{1.5}(\vec{k})$ in Figure 34, we can see a complex of dotted cobordisms which satisfies the conditions of Lemma 6.6 where we choose to move

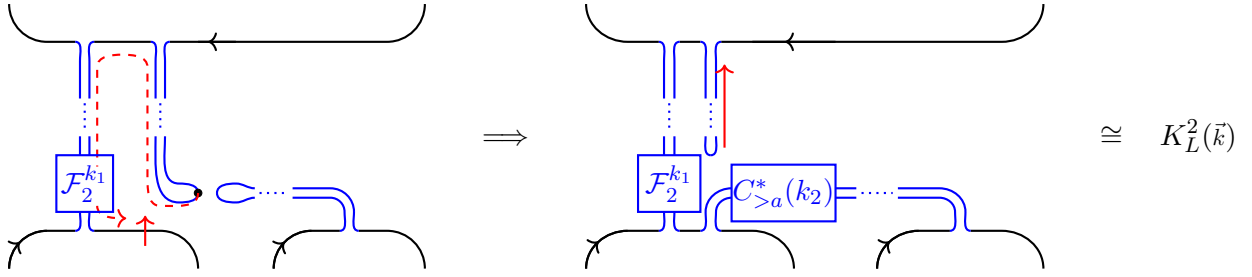


Figure 35: The left dot of the dotted cobordisms in Equation 43 can be slid along $K_L^{1.5}(\vec{k})$ as shown by the dashed red arrow. Along the way it will pass over and under an even number of crossings, so that the overall complex remains unchanged. The solid red arrows indicate simple planar isotopies that make the resulting complex equivalent to $K_L^2(\vec{k})$; see Figure 29.

the dot only on the ‘left-dotted cobordisms’ $\mathfrak{D}\mathfrak{C}$, viewing the ‘right-dotted cobordisms’ as the extra maps $\tilde{\phi}$ in that lemma’s notation (note that these maps do indeed alternate in sign as required). In this way, we can move the left dot first downwards then along sl_2 parallel to sl_1 , then back down along sl_1 , through the full twists $\mathcal{F}_2^{k_1}$, and finally settling at a point just to the right of Q_1 . See Figure 35. As can be seen there, the dot will slide through various crossing data along sl_2 as indicated by the dotted line there, but will then slide through the exact same crossing data along sl_1 . Finally, it slides through $\mathcal{F}_2^{k_1}$ which of course contains $2k_1$ crossings. In this way, we can guarantee that the dot passes an even number of crossings, so that the sign changes of applying Lemma 6.6 for each passed crossing all cancel.

We can now isotope the resulting diagram so that it clearly matches the diagram we would draw for $K_L^2(\vec{k})$ using an insertion point near P_2 (see Figure 29 for reference). Although the chain homotopy equivalence of Lemma 6.6 uses the full complex $\widetilde{KC}^*(\mathcal{F}_2^{k_1})$ on the left of our diagrams (as opposed to the truncated $C_{>-2k_1}^*(k_1)$ used to build $KC^*(K_L^{1.5})$), we still get isomorphisms on homology groups beyond the truncation point, allowing us to conclude in the limit that $Kh^*(K_L^{1.5}) \cong Kh^*(K_L^2)$ and so we are done.

Remark 6.8. We note here that, in this simple knotification scenario where all of our $n_i = 2$, we can also establish the invariance of our complex under the surgery wrap move utilizing Lemma 6.6 and a strategy similar to the proof of Theorem 6.7. In addition, the stabilization of the truncated complexes $C_{>-2k_i}^*(k_i)$ is already well-known via the formula of Equation 43. In particular, there is no need in this case to appeal to functoriality for cobordism maps commuting with very strong deformation retracts in large multicones in order to arrive at the desired result. It is our hope that this viewpoint may be helpful in lifting this construction to provide a stable homotopy type $\mathcal{X}(\mathcal{K}_L)$ for such knotifications $\mathcal{K}_L \subset M^r$ as in the work of Lipshitz-Sarkar and Lawson-Lipshitz-Sarkar [LS14, LLS], using techniques similar to those used in the author’s construction of a colored homotopy type $\mathcal{X}_c(L)$ in [Wil18]. We look to pursue this further in a future paper. □

References

- [AW] Michael Abel and Michael Willis. Colored Khovanov-Rozansky homology for infinite braids. *to appear in Algebr. Geom. Topol.* arXiv:1709.06666.
- [BK91] A I Bondal and M M Kapranov. Enhanced triangulated categories. *Mathematics of the USSR-Sbornik*, 70(1):93, 1991.
- [BN05] Dror Bar-Natan. Khovanov’s homology for tangles and cobordisms. *Geom. Topol.*, 9:1443–1499, 2005.
- [BN07] Dror Bar-Natan. Fast Khovanov homology computations. *J. Knot Theory Ramifications*, 16(3):243–255, 2007.
- [CH15] Benjamin Cooper and Matt Hogancamp. An exceptional collection for Khovanov homology. *Algebr. Geom. Topol.*, 15(5):2659–2707, 2015.
- [CK12] Benjamin Cooper and Vyacheslav Krushkal. Categorification of the Jones-Wenzl projectors. *Quantum Topol.*, 3(2):139–180, 2012.
- [CS98] J. Scott Carter and Masahico Saito. *Knotted surfaces and their diagrams*, volume 55 of *Mathematical Surveys and Monographs*. American Mathematical Society, Providence, RI, 1998.
- [EHa] Ben Elias and Matt Hogancamp. Categorical diagonalization. arXiv:1707.04349.
- [EHb] Ben Elias and Matt Hogancamp. Categorical diagonalization of full twists. arXiv:1801.00191.
- [HP92] Jim Hoste and Józef H. Przytycki. A survey of skein modules of 3-manifolds. In *Knots 90 (Osaka, 1990)*, pages 363–379. de Gruyter, Berlin, 1992.
- [HP95] Jim Hoste and Józef H. Przytycki. The Kauffman bracket skein module of $S^1 \times S^2$. *Math. Z.*, 220(1):65–73, 1995.
- [IW18] Gabriel Islambouli and Michael Willis. The Khovanov homology of infinite braids. *Quantum Topol.*, 9(3):563–590, 2018.
- [Kho00] Mikhail Khovanov. A categorification of the Jones polynomial. *Duke Math. J.*, 101(3):359–426, 2000.
- [Kho02] Mikhail Khovanov. A functor-valued invariant of tangles. *Algebr. Geom. Topol.*, 2:665–741, 2002.
- [KL94] Louis H. Kauffman and Sóstenes L. Lins. *Temperley-Lieb recoupling theory and invariants of 3-manifolds*, volume 134 of *Annals of Mathematics Studies*. Princeton University Press, Princeton, NJ, 1994.
- [LLS] Tyler Lawson, Robert Lipshitz, and Sucharit Sarkar. The cube and the Burnside category. arXiv:1505.00512.

- [LS87] Larry Lambe and Jim Stasheff. Applications of perturbation theory to iterated fibrations. *manuscripta mathematica*, 58:363–376, 09 1987.
- [LS14] Robert Lipshitz and Sucharit Sarkar. A Khovanov stable homotopy type. *J. Amer. Math. Soc.*, 27(4):983–1042, 2014.
- [Mar01] Martin Markl. Ideal perturbation lemma. *Communications in Algebra*, 29(11):5209–5232, 2001.
- [OS04] Peter Ozsváth and Zoltán Szabó. Holomorphic disks and knot invariants. *Adv. Math.*, 186(1):58–116, 2004.
- [Ras10] Jacob Rasmussen. Khovanov homology and the slice genus. *Invent. Math.*, 182(2):419–447, 2010.
- [Roz] Lev Rozansky. A categorification of the stable $su(2)$ Witten-Reshetikhin-Turaev invariant of links in $S^2 \times S^1$. arXiv:1011.1958.
- [Roz14] Lev Rozansky. An infinite torus braid yields a categorified Jones-Wenzl projector. *Fund. Math.*, 225(1):305–326, 2014.
- [RT91] N. Reshetikhin and V. G. Turaev. Invariants of three manifolds via link polynomials and quantum groups. *Invent. Math.*, 103:547–597, 1991.
- [Wen87] Hans Wenzl. On sequences of projections. *C. R. Math. Rep. Acad. Sci. Canada*, 9(1):5–9, 1987.
- [Wil18] Michael Willis. A colored Khovanov spectrum and its tail for B -adequate links. *Algebr. Geom. Topol.*, 18(3):1411–1459, 2018.
- [Wit89] Edward Witten. Quantum field theory and the jones polynomial. *Commun. Math. Phys.*, 121:351–399, 1989.